

THE UNIVERSITY OF MANITOBA

THE GEOLOGY OF THE
WHITEROCKS MOUNTAIN ALKALIC COMPLEX
IN SOUTH-CENTRAL BRITISH COLUMBIA

by

DAVID T. MEHNER

A THESIS SUBMITTED TO THE FACULTY OF GRADUATE STUDIES
IN PARTIAL FULFILMENT OF THE REQUIREMENTS FOR THE DEGREE OF
MASTER OF SCIENCE
DEPARTMENT OF EARTH SCIENCES

WINNIPEG, MANITOBA

April, 1982

THE GEOLOGY OF THE
WHITEROCKS MOUNTAIN ALKALIC COMPLEX
IN SOUTH-CENTRAL BRITISH COLUMBIA

BY

DAVID T. MEHNER

A thesis submitted to the Faculty of Graduate Studies of
the University of Manitoba in partial fulfillment of the requirements
of the degree of

MASTER OF SCIENCE

© 1982

Permission has been granted to the LIBRARY OF THE UNIVERSITY OF MANITOBA to lend or sell copies of this thesis, to the NATIONAL LIBRARY OF CANADA to microfilm this thesis and to lend or sell copies of the film, and UNIVERSITY MICROFILMS to publish an abstract of this thesis.

The author reserves other publication rights, and neither the thesis nor extensive extracts from it may be printed or otherwise reproduced without the author's written permission.

ABSTRACT

The Whiterocks Mountain stock is a small intrusive complex consisting of an alkalic suite and a calc-alkalic suite of rocks, intruding Paleozoic metasediments and metavolcanics, 25 km northwest of Kelowna, British Columbia. Crosscutting relationships indicate that the oldest alkalic unit is mafic syenite-monzonite, with biotite pyroxenite, amphibole pyroxenite, porphyritic monzonite and leucocratic quartz monzonite being successively younger. All but the leucocratic quartz monzonite lack quartz. Weakly developed copper sulphide mineralization occurs in the amphibole pyroxenite. Major, minor and trace element geochemistry suggest the alkalic units are related through crystal-liquid fractionation that involved the early separation of biotite, followed by ferrohastingsite and plagioclase.

The calc-alkalic rocks of the stock are younger. They consist predominantly of quartz monzonite, granodiorite and quartz diorite dykes that crosscut the alkalic rocks. They have a distinct, sub-alkaline trend on the diagram $\text{Na}_2\text{O} + \text{K}_2\text{O}$ vs. SiO_2 . On this diagram, the leucocratic quartz monzonite is transitional between the two suites.

K/Ar and Rb-Sr ages have yielded dates of between 154 m.y. and 145 m.y. for the calc-alkalic rocks. This age is identical to that obtained for similar rocks belonging to the Okanagan intrusive complex to the south. K/Ar dates of 169 m.y. and 174 m.y. for the alkalic rocks suggest they may represent some of the oldest rocks in the Okanagan intrusive complex. Rb-Sr dates of 291 ± 38 m.y. and 338 ± 37 m.y. for the same alkalic rocks contradict the younger age and suggest they may represent some of the oldest intrusive rocks in southern B.C.

TABLE OF CONTENTS

	<u>page</u>
ABSTRACT	i
LIST OF FIGURES	iv
LIST OF TABLES	vi
APPENDICES	vii
 <u>CHAPTER I</u> INTRODUCTION	 1
Statement of Problem	1
Location and Access	1
Previous Work	2
 <u>CHAPTER II</u> GEOLOGICAL SETTING	 5
Introduction	5
Regional Geology	5
Regional Structure	7
Orogeny	7
 <u>CHAPTER III</u> WHITEROCKS MOUNTAIN STOCK	 9
Introduction	9
Alkalic Complex	10
Methodology	10
Intrusive Relationships	12
Rock Description	19
A. Mafic Syenite-Monzonite	19
B. Alkalic Pyroxenites	21
i biotite pyroxenite	22
ii amphibole pyroxenite	24
iii hornblendite dykes	29
C. Porphyritic Monzonite	29
D. Hybrid Zone	34
E. Leucocratic Quartz Monzonite	35
F. Porphyritic Leucocratic Quartz Diorite	37
Calc-Alkalic Complex	38
 <u>CHAPTER IV</u> AMPHIBOLES	 40
Introduction	40
Results	40
 <u>CHAPTER V</u> METALLIC MINERALIZATION	 43
Introduction	43
Copper Content of Rocks	43
Nickel Content of Rocks	46
Mode of Mineralization	48
Factors Controlling Copper Mineralization	49
Economic Significance of Mineralization	52

	<u>page</u>
<u>CHAPTER VI</u> ALTERATION	54
Introduction	54
Temperature-Pressure Conditions of Late Magmatic Alteration	55
<u>CHAPTER VII</u> PETROCHEMISTRY	56
Introduction	56
Major and Minor Elements	56
A. Alkalic Suite of Rocks	56
B. Calc-alkalic Suite of Rocks	64
C. Porphyritic Leucocratic-Quartz Diorite Dykes	64
Petrogenetic Trace-Elements: Ba, Rb and Sr ..	65
Rock Geochemical Results and Their Interpretation	67
<u>CHAPTER VIII</u> AGE DETERMINATIONS	74
Introduction	74
Ages and Interpretation	74
<u>CHAPTER IX</u> CONCLUSIONS	78
<u>CHAPTER X</u> ACKNOWLEDGEMENTS	80
REFERENCES	81

LIST OF FIGURES

	page
FIGURE 1. Location Map and General Geology of the Whiterocks Mountain Area.	3
FIGURE 2. Semi-detailed Geological Map of the Whiterocks Mountain Stock.	11
FIGURE 3. Classification of Feldspar Rich-Rocks on the Basis of Modal Plagioclase, K-Feldspar, and Quartz From the Quartz-Poor Portion of the Whiterocks Mountain Stock.	13
FIGURE 4. Classification of Feldspar-Rich Rocks on the Basis of Modal Plagioclase, K-feldspar and Coloured Minerals Plus Opaques from the Quartz-Poor Portion of the Whiterocks Mountain Stock.	14
FIGURE 5. A Comparison of the Mafic-Rich Rocks From the Quartz-Poor Portion of the Whiterocks Mountain Stock on the Basis of Modal Pyroxene, Amphibole and Biotite.	15
FIGURE 6. Schematic Section Through the Alkalic Portion of the Whiterocks Mountain Stock Showing the Various Intrusive Relationships.	16
FIGURE 7. Geological Map of the Whiterocks Mountain Alkalic Complex, scale 1:5000. Map in pocket in back of thesis.	pocket
FIGURE 8. Photograph of a composite dyke consisting of hornblendite borders with a mafic-poor, porphyritic monzonite core cutting mafic syenite- monzonite.	18
FIGURE 9. Microphotograph under polarized light of biotite pyroxenite with well developed "sagenitic" texture in the biotite.	23
FIGURE 10. Photograph of brecciated biotite pyroxenite with coarse hydrothermal biotite surrounding partly rounded pyroxenite fragments.	23
FIGURE 11. Microphotograph under polarized light of amphibole pyroxenite with poikilitic ferrohastingsite enclosing euhedral to subhedral aegirine-augite.	26
FIGURE 12. Microphotograph under plane light of amphibole pyroxenite with ferrohastingsite replacing aegirine-augite.	26
FIGURE 13. Microphotograph under plane light of euhedral ferrohastingsite crystals within a hornblendite dyke being replaced by late stage hornblende.	28

	page
FIGURE 14. Photograph of late stage hornblendite dykes cutting medium grained biotite pyroxenite.	30
FIGURE 15. Photograph of porphyritic monzonite showing "blocky" microcline phenocrysts set in a medium grained monzonite groundmass.	31
FIGURE 16. Photograph of porphyritic monzonite showing aligned microcline phenocrysts separated by thin bands of mafic-rich monzonite into units characterized by phenocrysts of a fairly uniform size.	31
FIGURE 17. Histogram Showing the Copper Distribution in Rocks from the Whiterocks Mountain Stock.	45
FIGURE 18. Microphotograph under plane light showing opaque minerals and biotite filling the interstices between subhedral to euhedral aegirine-augite crystals.	50
FIGURE 19. Microphotograph under polarized light showing opaque minerals and biotite filling interstices and rimming euhedral to aegirine-augite crystals.	50
FIGURE 20. Variation Diagram Showing Total Alkalis vs. SiO_2 for Rocks from the Whiterocks Mountain Stock.	59
FIGURE 21. Chemical Variation Diagram Showing $\text{K}_2\text{O} + \text{Na}_2\text{O}$ and CaO vs. SiO_2 and the Peacock Index for Rocks from the Whiterocks Mountain Stock.	60
FIGURE 22. Harker Variation Diagrams Showing Major Oxides vs. SiO_2 for the Alkalic Rocks from the Whiterocks Mountain Stock.	62
FIGURE 23. Total Alkalis - Total Iron - Total Magnesium Ternary Diagram for Rocks from the Whiterocks Mountain Stock.	63
FIGURE 24. Chemical Variation Diagram Showing Sr vs. Rb for the Whiterocks Mountain Stock.	66
FIGURE 25. Chemical Variation Diagram Showing Sr vs. Ba for the Whiterocks Mountain Stock.	68
FIGURE 26. Chemical Variation Diagram Showing Ba vs. Rb for the Whiterocks Mountain Stock.	69
FIGURE 27. Chemical Variation Diagram Showing Ca/Sr vs. K/Rb for the Whiterocks Mountain Stock.	70

LIST OF TABLES

	page
TABLE 1. Calculated Cell Dimensions For Amphiboles From the Amphibole Pyroxenite, Hornblendite Dykes and the Porphyritic Monzonite-Pyroxenite Hybrid Zone of the Whiterocks Mountain Alkalic Complex and A Comparison With Values For Ferrohastingsite Determined by Borley and Frost (1962).	41
TABLE 2. Copper and Nickel Contents of Some Rocks from the Alkalic Portion of the Whiterocks Mountain Stock.	44
TABLE 3. A Comparison of Major, Minor and Trace Element Contents of Some Average Mafic and Ultramafic Rocks with the Whiterocks Mountain Stock Pyroxenites.	47
TABLE 4. Major, Minor and Trace Element Contents of Some Rocks from the Alkalic Portion of the Whiterocks Mountain Stock.	57
TABLE 5. Major, Minor and Trace Element Contents of Some Rocks from the Calc-Alkalic Portion of the Whiterocks Mountain Stock.	58

APPENDICES

	page
APPENDIX A. Modal Mineralogy in Volume Percent for Some Rocks From the Alkalic Portion of the Whiterocks Mountain Stock.	85
APPENDIX B. Partial Modes in Volume Percent for Some Rocks From the Whiterocks Mountain Alkalic Complex.	86
APPENDIX C. X-Ray Results from Three Analyzed K-Spar Phenocrysts From the Porphyritic Monzonite of the Whiterocks Mountain Alkalic Complex.	87
APPENDIX D. C.I.P.W. Norms for Some Rocks From the Whiterocks Mountain Alkalic Complex.	88
APPENDIX E. Calculated Ratios of Various Elements and Oxides for Rocks from the Whiterocks Mountain Stock.	89

CHAPTER I

INTRODUCTION

Statement of Problem

The Whiterocks Mountain stock is a small plutonic complex intruding metamorphosed Upper Paleozoic to Upper Triassic volcanics and sediments that lie north of the Okanagan intrusive complex in south-central British Columbia.

The purpose of this study is to establish the age and chemistry of the stock and to study the petrology of a suite of weakly mineralized quartz deficient, alkalic rocks that make up a portion of the Whiterocks Mountain intrusive complex.

The study of the alkalic rocks is based on geological mapping at 1:5000 scale, microscopic investigation of forty thin sections and sixty-five stained rock slabs, geochemical data from over forty rock samples and calculated cell dimensions from sixteen X-rayed amphiboles. The rock geochemical data includes thirty-one specimens analyzed for major and minor elements and five trace elements, including Ni, Cu, Ba, Rb and Sr for the quartz-poor rocks.

In addition, eight specimens, analyzed for major, minor and trace elements plus an extra seven specimens analyzed only for trace elements, were collected from the remainder of the stock by M. Osatenko and J. K. Russell of Cominco Ltd. Also, two Rb/Sr isochrons for the stock were determined by R. L. Armstrong of University of British Columbia for Cominco Ltd. An additional two Rb/Sr isochrons and two K/Ar age determinations were made by Wilkins (1981) for a B.Sc. thesis at University of British Columbia.

Location and Access

The Whiterocks Mountain stock is located about 25 km northwest of

Kelowna, British Columbia (Figure 1), at $119^{\circ}44'$ west longitude and $50^{\circ}02'$ north latitude. The quartz-deficient portion of the stock is largely confined to the western and southern slopes of Whiterocks Mountain with known outcrops only above 5300 feet elevation. Access to the area is easily obtained by car or truck along well marked logging roads (maintained by Crown Zellerbach of Kelowna, B.C.) that lead directly to Whiterocks Mountain from Westside Road along the west side of Okanagan Lake. Numerous logging and mining exploration drill roads cover portions of the stock.

Previous Work

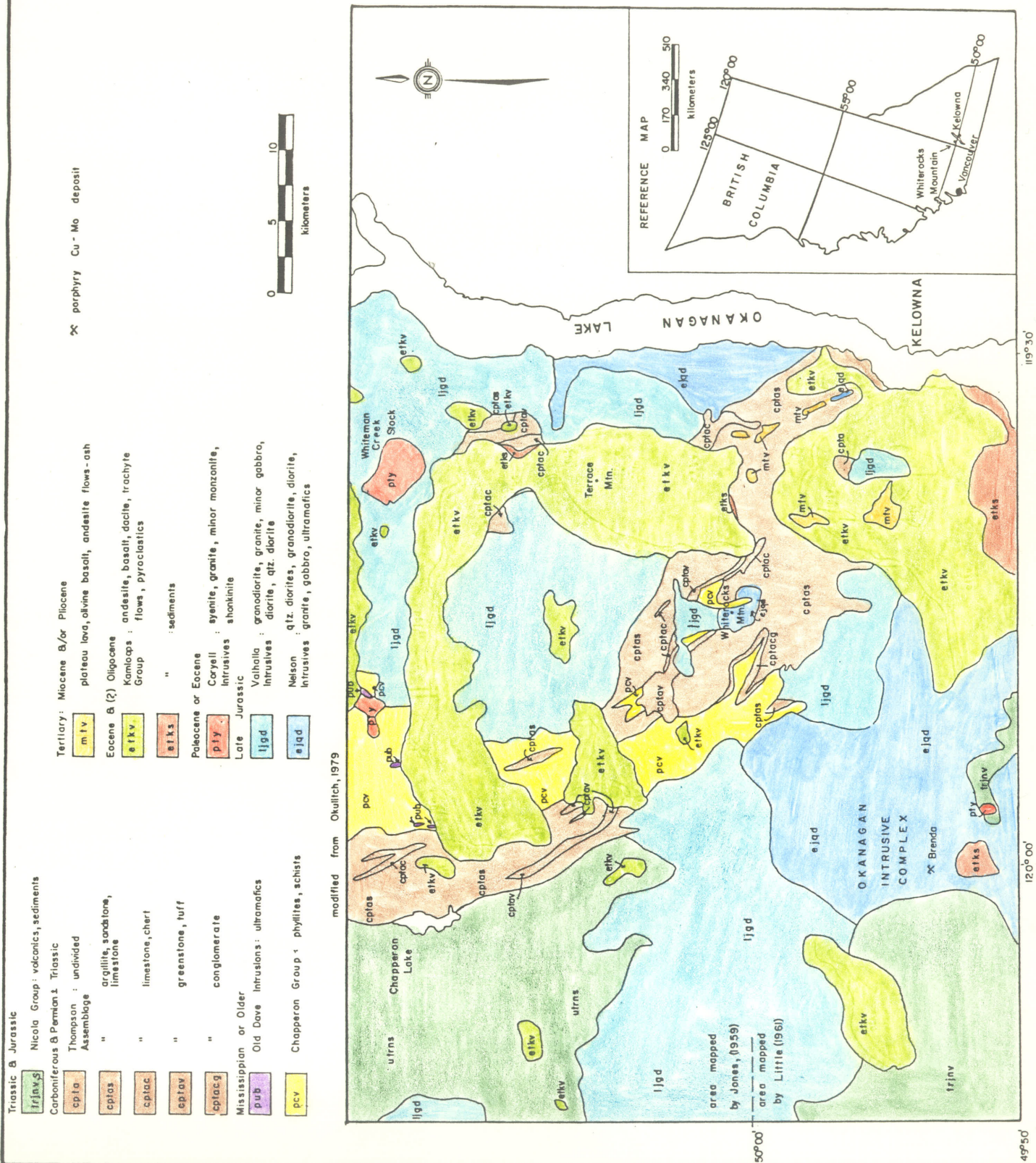
The northern half of the Whiterocks Mountain stock was originally mapped by Jones (1959) of the Geological Survey of Canada when he carried out 1 inch = 4 miles scale mapping of the Vernon map sheet area during 1945-51. The southern portion of the stock was first mapped for the G.S.C. in 1936 by Cairnes (1940) and later by Little (1961), both of whom carried out 1 inch = 4 miles scale mapping of the Kettle River, west half map sheet area.

Most recently a 1:250,000 scale geology compilation and mapping study of the area was completed by Okulitch (1979) of the Geological Survey of Canada.

Besides the work carried out by the G.S.C., numerous mining companies have worked in the area, particularly on the alkalic (quartz-deficient) suite of rocks where visible chalcopyrite mineralization exists. The work includes geological mapping, soil geochemical, induced polarization and ground magnetic surveys and percussion and diamond drilling. Companies that have filed reports of their work with the Mining Recorder

FIGURE 1

LOCATION MAP AND GENERAL GEOLOGY OF THE WHITEROCKS MOUNTAIN AREA



for the purpose of property assessment credits include Texas Gulf Sulphur, 1968; Atlas Exploration, 1969; and Cominco Ltd., 1978-80 (copies of assessment reports covering part or all of the stock are located at the Mining Recorder's Office in Vernon, Vancouver or Victoria, B.C. These reports are kept confidential for one year after being submitted to the government).

Reference to the area is also made in the B.C. Department of Mines and Petroleum Resources G.E.M. Report, 1969 (p. 299-300) and 1970 (p. 406) and in Table 1 of Characteristics of Some Canadian Cordilleran Porphyry Prospects (Pilcher and McDougall, 1976).

Besides work done directly on the stock itself, a number of studies have been carried out on the nearby Okanagan intrusive complex. These include Petß, 1970, 1973; Roddick et al., 1972; Preto, 1974; Gabrielse and Reesor, 1974; Medford, 1975; and Petß and Armstrong, 1976.

CHAPTER II

GEOLOGICAL SETTING

Introduction

The Whiterocks Mountain stock is a small pluton located along the eastern boundary of the Intermontane Tectonic Belt (Sutherland Brown et al., 1971) of south-central British Columbia. The Intermontane Tectonic Belt is one of five major sub-parallel, facies and tectonic belts arranged parallel to the length of the Canadian Cordillera. It is composed of Upper Paleozoic to Jurassic volcanic and volcanoclastic "eugeosynclinal" rocks and Jurassic and Tertiary plutons and stocks (Ney and Hollister, 1976). It also contains most of British Columbia's porphyry copper deposits including all the deposits associated with alkaline rocks (Christopher and Carter, 1976).

Structurally, the belt as a whole is characterized by normal faulting with only moderate amounts of folding and thrusting present.

Regional Geology

In the area around Whiterocks Mountain (Figure 1), the oldest known rocks are the metamorphic rocks of the Mississippian or possibly older, Chapperon Group (Okulitch, 1979). These are intruded by a number of small, serpentized ultramafic sills and dykes known as the Old Dave Intrusions. These ultramafic bodies are not found intruding younger rocks. Unconformably overlying the Chapperon Group and country-rock for the Whiterocks Mountain stock are weakly to moderately metamorphosed argillites, siltstones, quartzites, conglomerates, limestones and minor andesite to rhyolite tuffs and flows of the Thompson Assemblage (Okulitch, 1979). Yielding fossils that range in age from Upper Mississippian to Pennsylvanian and Permian, the Thompson Assemblage has also produced

fossils that are Upper Triassic in age (Campbell and Okulitch, 1972; Monger and Price, 1979). In the past (Jones, 1959; Little, 1961) these rocks were mapped as part of the Cache Creek Group, but recent work by Monger (1975) on the type locality for Cache Creek Group rocks has distinguished these on the basis of lithology and fauna.

Intruding both the Chapperon Group and Thompson Assemblage are Lower to Upper Jurassic granitic rocks. Composed of quartz diorite, granodiorite, granite and minor diorite, gabbro and ultramafic rocks, these batholith size plutons were called Okanagan Intrusives by Cairnes (1940), Coast intrusions by Jones (1959) and Nelson and Valhalla intrusions by Little (1961). Okulitch (1979) also refers to these plutonic rocks on the west side of Okanagan Lake as Nelson and Valhalla intrusions, while other recent workers have referred to the same rocks as the Similkameen Batholith (Pet8, 1973 a, b), the Okanagan Complex (Roddick et al., 1972, Preto, 1974) and the Pennask Batholith (Gabrielse and Reesor, 1974).

Following emplacement of the Jurassic intrusives a number of small Eocene to Paleocene plutons composed of syenite, granite, minor monzonite and shonkinite intruded the area (Little, 1961; Okulitch, 1979). These small intrusive bodies, including the Whiterocks Mountain Stock according to some workers, have been correlated with the Coryell plutonic rocks which are most abundant east of Okanagan Lake.

Unconformably overlying the Jurassic and older rocks in the area are sediments and volcanic flows and tuffs of the Eocene, Kamloops Group. According to Macdonald (1975) and Okulitch (1979) these also unconformably overlie the Paleocene or Eocene intrusives, however mapping in the vicinity of the Tertiary, Whiteman Creek stock (Figure 1) does not substantiate that hypothesis. Rather it indicates the stock is coeval with the

surrounding volcanics and in fact is likely the feeder to some of the overlying volcanics as suggested by Church (1979).

Conformably overlying the Kamloops Group are scattered occurrences of Miocene and/or Pliocene plateau lavas, related ash and breccia and minor basal sediments.

Regional Structure

The most obvious regional structures around Whiterocks Mountain occur in the metamorphosed sediments and volcanics where tight, upright folds, plunging gently northwest are common in the Chapperon Group but less well developed in the younger, Paleozoic rocks (Okulitch, 1979). Later folding, possibly related to emplacement of Jurassic plutons changed the orientation of earlier folds and may be responsible for the arcuate shape of the belt of Thompson Assemblage rocks (see Figure 1).

In the immediate vicinity of the Whiterocks Mountain stock, well preserved bedding in the metasediments parallels foliation. Strike ranges from 125° - 150° and dip averages 70° W. No significant folding was observed.

Metamorphic foliation is also observed in the Mesozoic plutonic rocks where foliation is quite strong in the Lower Jurassic, Nelson Intrusives and faint to absent in the younger, more massive Upper Jurassic, Valhalla plutons.

Steep angle faulting greatly affected the area from the time following emplacement of the Mesozoic intrusives, right up to the extrusion of the Miocene and younger, plateau basalts.

Orogeny

The area in and around Whiterocks Mountain has undergone at least three significant periods of orogeny.

The first period occurred in Permo-Triassic times and consisted of plutonism, uplift and erosion and associated deformation and low grade metamorphism (Okulitch, 1979).

This was followed by the Columbian Orogeny which lasted from Early Jurassic to Mid-Cretaceous times. It was by far the most significant of the orogenic events to affect the area and consisted of extensive plutonism, polyphase folding, faulting and regional metamorphism (Monger and Price, 1979; Okulitch, 1979).

This was followed by an intense regional Tertiary thermal event that took place about 50 m.y. ago and is associated with the Eocene plutonic (Coryell intrusives) and volcanic rocks found in the area (Ross, 1974; Medford, 1975).

In addition to these three major orogenic periods, fault movement and gentle crustal warping associated with extrusion of Eocene flows and possibly due to post-orogenic crustal uplift, erosion and cooling has taken place (Okulitch, 1979).

CHAPTER III
WHITEROCKS MOUNTAIN STOCK

Introduction

The Whiterocks Mountain stock has been until very recently a poorly documented intrusive complex. Straddling the southern boundary of the Vernon map sheet, it was mapped by Jones (1959) as part of the Late Mesozoic, calc-alkaline Coast Batholith Complex. These include quartz-monzonites, granodiorites and granites and locally minor syenites in the area of Whiterocks Mountain. The Kettle River, west half map sheet contains the southern half of the stock and was first mapped by Cairnes (1940) and then later by Little (1961). Cairnes (1940), recognized the alkalic character of the rocks and mapped them as Jurassic or Later, syenites and alkali-rich granitic rocks. Little (1961) considered the plutonic rocks to be much younger in age and mapped them as part of the Oligocene, Coryell intrusive complex. These are alkaline intrusions characterized by coarse to medium grained, inequigranular, reddish to pale buff syenites with some granites, monzonites and shonkinites (Little, 1960, p. 90).

Okulitch (1979), has recently produced an updated map which covers areas mapped by Cairnes (1940), Jones (1959) and Little (1961) and includes all of the Whiterocks Mountain stock. On the basis of similarity in lithology, Okulitch (1979) has correlated the stock with Coryell intrusives of Eocene to Paleocene age that occur in the Okanagan Plutonic and Metamorphic Complex to the east.

Recent mapping by Osatenko (1978 & 1979) shows the Whiterocks Mountain stock consists of two distinct suites of rocks. The one suite is a calc-alkalic assemblage that is characterized by the presence of quartz and

brown biotite. It forms a north-northwesterly trending plug (Figure 2) that includes granodiorite and quartz porphyry with minor feldspar porphyry, alaskite and aplite dykes.

The second and apparently older of the two intrusive complexex making up the Whiterocks Mountain stock is a pyroxenite to leucocratic quartz-monzonite assemblage of alkalic rocks that are dominantly quartz-deficient.

The contact between the two complexes is generally obscured by overburden or finely laminated metasediments, however cross-cutting porphyritic leucocratic quartz diorite dykes of the calc-alkalic complex indicate these rocks are younger.

Alkalic Complex

Geological mapping of the Whiterocks Mountain alkalic complex has delineated four distinct intrusive units that include mafic syenite-monzonite, alkalic pyroxenite, porphyritic monzonite and leucocratic quartz monzonite.

Methodology

Rock types of the alkalic complex were petrographically studied with the use of slabbed specimens etched in nitric acid (HNO_3) and stained with sodium cobaltinitrite $[\text{Na}_3\text{Co}(\text{NO}_2)_6]$. The stained slabs were then point counted to quantitatively determine the proportion of felsic and mafic plus-opaque mineral constituents. Thin sections from the same rock specimens were used to identify the various felsic and mafic minerals (all coloured minerals including epidote). Modes are listed (Appendices A and B) and results plotted on the quartz-plagioclase-K-feldspar (QPK) diagram

FIGURE 2
SEMI DETAILED GEOLOGICAL MAP OF THE WHITEROCKS
MOUNTAIN STOCK

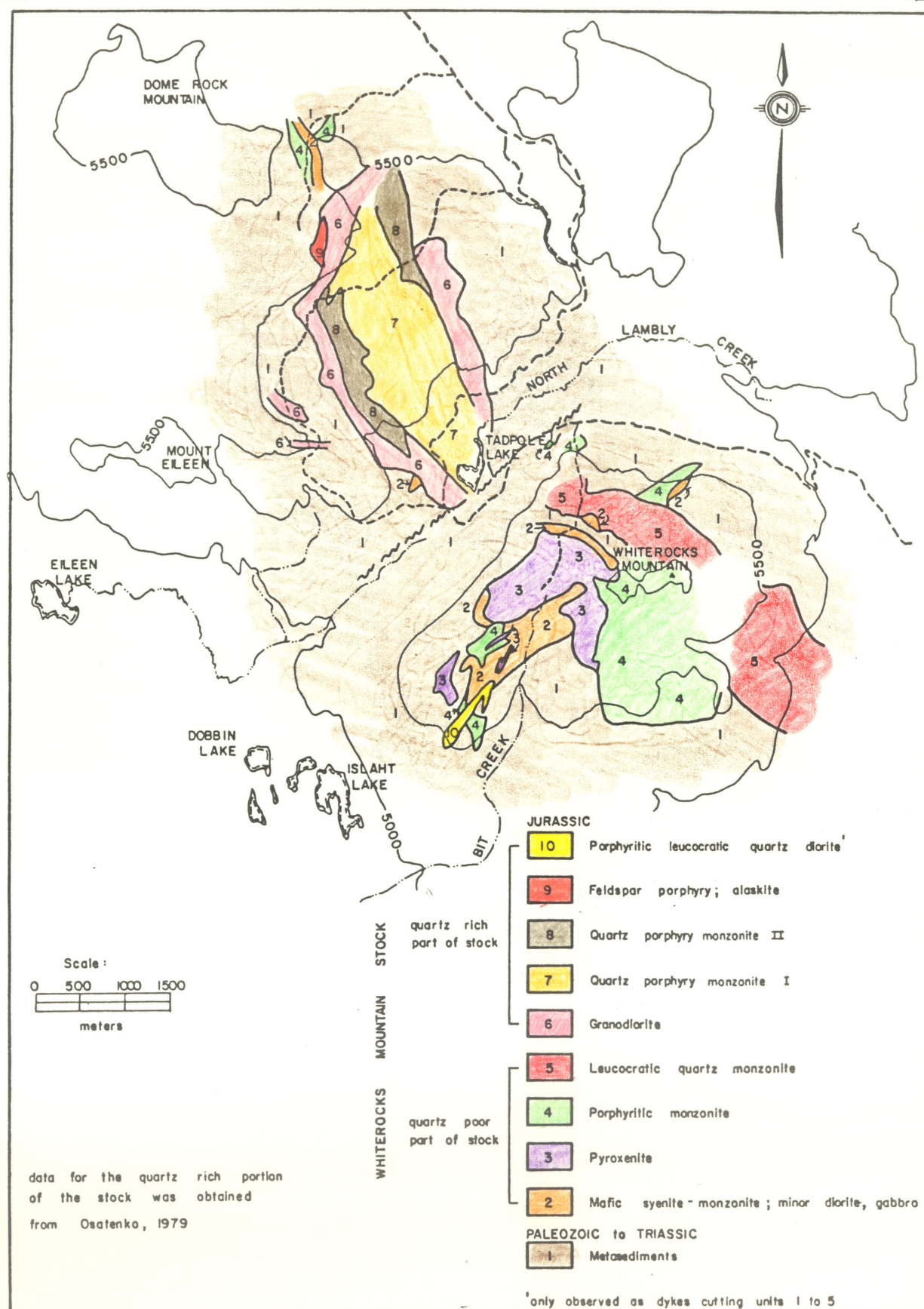


(Figure 3). Since most of the rocks have a relatively high proportion of mafic minerals and low proportions of quartz and feldspathoids, modes were also plotted on the mafics-plagioclase-K-feldspar (MPK) ternary diagram (Figure 4). A third ternary diagram (Figure 5) using biotite-pyroxene-amphibole (BPA) was used to compare the mafic rich rock types.

Intrusive Relationships

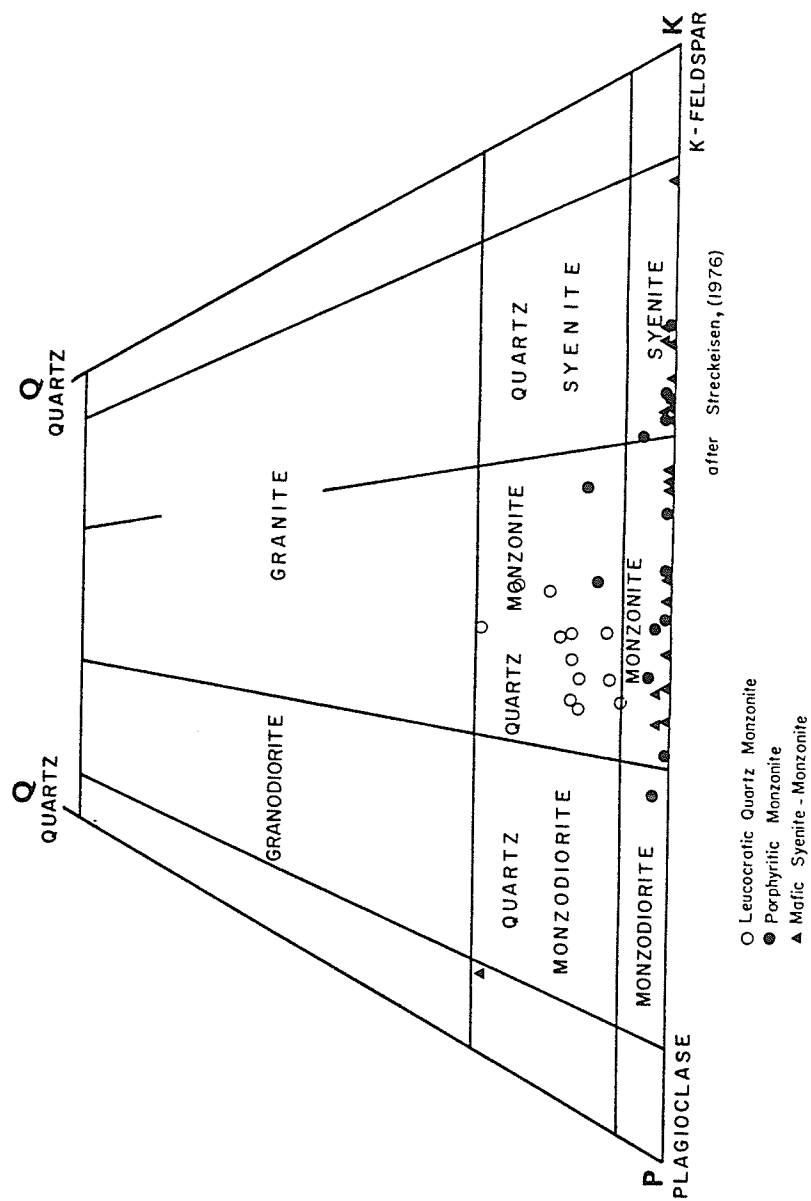
An actual contact between the quartz-poor and quartz-rich complexes of the Whiterocks Mountain stock has not yet been observed, however cross-cutting relationships between various phases of the quartz-deficient, alkalic rocks have been documented.

Based on these cross-cutting relationships (Figure 6) the oldest alkalic unit is the mafic syenite-monzonite. It tends to form sharp contacts with the porphyritic monzonite and leucocratic quartz monzonite but varies from sharp to highly irregular, gneissic looking contacts with the pyroxenite. Stringers and dykes of pyroxenite intruding the mafic syenite-monzonite are common. Also fracturing and localized hydrothermal alteration and sparse sulphide mineralization can be found associated with the pyroxenite-mafic syenite-monzonite contacts. Rare (less than 1 cm) diorite xenoliths and very rare pyroxenite xenoliths have been found in the mafic syenite-monzonite phase.

The pyroxenite is the second oldest unit based on cross-cutting relationships, despite the presence of a pyroxenite xenolith in mafic syenite-monzonite rocks. In addition to the small pyroxenite stringers and dykes found cutting the mafic syenite-monzonite, angular xenoliths of the mafic syenite-monzonite are common along intrusive contacts within the pyroxenite.

FIGURE 3

CLASSIFICATION OF FELDSPAR - RICH ROCKS ON THE BASIS OF MODAL
PLAGIOCLASE, K-FELDSPAR AND QUARTZ FROM THE QUARTZ - POOR
PORTION OF THE WHITEROCKS MOUNTAIN STOCK



NOTE: data from appendices 'A' and 'B'

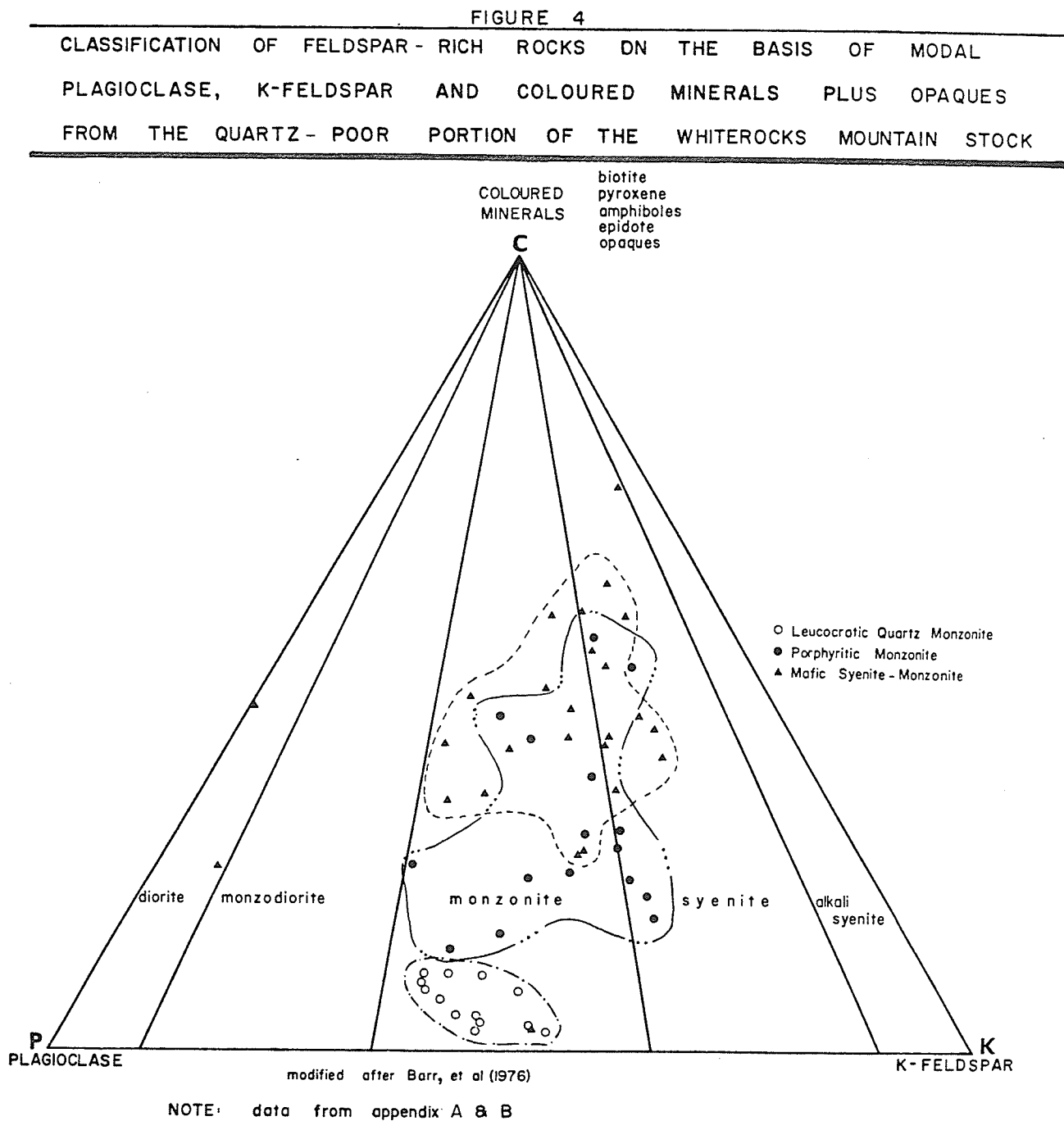


FIGURE 5
A COMPARISON OF THE MAFIC - RICH ROCKS FROM THE QUARTZ - POOR PORTION OF THE WHITEROCKS MOUNTAIN STOCK ON THE BASIS OF MODAL PYROXENE, AMPHIBOLE AND BIOTITE

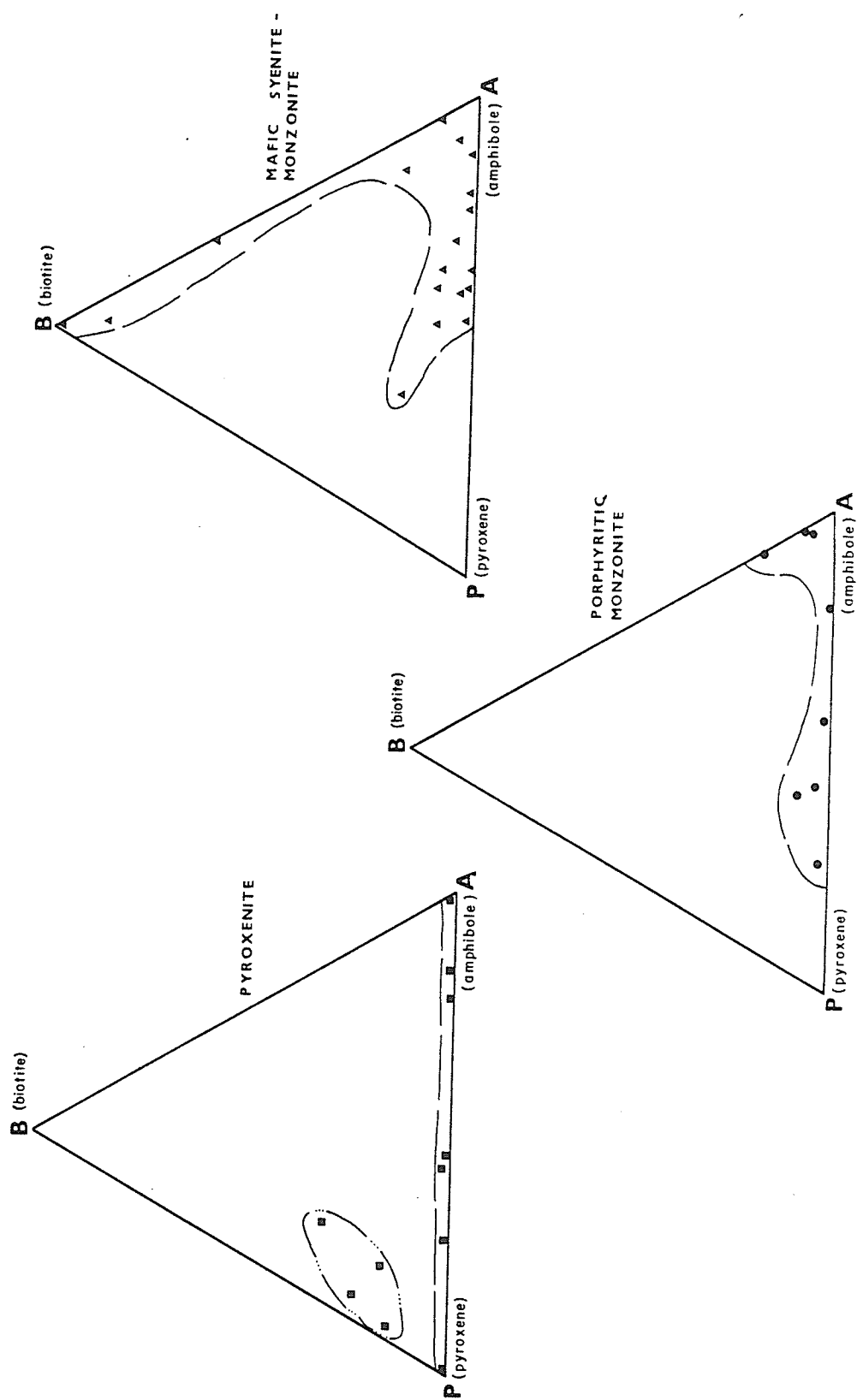
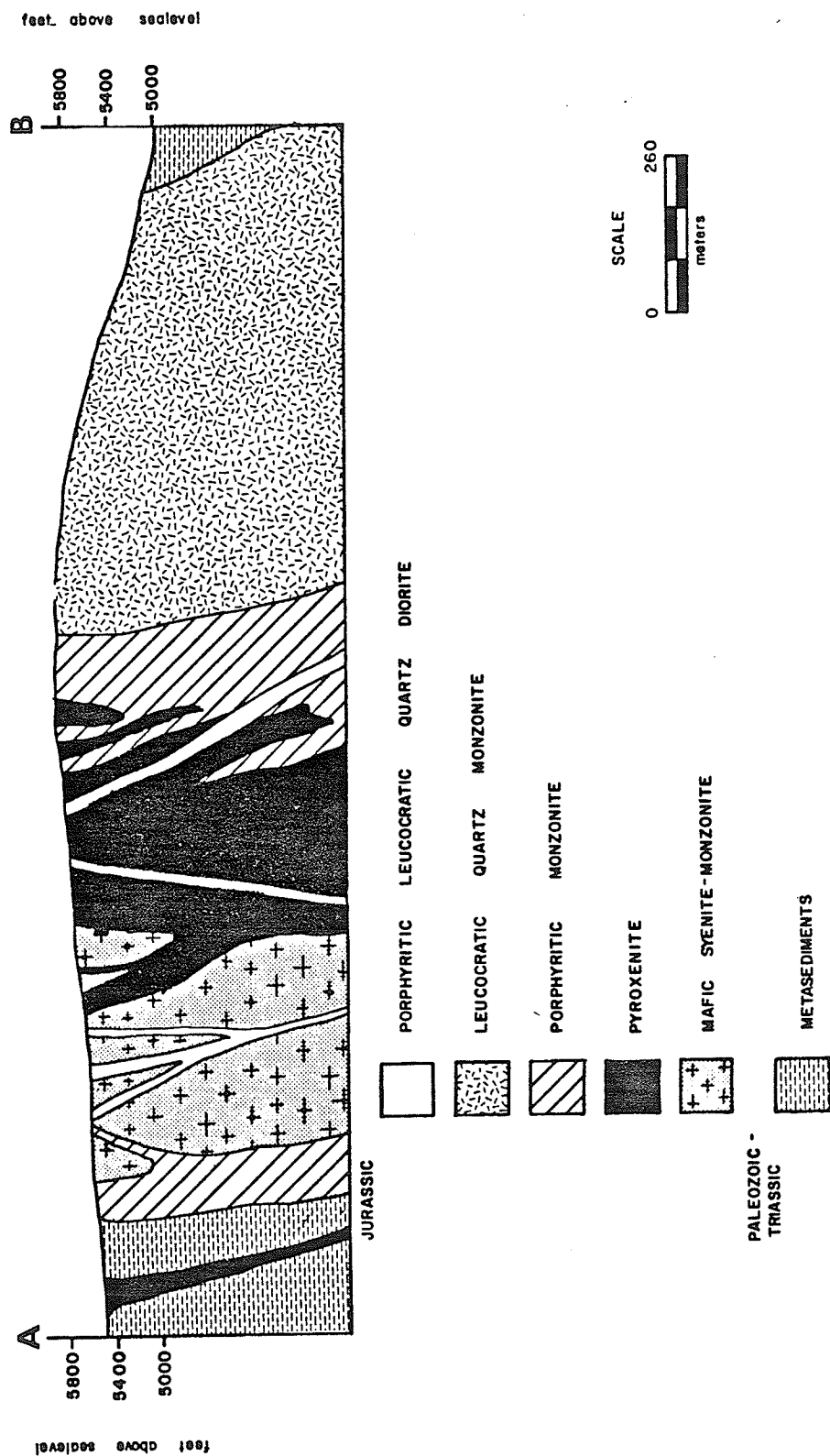


FIGURE 6
SCHEMATIC SECTION THROUGH THE ALKALIC PORTION OF THE WHITE-
ROCK MOUNTAIN STOCK SHOWING THE VARIOUS INTRUSIVE RELATIONSHIPS
refer to figure 7 for section location



Typically the contact between the pyroxenite and porphyritic monzonite is "gneissic" in appearance, especially where larger bodies of the two rock types are in contact with each other as along the eastern side of the main pyroxenite body. Here the monzonite and pyroxenite form a 5-80 meter wide hybrid zone (Figure 7). Away from the hybrid zone and more towards the central and western parts of the alkalic complex, dykes of porphyritic monzonite cut the pyroxenite, usually with sharp intrusive contacts and often containing xenoliths of pyroxenite. Where the dykes contain a large number of these angular pyroxenite xenoliths the rock resembles an igneous breccia with a porphyritic monzonite matrix. Throughout the alkalic complex a number of porphyritic monzonite composite dykes can be found, usually with mafic-rich borders (ferrohastingsite) and leucocratic cores (plagioclase and K-spar), suggesting there was more than one episode of porphyritic monzonite magma injection (Figure 8).

Leucocratic quartz monzonite is probably the youngest alkalic intrusive phase although it has only been found crosscutting pyroxenite and mafic syenite-monzonite. Along the southeastern part of the stock, rounded xenoliths of pyroxenite and metasediments have been found in the leucocratic quartz monzonite.

In addition to the alkalic units, numerous porphyritic, leucocratic quartz diorite to locally porphyritic granodiorite and quartz monzonite dykes cut all phases of the alkalic complex. The contacts between these dykes and the alkalic rocks are sharp, though quartz stringers associated with the dykes often cut across the contact and intrude the alkalic rocks. In the N.W. quadrant of the area mapped (see Figure 7), vein, stringer and fracture-controlled quartz cut all phases of the alkalic complex. The quartz appears related to the dykes, which seem to be more common in this



Figure 8. A composite dyke with a mafic rich, hornblendite border and a mafic poor, porphyritic monzonite core. The porphyritic monzonite shows no variation in grain size while the hornblendite becomes coarser towards the centre of the dyke. Sample location 23, Figure 7.

part of the project area (this area is closest to the calc-alkalic portion of the Whiterocks Mountain stock).

Pre-dating the quartz-veining but cutting both the alkalalic and calc-alkaline rocks of the stock are thin, pink aplite dykes.

Mafic dykes which cut the alkalalic rocks on the west side of the project area are likely related to Tertiary volcanism and thus represent the youngest plutonic rocks cutting the stock.

Although the shape of the alkalalic complex is highly irregular, and appears to be elongated in a north-easterly, south-westerly direction, the complex does display a definite zonation from an ultramafic core to a fairly leucocratic periphery. This zonation can be directly related to the sequence of intrusive events just described.

Rock Description

A. Mafic Syenite-Monzonite (Unit 2, Figure 7)

The mafic syenite-monzonite is a weakly to moderately altered, medium grained, equigranular, hypidiomorphic granular rock. Poor to locally strongly developed mineral foliation exists and is likely the result of regional metamorphism.

Characteristically the rock is high in mafic minerals (30-50%; Figure 4 and Appendix A and B) and in hand specimen resembles a medium grained gabbro to mafic diorite. Both quartz and feldspathoids are absent. Euhedral crystals of aegirine-augite are present in all but the most altered rocks. They form short, stubby, light green crystals, the pleochroism of which varies from very weak to moderately strong with deep green to bright green parallel to α , yellowish green parallel to β and brownish green parallel to γ . Size averages from 0.5 mm to 2.0 mm with some crystals reaching 3 mm to 4 mm.

The type (plagioclase or K-feldspar) and percentage of feldspar in the mafic syenite-monzonite varies considerably. This is particularly evident in the M.P.K. ternary diagram (Figure 4) where the greatest number of samples studied plot over a wide area in both the syenite and monzonite fields. Although it can't be shown on the map, many of the samples that are richer in mafics and K-spar and plot in the syenite field of Figure 4 tend to be finer grained than those rocks that contain fewer mafics and K-spar and plot predominantly in the monzonite field.

Plagioclase crystals vary from euhedral to subhedral. They average 0.3 mm to 0.6 mm in length and comprise 20% to 50% of the mafic syenite-monzonite phase. Crystal contacts are often irregular and partly recrystallized. Rare plagioclase megacrysts, 1 cm to 2 cm long can be found, usually close to a contact with pyroxenite.

K-feldspar varies from 5% to 40%. It is almost always interstitial, usually in the form of orthoclase. In some specimens faint microcline twinning is present although it is typically uncommon for the unit. Rare, weakly perthitic K-feldspar crystals reaching 2 mm to 4 mm in length and containing plagioclase crystals less than 0.1 mm in length are present.

Alteration does exist in the mafic syenite-monzonite rocks and is best illustrated on the biotite-pyroxene-amphibole, ternary diagram (Figure 5). The large scatter of mafic minerals, particularly biotite is interpreted to be the result of late magmatic processes combined with metamorphic alteration, which may be partly due to regional metamorphism but is most likely due to the effects of subsequent intrusives.

During alteration, aegirine-augite is replaced by darker green ferrohastingsite and less commonly by blue-green hornblende and green biotite. The ferrohastingsite occurs as irregular grains, usually rimming or poikilitically enclosing pyroxene and biotite and sometimes small plagioclase

crystals. Biotite is present as both a product of late magmatic crystallization, rimming pyroxenes and filling interstices between pyroxene crystals, as well as an alteration mineral associated with ferrohastingsite. Hornblende, chlorite and epidote are very late alteration minerals. Hornblende replaces ferrohastingsite and some pyroxene. Chlorite is present in only minor amounts, usually replacing biotite although some chlorite forms at the expense of pyroxene. Epidote occurs as part of the late alteration assemblage replacing pyroxene, ferrohastingsite and plagioclase. Plagioclase is also replaced by a fine grained assemblage of undetermined clay minerals and sericite. The anorthite molecule content of plagioclase shows considerable variation, ranging from a low An 8 in highly altered and recrystallized specimens to a high An 38 in relatively fresh, unaltered rock.

B. Alkalic Pyroxenites (Unit 3, Figure 7)

The alkalic pyroxenite rock unit is very complex and consists of two major phases. One is a relatively homogeneous biotite pyroxenite and the other is a weakly mineralized amphibole pyroxenite. The amphibole pyroxenite occurs as dykes cross-cutting biotite pyroxenite and as a pervasive, late magmatic or deuteric replacement of biotite pyroxenite. In addition, late pyroxenite stage, hornblendite dykes which may be of similar age to the amphibole pyroxenite cross-cut biotite pyroxenite and mafic syenite-monzonite.

Variation between biotite and amphibole pyroxenites is clearly shown on the biotite-pyroxene-amphibole ternary diagram (Figure 5). Biotite pyroxenites plot in a small zone showing an abundance of pyroxene, some variability in the biotite content and limited variation in total amphiboles. Any amphibole increase that does occur is accompanied by a small increase in epidote and a decrease in pyroxene content (Appendix A).

Amphibole rich pyroxenite is characterized by an almost complete absence of biotite and extreme variation in the pyroxene and amphibole content. Epidote content is up considerably in the amphibole pyroxenites.

(i) biotite pyroxenite (Unit 3a, Figure 7)

The biotite pyroxenite is medium to fine grained, equigranular and shows hypidiomorphic-granular texture. It weathers black to greenish black. In its least altered state, it consistently contains over 60% of euhedral aegirine-augite, more than 10% of anhedral to subhedral biotite and less than 10% of anhedral amphiboles. Accessory minerals including apatite, sphene and some carbonate make up the remainder of the rock.

The stubby, euhedral aegirine-augite crystals range in size from 1.0 mm to 1.5 mm long. Pleochroism is weak to moderate with colours changing from deep green to bright green parallel to α , yellowish green parallel to β and brownish green parallel to γ . Minor zoning is present, with light green crystals lined by darker green (possibly more aegirine-rich) rims.

Interstitial, dark green biotite is present as anhedral to subhedral grains among pyroxene crystals. Pleochroism is moderate to strong, ranging from brownish green parallel to α to dark green parallel to β and γ . Much of the biotite is in the form of "sagenite", with tiny rutile crystals forming triangular patterns within the grains (Figure 9). A small amount of biotite appears to be replacing pyroxene crystals as indicated by the corroded edges. Also within the biotite pyroxenite phase, coarse secondary biotite is developed as clots within the groundmass or as filling along fracture. At least two occurrences of hydrothermal biotite breccia (Figure 10) are known, indicating that some hydrothermal activity has taken place in the alkalic complex.

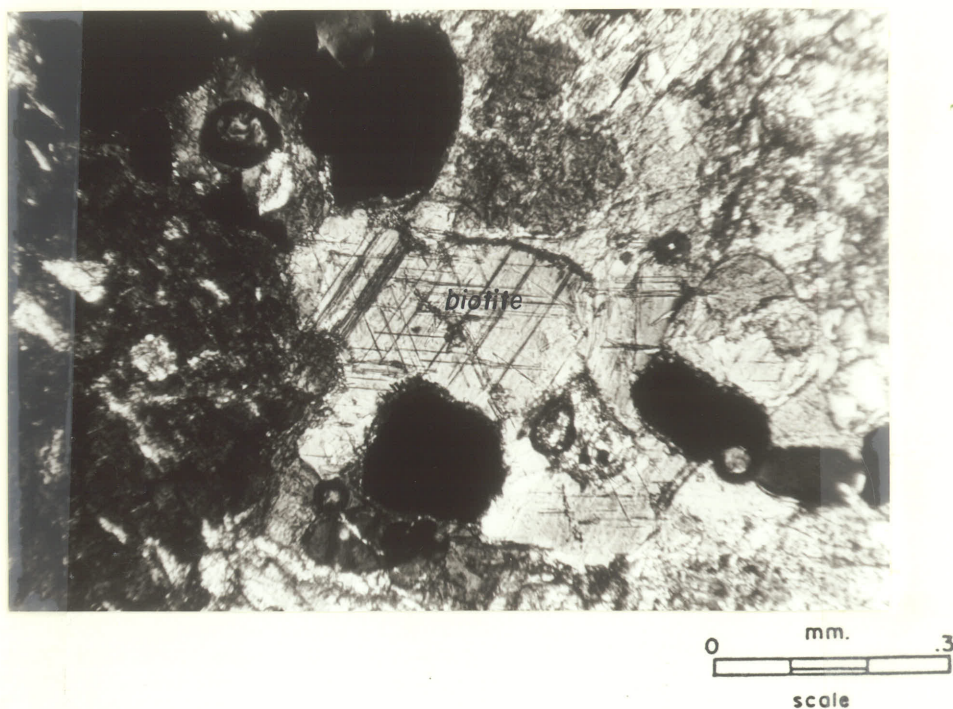


Figure 9. Biotite pyroxenite with late stage sagenitic biotite. Needlelike rutile crystals form triangular lattices in the biotite, intersecting at angles of 60 degrees. Microphotograph taken under polarized light. Sample location 39, Figure 7.

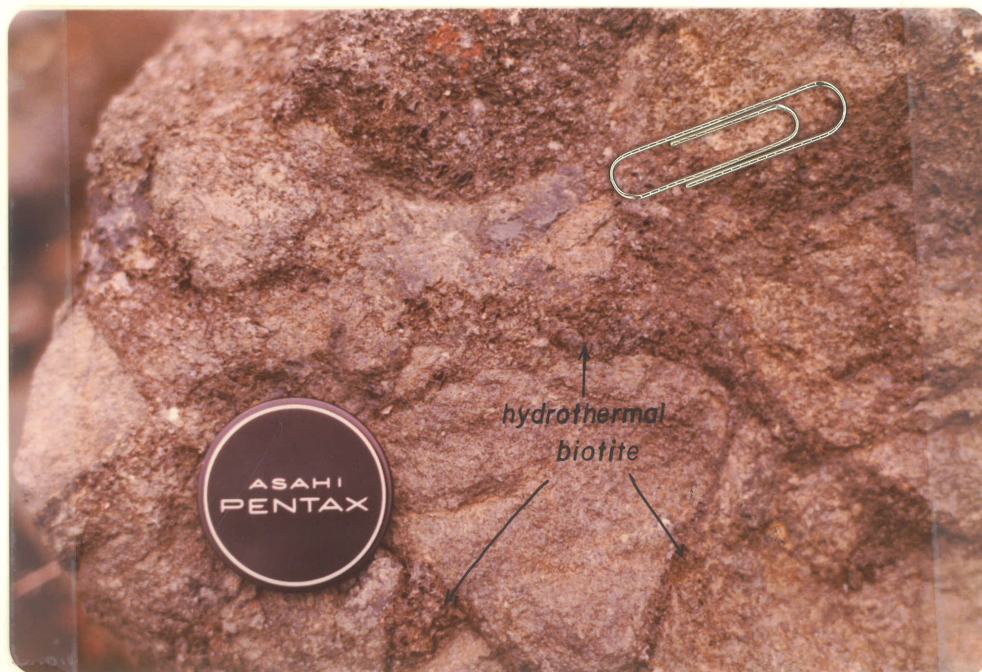


Figure 10. Brecciated biotite pyroxenite, with coarse hydrothermal biotite surrounding partly rounded biotite pyroxenite fragments. Sample location 196, Figure 7.

Where present in the biotite pyroxenite, amphibole consists of two varieties. Ferrohastingsite, the most common of the two, is strongly pleochroic, ranging from yellowish green parallel to α , brownish green parallel to β and dark green parallel to γ . Typically a late stage mineral, it rims and replaces aegirine-augite. Hornblende, the second and less common of the two amphiboles is green to bluish green in colour and is present as fine, acicular crystals replacing ferrohastingsite. Both amphiboles are most common along fractures cutting the biotite pyroxenite.

Although minor amounts of epidote are found with the amphiboles, it usually occurs as a fracture filling or alteration associated with a fracture.

Accessory euhedral apatite and subhedral to anhedral sphene are found throughout the groundmass. Apatite is also present as inclusions in pyroxene and biotite. Up to 12% magnetite occurs interstitially between aegirine-augite crystals.

Trace amounts of interstitial plagioclase and K-feldspar are found along fractures or within zones of amphibole crystallization. Similar amounts of intergranular carbonate (calcite) may be found with the feldspars.

(ii) amphibole pyroxenite (Unit 3b, Figure 7)

The amphibole pyroxenite varies in appearance from a coarse, "spotted", porphyritic pyroxenite with 30%, 6 mm to 8 mm long amphibole phenocrysts to a very fine grained, light green, massive, "volcanic" appearing rock with minor amphibole phenocrysts.

Throughout the alkalic complex, the amphibole pyroxenite exists as dykes cutting biotite pyroxenite or as a weak to strong pervasive alteration

(replacement) of the biotite pyroxenite. The fluids responsible for forming these dykes and alteration are late magmatic fluids of the pyroxenite phase and not those belonging to some later hydrothermal event. The evidence used to support this hypothesis is the lack of appreciable alteration or replacement of similar composition in adjacent younger intrusive rocks and the apparent crystallization, at least in part, of the biotite pyroxenite prior to the appearance of the amphibole pyroxenite fluids.

In the amphibole pyroxenite aegirine-augite makes up less than 50% of the rock with amphibole averaging more than 30% and biotite less than 2%. Accessory minerals make up the remainder of the rock. Uncommon zones of recrystallized pyroxenite do occur. In these instances the pyroxene content of the rock increases dramatically while the amphibole content is sharply reduced.

The aegirine-augite pyroxenes generally occur as either stubby, green, euhedral crystals varying in size from 0.5 mm to 1.5 mm or as tiny recrystallized anhedral grains with sutured boundaries in a mosaic pattern. Some recrystallized pyroxene form 1 mm grains poikilitically enclosing very small, subhedral pyroxenes. Zoning in the pyroxenes is common, though the more recrystallized specimens lack any internal features. Instead they are light green in colour, moderate to strongly pleochroic, subhedral featureless grains with pleochroism ranging from dark green parallel to α , light green parallel to β and light brown parallel to γ .

Ferrohastingsite and hornblende are the two varieties of amphibole in the amphibole pyroxenite. Dark green ferrohastingsite is most commonly found as anhedral to subhedral grains up to 1 cm across that poikilitically enclose and replace pyroxene (Figures 11 and 12). Hornblende occurs as

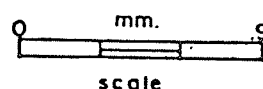
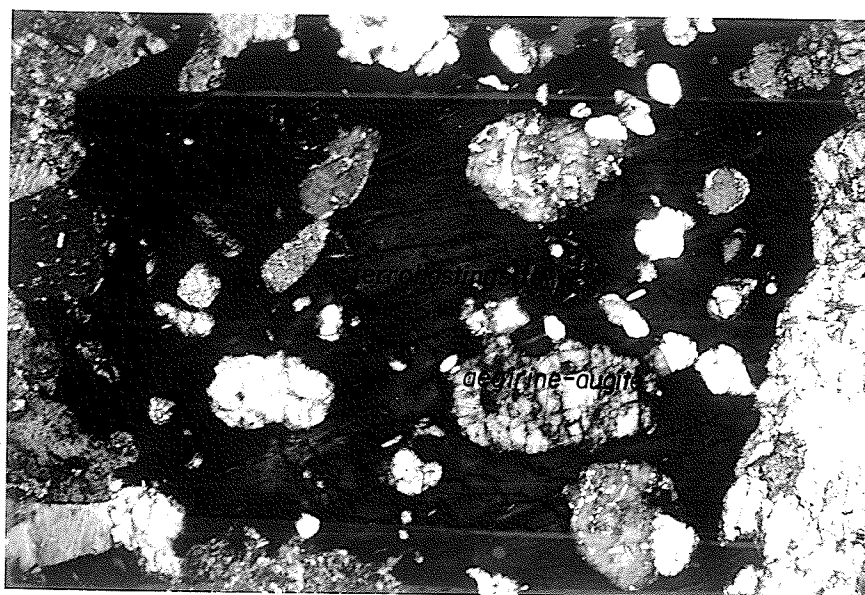


Figure 11. Amphibole pyroxenite with poikilitic ferrohastingsite (dark grey) enclosing euhedral to subhedral aegirine-augite. Microphotographs taken under polarized light. Sample location 128a, Figure 7.

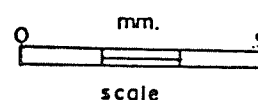
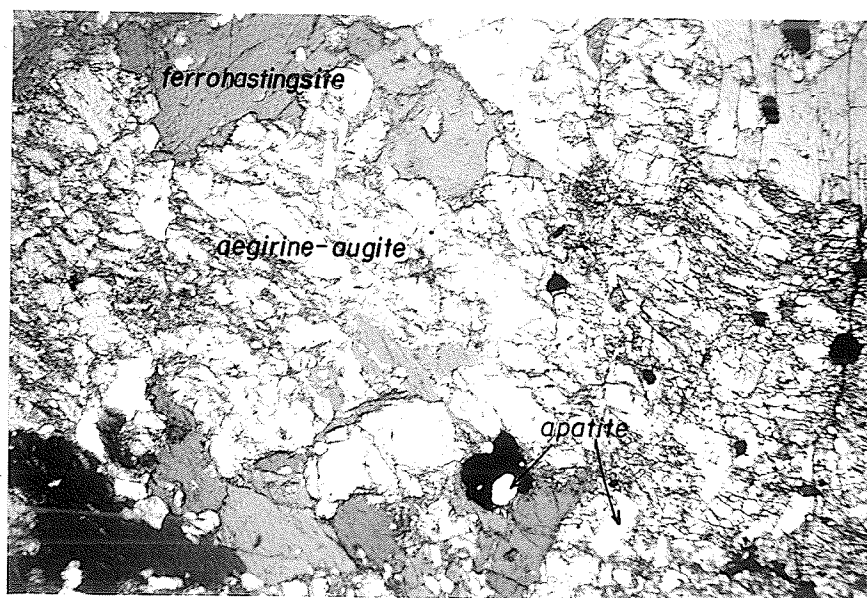


Figure 12. Amphibole pyroxenite with ferrohastingsite (dark grey) replacing aegirine-augite (light grey). Opaques are confined to interstices and as inclusions within the ferrohastingsite. Note the euhedral apatite crystals (very light grey) found as inclusions in the aegirine-augite, ferrohastingsite, and opaques. Microphotograph taken under plain light. Sample location 128a, Figure 7.

both blue green, acicular crystals less than 1 mm in length and as green, anhedral grains. It is most commonly found filling fractures and replacing ferrohastingsite although minor replacement of pyroxene does exist (Figure 13).

Biotite is rare in the amphibole pyroxenite, particularly in the more recrystallized portions. Some relic, green biotite is present as anhedral grains enclosed in amphibole. Minor, coarse to fine grained (up to 1 cm) green hydrothermal biotite similar to the hydrothermal biotite found in the biotite pyroxenite occurs along hairline fractures or as clots in highly altered, fine grained pyroxenite.

Epidote is closely associated with the amphibole pyroxenite, where it is found as a late alteration mineral replacing pyroxene and ferrohastingsite. In intensively altered portions, epidote occurs throughout the groundmass, giving the rock a light green appearance. In late stage dykes and veins, epidote commonly makes up the majority of the groundmass, producing a light green rock with dark green amphibole phenocrysts. Trace amounts of calcite occur with hornblende and epidote along fractures and in the groundmass.

Accessory minerals include euhedral apatite, subhedral sphene and up to 15% disseminated and fracture controlled magnetite. The apatite is present as small, euhedral inclusions within pyroxene and amphibole crystals or as crystal aggregates or concentrations in pyroxene-rich, recrystallized pyroxenite. The magnetite occurs as disseminated grains in poikilitic ferrohastingsite grains that are replacing aegirine-augite.

Plagioclase and K-feldspar occur as minor interstitial minerals in the more altered (magmatically) pyroxenites.

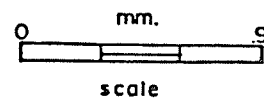
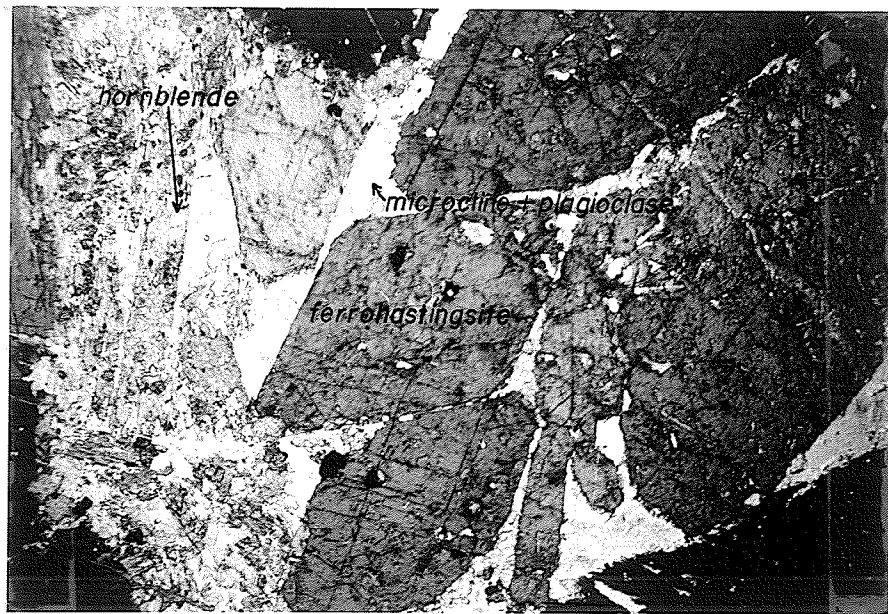


Figure 13. Hornblendite dyke with euhedral ferrohastingsite crystals (dark grey) surrounded by microcline-plagioclase groundmass. The prismatic mineral to the far left (medium grey) is late stage hornblende which replaces the ferrohastingsite. Microphotograph taken under plain light. Sample location 23, Figure 7.

(iii) hornblendite dykes (part of Unit 3b, Figure 7)

Late pyroxenite stage hornblendite dykes are found cutting all rocks older than the pyroxenite as well as the biotite and more weakly developed amphibole pyroxenite phases (Figure 14). Texturally and mineralogically the dykes resemble the amphibole pyroxenite, though the feldspar content is much greater in the dykes.

Typically, the dykes consist of 40% to 80% of slender, euhedral, ferrohastingsite phenocrysts averaging 0.5 cm to 1.0 cm in length with coarser pegmatitic zones containing crystals up to 4 cm long. Groundmass is made up of very fine grained blue green hornblende and varying amounts of epidote. Biotite is generally absent, though it may be present in amounts of up to 5%. This biotite may be secondary in origin and not part of the primary dyke material. Microcline and plagioclase are present as interstitial minerals in most dykes and may compose up to 50% of an individual dyke.

C. Porphyritic Monzonite (Unit 4, Figure 7)

The porphyritic monzonite is a medium to coarse grained, highly porphyritic unit with aligned microcline phenocrysts. Averaging 1.5 cm to 2.0 cm in length, these feldspar phenocrysts produce a highly trachytic texture that varies in orientation throughout the unit. At two locations (Unit 4b, Figure 7) the phenocrysts tend to be quite large and reach lengths up to 15 cm (Figure 15). In both instances, aligned mafic minerals separate the porphyritic monzonite into units 3 cm to 15 cm wide that are characterized by microcline crystals of similar shape and size (Figure 16). Individual units vary from those with predominantly 2 cm long microcline crystals to those with 12 cm to 15 cm long microcline crystals. No gradation in size exists between successive units.



Figure 14. Late stage hornblendite dykes cutting medium grained biotite pyroxenite. Dark mineral in dyke is ferro-augite set in a feldspar groundmass. Green colour in dyke groundmass is due to epidote. Sample location 196, Figure 7.



Figure 15. "Blocky" microcline phenocrysts set in a medium grained monzonite groundmass. Photo taken of unit 4b (porphyritic monzonite with microcline phenocrysts greater than 2 cm), near sample location 139 in Figure 7.



Figure 16. Porphyritic monzonite with aligned microcline phenocrysts separated into different units by thin bands of mafic rich monzonite. Individual units are characterized by phenocrysts of a certain size, with no apparent systematic change existing between the successive units. The texture resembles magmatic layering in a tilted sequence of igneous rocks. Photo taken near sample location 137 in Figure 7.

Compositionally, the entire porphyritic monzonite unit is intermediate, containing on average 20%-25% mafic minerals and rare free quartz (the quartz is at least in part related to quartz veining that exists in the N.W. quadrant of the alkalic complex).

The mafic minerals are relict, 0.2 mm to 1.0 mm large, euhedral aegirine-augite crystals that are largely replaced by subhedral to anhedral ferrohastingsite and hornblende. Biotite is found in minor amounts as green, possibly relict, anhedral grains that are poikilitically enclosed by ferrohastingsite grains. Chlorite is present in small amounts as a late alteration preferentially replacing biotite, though some replacement of ferrohastingsite takes place as indicated by chlorite pseudomorphs after ferrohastingsite. Similarly, hornblende also occurs as a late alteration mineral replacing ferrohastingsite.

Epidote exhibits considerable variation within the porphyritic monzonite, ranging from just over 5% to about 18% of the rock. It is characteristically a late alteration mineral, replacing both pyroxenes and amphiboles and commonly occurring as filling along fractures.

Plagioclase feldspars make up an average of 20% to 25% of the porphyritic monzonite. They are typically euhedral to subhedral crystals, 0.4 mm to 1.0 mm in length. Rare crystals of up to 1.5 cm in length have been found. The average An molecule content for the plagioclase is 28 %. Minor mineral replacement by sericite and unidentified clay minerals is likely due to some localized hydrothermal alteration and weathering.

Potassium feldspar occurs as both anhedral interstitial microcline and perthite grains and as euhedral appearing phenocrysts that range in size from 0.5 cm to 15.0 cm long. Microscopically the phenocrysts are predominantly subhedral microcline perthite megacrysts with irregularly

shaped boundaries. They display discontinuous zoning by enclosed plagioclase crystal inclusions that are less than 3 mm long and are aligned parallel to the phenocrysts' edges. Rare, similarly oriented pyroxene crystals are found as well.

The shape and texture of the microcline perthite phenocrysts and their relationship to other minerals in the rock suggests they crystallized after pyroxene and at least some of the plagioclase. Crystal growth appears to have taken place around a plagioclase crystal that acted as a nucleus. As the microcline perthite crystals grew, small plagioclase and rarely pyroxene crystals were incorporated into the crystal by adhering themselves parallel to the edge of the crystal as it existed at that time. Continued growth allowed for continual incorporation of small crystal inclusions that give the overall appearance of concentric zoning. Similar textures and phenomenon have been discussed by Hibbard (1965) who also noted a systematic variation in the An molecule content of the enclosed plagioclase crystals. He suggests that crystals of plagioclase and alkali feldspar may be suspended in a mobile belt, and through the process of turbulence related to magmatic flow, the growing crystals were able to come into contact with one another and produce the resulting zoned microcline perthites.

Factors which suggest that such a process took place within the porphyritic monzonite phase include the alignment of the microcline crystals, which varies in orientation from place to place (Figure 7) and is thus likely the result of magmatic flow. Also, the occurrence of aligned inclusions within microcline phenocrysts (which have lengths < 15 cm and irregular contacts) suggests both an abundance of mobile melt and a stable enough environment to allow crystal growth.

Examination of the 201 reflection (Smith 1974, p. 283) from X-ray powder diffractograms obtained for three K-feldspar phenocrysts (plus inclusions) from the porphyritic monzonite indicates the feldspars vary from $\text{Or}_{71}\text{Ab}_{29}$ to $\text{Or}_{54}\text{Ab}_{46}$ in composition. Triclinicity (Smith 1974, p. 287) ranges from 0.89 to 0.53 (Appendix C).

D. Hybrid Zone (see Figure 7)

Along the contact between the main body of pyroxenite and the porphyritic monzonite is a zone up to 80 meters wide that grades from a plutonic-looking rock into a foliated, gneissic-looking rock. Compositionally the foliated rock varies from a coarse to medium grained monzonite through monzodiorite and amphibole gabbro to hornblendite.

The mineralogy and hence overall appearance of the rock is very similar to the hornblendite dykes though locally the hybrid zone is considerably more leucocratic than the dykes. The main mafic minerals are ferrohastingsite and epidote. Varying in content throughout, these two minerals combine to give much of the rock a "streaky" black to green appearance. Plagioclase tends to be the dominant feldspar occurring as euhedral to subhedral crystals up to 5 mm long. Rare plagioclase crystals up to 2 cm long have been observed. K-feldspar is most common in the epidote-poor zones where it is interstitial. Weak microcline twinning is found throughout the K-spars.

The presence of a highly foliated zone between the pyroxenite and porphyritic monzonite suggests a reaction between the two phases has taken place. Previously described hornblendite dykes which texturally and compositionally resemble the hybrid zone and which cut the pyroxenite are traceable into the hybrid zone but do not pass through it. This indicates the dykes and the hybrid zone are similar in age and possibly related.

Since the hybrid zone is spatially restricted to the contact area between a large body of porphyritic monzonite and a similarly large body of pyroxenite, it seems likely that the zone resulted from the interaction of fluids from at least a partially liquid porphyritic monzonite with a solid pyroxenite. The hornblendite dykes which are seen cutting the mafic syenite-monzonite and pyroxenite probably formed from some of the same fluids and likely give a good representation of the overall composition of the fluids which helped produce the hybrid zone. However, many of the dykes do exhibit compositional and textural differences which may be the result of contamination as the liquids intruded the pyroxenite and older rocks or it may be that there were several "magmatic" pulses with each pulse producing a number of small dykes of slightly different composition.

E. Leucocratic Quartz Monzonite (Unit 5, Figure 7)

The leucocratic quartz monzonite is a coarse grained, equigranular to weakly porphyritic, massive to moderately foliated, buff white coloured unit. It is the only unit in the alkalic complex to contain primary quartz and aside from differences in the quartz content, the rocks have limited compositional variation and plot in relatively small clusters on both the quartz-plagioclase-K-feldspar ternary diagram (Figure 3) and the mafics-plagioclase-K-feldspar ternary diagram (Figure 4).

Mineralogically the rock is characterized by equal amounts of plagioclase and K-feldspar, less than 10% mafic minerals and an average of 10% quartz (Appendix A & B).

Mafic minerals include euhedral to anhedral, green ferrohastingsite which typically constitutes less than 5% of the leucocratic quartz monzonite and minor amounts of hornblende and epidote which are replacing the ferrohastingsite. Rare, relict aegirine-augites have been found with ferro-

hastingsite and epidote replacing them. Brown to greenish brown biotite is found in minor, local concentrations.

Subhedral to euhedral plagioclase crystals averaging 0.5 mm to 2.5 mm in length and reaching 4 mm in places make up 26% to 50% of the rock. Compositional zoning is well developed and common. Plagioclase alteration is virtually absent with only trace amounts of sericite and clay minerals present along fractures replacing the feldspar. The An molecule content of the plagioclase varies from An 30 to An 12 thus labelling the feldspars oligoclase.

Potassium feldspar is present as both microcline and microcline perthite minerals. The well developed microcline occurs both interstitially and as 2.0 mm to 5.0 mm long, subhedral laths with irregular edges (as in the porphyritic monzonite). Microcline perthite forms subhedral to anhedral, 0.5 mm to 2.0 mm long grains. Inclusions of plagioclase epidote and hornblende are common.

Quartz is common as fracture-filling small veins, and as interstitial grains in the groundmass. Though the unit as a whole averages about 10% quartz, two subtle sub-units are apparent. The first sub-unit 5A, Figure 7, consists of quartz contents from 5.3% to 10.1%, averaging 8.0%. This portion of the leucocratic quartz monzonite phase corresponds to that along the northern boundary of the Whiterocks Mountain alkalic complex.

The second sub-unit, 5B, contains 8.5% to 19.0% with an average of 13.8% quartz, and corresponds to the leucocratic quartz monzonite along the southeastern portion of the complex. In addition, this sub-unit seems to contain slightly more K-feldspar and less epidote and plagioclase than the sub-unit to the north. However, the textures and remaining mineralogy of the two sub-units are very similar and when modes are plotted on the

ternary diagrams, Figures 3 and 4, the sub-units plot in an unseparable field. Since no contact between the two sub-units was observed, it is impossible to determine if the two sub-units represent entirely different intrusive events with similar compositions or if they are part of one intrusive phase that shows a certain amount of variability.

F. Porphyritic Leucocratic Quartz Diorite (Unit 6, Figure 7)

Fine to medium grained, porphyritic leucocratic quartz diorite dykes cut all phases of the alkalic complex and the metasediments and meta-volcanics. Considerable variation in appearance of the dykes exists among the various localities shown on Figure 7 and in those occurrences where the dykes were too small to include on the map. However some of the common characteristics include weathering to a light grey colour, the presence of blocky plagioclase phenocrysts, a weak though visible foliation and the existence of fine, feathery biotite.

Mafic minerals make up to 10% of the rock, mostly fine, feathery flakes of brown to greenish brown biotite. Local concentrations of 1 mm to 2 mm long hornblende crystals do occur but never in amounts greater than 5%. Green chlorite replacing biotite is common.

Plagioclase is present as zoned 0.1 mm to 2.0 mm phenocrysts and as a major component in the undifferentiated quartz-feldspathic ground-mass. Weak clay and sericite replacement of some plagioclase phenocrysts exists.

Potassium feldspar is found in varying amounts but never exceeds 10% of the dykes. Most commonly it is present as small interstitial grains but has also been found as 1 mm in diameter, blocky, subhedral grains filling voids between euhedral plagioclase crystals.

Quartz occurs interstitially in the groundmass and as fracture filling or small veins, often branching out from the dykes into the host, country rocks. An estimate of average quartz content is 15% to 25%.

Associated with the porphyritic leucocratic quartz diorite dykes is the development of coarse, secondary biotite in the pyroxenites, some biotite replacement of mafics in the mafic syenite-monzonite and sericite development in the porphyritic monzonite. This is particularly evident in areas where the dykes are quite common. Two such localities exist in the pyroxenite unit where a number of porphyritic leucocratic quartz diorite dykes cut the pyroxenite and have produced hydrothermal breccias (Figure 7). In both cases rounded fragments of biotite pyroxenite are enclosed in a matrix of coarse, secondary biotite (see Figure 10). Similarly, mafic minerals in nearby mafic syenite-monzonites have been almost completely replaced by biotite.

These late dykes were associated with an abundance of hydrothermal fluids that has led to intense, localized hydrothermal alteration.

Calc-Alkalic Complex

Though little work has been done on the calc-alkalic portion of the Whiterocks Mountain stock by the author, considerable information has been gathered on these rocks from 1977 to 1980 by M. J. Osatenko and by J. K. Russell of Cominco Ltd. (oral communication and/or from information documented in reports filed on the Tad mineral claims, Vernon Mining Division, B.C.). The results of their work indicate the calc-alkalic rocks form an elliptical, northwest trending body consisting of a core of quartz porphyry monzonite surrounded by a coarser grained quartz porphyry monzonite and an equigranular granodiorite. Contacts are sharp but no age relationships are known between the quartz monzonites and the granodiorite. Cutting these intrusive rocks are fine grained aplite and fel-

site dykes; cutting the dykes and earlier intrusives are three different orientations of quartz-veins. Finally the entire calc-alkalic portion of the Whiterocks Mountain stock was subjected to a NW-SE trending, pervasive fracturing (this pervasive fracturing was not as evident in the alkalic rocks).

Mineralogically the rocks are characterized by K-feldspar, plagioclase, interstitial quartz and quartz phenocrysts and biotite, usually brown in colour. Hydrothermal alteration is locally intense with pervasive sericite development occurring in these zones.

Overall the calc-alkalic rocks belonging to the northern portion of the Whiterocks Mountain stock strongly resemble the porphyritic leucocratic quartz diorite dykes cutting the alkalic complex. Some of the common features of both rock units include the presence of abundant quartz either as crystals or interstitial material, the widespread persistence of quartz veining and fracture filling and the virtual absence of ferrohastingsite and dominance of brown to brownish green biotite as the main mafic mineral.

CHAPTER IV

AMPHIBOLES

Introduction

Common to all phases of the alkalic complex are euhedral to anhedral green amphiboles, that based on colour and extinction angles appear to be ferrohastingsite.

In order to confirm ferrohastingsite cell dimensions, and to see if any systematic changes in composition exist between the amphiboles sampled from different alkalic phases, sixteen specimens were analyzed by means of X-ray powder diffraction.

Results

The results show a wide range in β values, ranging from a high of 106.67° to a low of 104.35° (Table 1). Aside from the first three samples which came from the hybrid zone and have relatively high β angles, the remainder of the samples X-rayed have β angles which are typical of ferrohastingsite (Borley and Frost, 1962). The fact that three of the four analyzed amphiboles from the hybrid zone have the highest β angles determined suggests they are different from the rest of the amphiboles and are probably not ferrohastingsites. According to Borley et al. (1962), the increased size in β angles in amphiboles may be explained by greater Ca content in the crystal structure.

The amphiboles that come from the hornblendite dykes and the amphibole pyroxenite have very similar β angles, though there is a suggestion that the ferrohastingsites derived from the dykes have slightly larger angles. If so, it may be inferred that the dykes have amphiboles that are slightly richer in Ca.

TABLE I

CALCULATED CELL DIMENSIONS FOR AMPHIBOLES FROM THE AMPHIBOLE PYROXENITE, HORNBLENDITE DYKES AND THE PORPHYRITIC MONZONITE - PYROXENITE HYBRID ZONE OF THE WHITEROCKS MOUNTAIN ALKALIC COMPLEX AND A COMPARISON WITH VALUES FOR FERROHASTINGSITE DETERMINED BY BORLEY AND FROST (1962).

	a(Å)	b(Å)	c(Å)	β°
40 (H)	10.081(4)*	18.017(13)	5.435(3)	106.67(.05)
79a (H)	9.988(7)	18.117(2)	5.413(4)	106.13(.05)
37 (H)	9.946(14)	18.093(47)	5.321(22)	105.37(.16)
23a (H)	9.937(7)	18.188(16)	5.310(6)	105.17(.08)
1a (P)	9.948(13)	18.083(48)	5.348(35)	105.15(.17)
165b (M)	9.967(11)	18.209(24)	5.309(12)	105.12(.12)
1e (P)	9.938(13)	18.193(21)	5.302(17)	105.08(.18)
8 (M)	9.938(10)	18.202(26)	5.306(15)	105.05(.10)
165a (M)	9.839(16)	18.174(14)	5.329(11)	105.03(.14)
166 (M)	9.911(14)	18.102(30)	5.297(29)	105.03(.19)
23b (P)	9.961(14)	18.041(13)	5.324(4)	105.02(.08)
40a (H)	9.927(10)	18.192(11)	5.297(8)	104.85(.14)
179 (M)	9.846(2)	18.213(2)	5.286(2)	104.82(.02)
1b (P)	9.892(15)	18.145(13)	5.263(6)	104.80(.08)
123 (M)	9.638(13)	18.250(24)	5.318(5)	104.77(.09)
9 (M)	9.798(14)	18.364(37)	5.276(9)	104.35(.12)
6'	9.882	18.080	5.322	105.32
A.24'	9.926	18.221	5.324	104.88
A.25'	9.923	18.180	5.319	104.15

H- hybrid zone; P- dike phenocryst; M- metacryst

' from G.Borley and M.T. Frost, 1962

* $10.018 \pm .004$ angstroms

Note: sample locations given in Figure 7

The amphiboles coming from rocks having plagioclase (hybrid zone and some hornblendite dykes) tend to have the largest β angles while those that come from feldspar-poor ultramafic phases (amphibole pyroxenite) have the smallest angles. This observation may reflect minor amounts of magmatic differentiation which allows for more free Ca to produce both plagioclase feldspar and Ca rich amphiboles in the slightly younger, more evolved rocks.

CHAPTER V

METALLIC MINERALIZATION

Introduction

Several small, weakly mineralized showings occur throughout the ultramafic rocks, usually within the amphibole pyroxenite phase. Mineralization consists of chalcopyrite, magnetite and minor pyrite, either as disseminated minerals or as vein and fracture fillings. As part of the study on the alkalic complex, the mineralization has been examined in an attempt to determine what factors control its presence.

Copper Content of Rocks

Forty-six rock samples were analyzed for their copper content (values in Table 2, locations in Figure 7).

These results show a definite decrease in copper content that correlates with a decrease in the total mafic mineral content of all the alkalic rocks (Appendix A and B). The intermediate and felsic alkalic rock types average less than 50 ppm copper while the mafic syenite-monzonite averages over 110 ppm copper. The ultramafics range from 6 to 5550 ppm copper with the greatest values in the amphibole pyroxenites where copper values vary from 129-5550 ppm and average 853. This large range in values for the amphibole pyroxenite reflects varying degrees of alteration and chalcopyrite development. The biotite pyroxenite has copper contents ranging from 6-357 ppm and averages 142 ppm. It contains only rare chalcopyrite as indicated by the relatively low copper values. However, it does display a weakly developed bimodal distribution (Figure 17) that appears related to the type of biotite present. Those samples collected from areas where coarse, secondary biotite was observed

TABLE 2

COPPER AND NICKEL		CONTENTS		OF SOME		ROCKS		FROM		THE		ALKALIC		PORTION		OF THE		WHITEROCKS	

have copper values ranging from 6-103 ppm; those samples collected from areas containing only primary biotite have values in the 190-357 ppm range. Exceptions to this rule do exist but invariably these exceptions are then accompanied by large ferrohastingsite crystals. The biotite pyroxenite having slightly higher copper contents contain about the same amount of copper as the average amphibole pyroxenite.

Due to the similarity between some hornblendite dykes and the amphibole pyroxenite, three samples of the dykes were analyzed for copper. The results vary considerably, ranging from a low of 70 ppm to a high of 400 ppm. Sulphides are rarely visible in the dykes.

Hydrothermal alteration associated with the mineralization is notably absent, aside from the weakly developed coarse, secondary biotite found with the biotite pyroxenite having slightly lower copper values. As was mentioned in Chapter III, this secondary biotite is also spatially related to the porphyritic, leucocratic quartz diorite dykes which cut the alkalic complex. The biotite pyroxenite having slightly higher copper contents lacks notable alteration including the replacement of other minerals by biotite or of biotite development along fractures, thus precluding any notion that the biotite itself is an alteration assemblage. In contrast, the amphibole pyroxenite shows varying degrees of late magmatic or deuteric alteration, usually in the form of epidote, hornblende and poikilitic ferrohastingsites.

Nickel Content of Rocks

Although only 19 samples were analyzed for nickel (Table 2), it is apparent that the Whiterocks Mountain alkalic pyroxenite has a low nickel content compared to other ultramafic rocks (Table 3). In general,

TABLE 3

A COMPARISON OF MAJOR, MINOR AND TRACE ELEMENT CONTENTS OF SOME AVERAGE MAFIC AND ULTRAMAFIC ROCKS WITH THE WHITEROCKS MOUNTAIN STOCK PYROXENITES								
	*1 AVERAGE ALKALINE PERIDOTITE	*1 AVERAGE ALKALINE PYROXENITE	*1 BIOTITE PYROXENITE	*6 AVERAGE OCEANIC THOLEITE	*6 AVERAGE ALKALINE BASALT	*5 SHOSHONITE BASALT	WHITEROCKS MTN. BIOTITE PYROXENITE	WHITEROCKS MTN. AMPHIBOLE PYROXENITE
SiO ₂	40.27	41.55	43.72	49.30	47.10	53.74	40.00	39.71
TiO ₂	1.30	3.31	2.51	1.80	2.70	1.05	1.28	1.41
Al ₂ O ₃	7.29	7.25	7.54	15.20	15.30	15.84	5.62	9.18
Fe ₂ O ₃	4.28	6.80	5.55	2.40	4.30	8.10	10.52	7.39
FeO	9.08	7.77	5.67	8.00	8.30		8.77	10.08
MnO	0.25	0.20	0.17	0.17	0.17		0.27	0.34
MgO	24.36	13.02	14.20	8.30	7.00	6.36	10.82	8.57
CaO	7.15	16.93	15.47	10.80	9.00	7.90	17.95	16.10
Na ₂ O	1.06	1.38	0.68	2.60	3.40	2.38	0.68	1.13
K ₂ O	0.62	0.70	2.76	0.24	1.20	2.57	0.76	1.35
P ₂ O ₅	0.38	0.59	0.74	0.21	0.41		1.50	1.22
K ₂ O/Na ₂ O	0.58	0.51	4.06	0.09	0.35	1.08	1.12	1.19
FeO+Fe ₂ O ₃ /MgO	0.55	1.12	0.79	1.25	1.80	1.27	1.78	2.04
Fe ₂ O ₃ /FeO	0.47	0.88	0.98	0.30	0.52		1.20	0.73

TRACE ELEMENTS (ppm)

Ni	2000 *2	2000 *2	1500 *2		120 *4	20 *5	60	43
Cu	10	20	30				210	535
Sr	1.0	10.0	20.0	130	500- ^{*3} 1000	700	371	538
Ba	0.4	6.0	0.4	14	300- 800	1000	390	253
Rb	0.2	2.0	1.0	10	30- 100	75	39	24

*1. Nockolds, S.R., (1954)

*2. Wyllie, P.J., (1967)

*3. Carmichael, I.S.E., et al, (1974)

*4. Lo, H.H. and Goles, G.G., (1976)

*5. Jakes, P. and White, A.J.R., (1972)

*6. Hyndman, D.W., (1972)

Ni is concentrated in more primitive ultramafics, which are richer in olivine, bronzite, and more Mg-rich augite (Stanton, 1972; Carmichael et al., 1974). The absence of these minerals along with the low nickel contents of the pyroxenites suggests an earlier, hidden process, whereby the minerals may have fractionated out of a parental magma at depth and depleted the residual magma (which formed the Whiterocks Mountain alkalic pyroxenites) in nickel.

Mode of Mineralization

Copper mineralization within the Whiterocks Mountain stock is found mainly in the amphibole pyroxenite with a few scattered occurrences in the biotite pyroxenite and the mafic syenite-monzonite. Overall the mineralization is very weak with the most significant mineralization confined to a relatively small portion of the amphibole pyroxenite near the centre of the stock (Figure 7).

In the amphibole pyroxenite mineralization consists of oxides, usually magnetite, and sulphides chalcopyrite and pyrite. The mineralization occurs as disseminated euhedral to subhedral crystals within anhedral, poikilitic ferrohastingsite grains which are replacing aegirine-augite, and as stringer and fracture fillings associated with epidote and blue-green hornblende. Of the opaques, magnetite is most common, occurring as disseminated grains averaging 3% to 5% of the amphibole pyroxenite, or locally occurring as clots and stringers and making up to 15% of the rock. Sulphides (pyrite much greater than chalcopyrite) are most common in areas with abundant epidote and locally constitute up to 5% of the rock but typically average less than 1%.

In addition, copper values are found in highly altered zones within the amphibole pyroxenite which contain primary and recrystallized (less

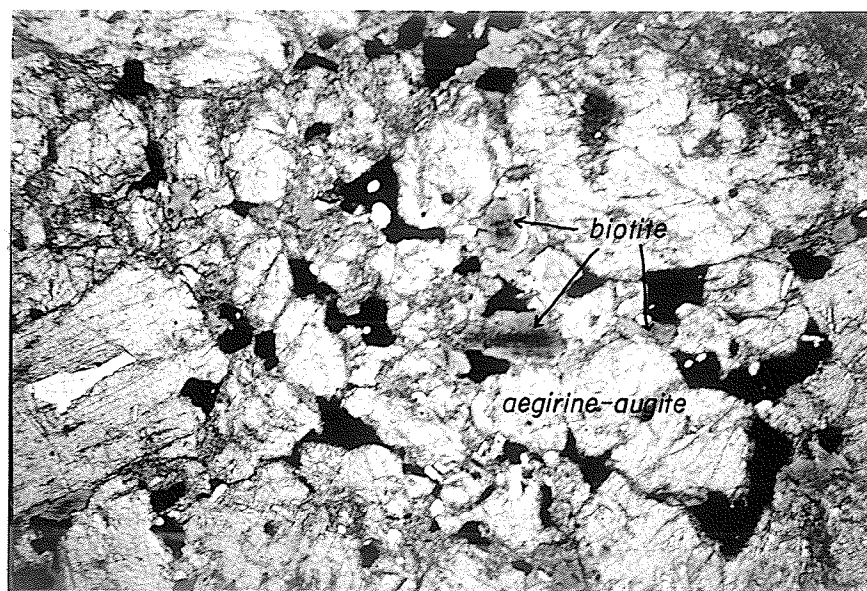
than 1 mm in diameter) aegirine-augites. Surrounding the aegirine-augites are anhedral opaques. Crude layering is developed where medium-grained recrystallized pyroxene layers grade into and alternate with fine-grained recrystallized pyroxene layers up to 1 cm thick. The layers contain 20% to 50% disseminated and stringer controlled opaque minerals. Separating the medium-grained layers from the fine-grained layers is a thin "ribbon" of apatite crystals.

In the biotite pyroxenite opaque minerals (predominantly magnetite, only rarely sulphides) occur with the biotite as euhedral to anhedral grains that fill the interstices between the pyroxenes or concentrate around their edges, rimming them (Figures 18 and 19). Minor amounts of pyrite and or chalcopyrite also occur along hairline fractures that cut the biotite pyroxenite but are lined with ferrohastingsite or coarse secondary biotite.

The largely disseminated character of the opaques, particularly magnetite, occurring in the biotite pyroxenite suggests they are primary magmatic in origin and crystallized at the same time as biotite but after the aegirine-augite. The hairline fractures containing sulphides and ferrohastingsite crystals are related to another event, probably the intrusion of the amphibole pyroxenite phase.

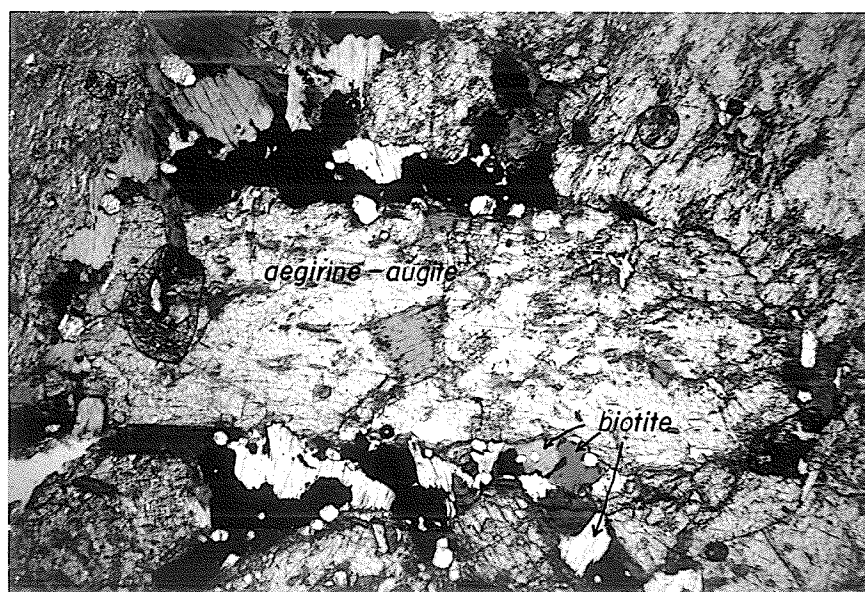
Factors Controlling Copper Mineralization

In the mafic syenite-monzonite, weak chalcopyrite and pyrite mineralization is present in an area adjacent to amphibole pyroxenite. Mineralization is stringer and fracture controlled and is associated with weak amphibole development along fractures. Hydrothermal alteration consists of localized weak to moderately intense, pervasive and



0 mm. 9
scale

Figure 18. Opaque minerals (black) along with minor biotite (medium grey) are filling the interstices between subhedral to euhedral aegirine - augite crystals (light grey). Opaques are largely magnetite. The rock is a biotite pyroxenite. Microphotograph taken under plain light.



0 mm. 9
scale

Figure 19. Opaque minerals (black) along with biotite (medium grey) are filling interstices and rimming euhedral to subhedral aegirine - augite (light grey) crystals. The rock is biotite pyroxenite. Microphotograph taken under polarized light.

fracture controlled epidote replacement, minor chlorite and widespread iron staining.

The mineralization in the amphibole pyroxenite occurs as disseminated grains, stringers and fracture fillings. As in the biotite pyroxenite, the mineralization postdates development of primary pyroxenes, occurring as interstitial grains between the aegirine-augites or rimming the edges of partly corroded crystals. Unlike the disseminated mineralization in the biotite pyroxenite, mineralization in the amphibole pyroxenite is spatially associated with the development of coarse, ferrohastingsite grains which are replacing primary aegirine-augite. The opaques (predominantly chalcopyrite, pyrite and magnetite) commonly occur as inclusions within the ferrohastingsites and are therefore thought to be both older and the same age as them. Alteration minerals do occur and are confined to epidote and hornblende development which are largely fracture controlled and vary in intensity from weak to strong.

The absence of visible mineralization or widespread hydrothermal alteration in rocks younger than the amphibole pyroxenite, particularly in the immediately adjacent rocks, infers the mineralization is preporphyritic monzonite. When combined with the lack of appreciable epigenetic mineralization or hydrothermal alteration in rocks older than the amphibole pyroxenite (aside from the isolated occurrences in biotite pyroxenite and the mafic syenite-monzonite which are both known to be associated with coarse ferrohastingsite), it seems likely that the fracture and stringer controlled mineralization (oxides and sulphides) is controlled by the same late pyroxenite stage magmatic fluids that produced the amphibole pyroxenite. This of course does not apply to the biotite pyroxenite in which textural evidence already cited indicates

the mineralization is not epigenetic but rather the result of primary magmatic crystallization, with intermediate oxygen partial pressure conditions (fO_2) suitable for the occurrence of magnetite.

The process by which the mineralization in the Whiterocks Mountain alkalic pyroxenite formed can be explained by magmatic differentiation. By this mechanism, copper and sulphur, both of which do not readily enter silicate lattices, would be enriched in the melt fraction of a fractionating magma until conditions were right for the crystallization of sulphides to occur (Graybeal, 1973; Bowen and Gunatilaka, 1977). Such a situation could have existed at Whiterocks Mountain from a fractionating melt of pyroxenite composition that crystallized and separated out a biotite pyroxenite and mafic syenite-monzonite phase, and the remaining melt fraction was enriched in a number of elements including copper and sulphur. The resulting melt subsequently intruded and replaced part of the biotite pyroxenite and locally the mafic syenite-monzonite. Having been slightly more "evolved", the melt was responsible for the formation of ferrohastingsite (after aegirine-augite), plagioclase, K-feldspar and visible sulphides. As in the crystallization of the biotite pyroxenite, oxygen partial pressure (fO_2) conditions would have been fairly high as indicated by the presence of abundant magnetite.

Economic Significance of Mineralization

The Whiterocks Mountain stock has been the subject of mineral exploration, due to the presence of visible sulphides in the pyroxenite. Besides being examined for its chrome and nickel potential, the ultramafic has been explored for its precious metal content, including gold, silver, platinum and palladium and most recently as a possible alkaline porphyry copper prospect.

The calc-alkalic portion of the stock has also been explored, primarily for its molybdenum potential (Geology, Exploration, and Mining in British Columbia, 1969, p. 300; Exploration in B.C., 1975, p. E52; 1977, p. E79-E80; 1978, p. E93).

To date, no known ore deposits exist in the Whiterocks Mountain stock and aside from the Brenda porphyry copper-molybdenum mine, 23 km southwest of Whiterocks Mountain, no ore deposits are known in the area.

Based on the present study, the potential of the alkalic rocks for containing an ore deposit is limited. The lack of any evidence of a significant hydrothermal system, including the development of intense, localized fracturing, precludes the possibility of a porphyry copper deposit. The amphibole pyroxenite phase does contain copper, but surface exposures indicate it is erratic in both size and grade and at present is far from being an ore deposit. Precious metals do occur (gold, silver and platinum minerals were identified in at least one polished section) within the amphibole pyroxenite, but again are very erratic in their distribution.

Nickel and chrome also appear to be unimportant in the pyroxenite. Although the possibility does exist that nickel may be found at depth, it is unlikely that exploration for it will be undertaken.

CHAPTER VI

ALTERATION

Introduction

Alteration within the Whiterocks Mountain alkalic complex consists of a combination of regional greenschist facies metamorphism, probably induced by the Columbian Orogeny, hydrothermal alteration associated with the porphyritic leucocratic quartz diorite dykes, and deuteric alteration that produced the amphibole pyroxenite.

The regional metamorphism, including that due to the intrusion of younger plutonic rocks, produced weak fracturing with epidote, chlorite and sericite minerals filling fractures. Much of the visible alteration in the mafic syenite-monzonite and in the porphyritic monzonite is of this type.

Hydrothermal alteration associated with porphyritic leucocratic quartz diorite dykes consists of coarse, secondary biotite development primarily along fractures in the amphibole and biotite pyroxenites and includes the formation of the hydrothermal biotite breccias and more localized biotite replacement of amphiboles and pyroxenes in the mafic syenite-monzonite. Locally, weak to moderate sericite mineral development, usually after plagioclase, can be observed in the porphyritic monzonite.

The most abundant and obvious alteration of the alkalic complex is the late magmatic or deuteric alteration that produced the amphibole pyroxenite and locally altered the mafic syenite-monzonite. This phase of alteration is both pervasive and fracture controlled. It is identified by the presence of large, poikilitic ferrohastingsite minerals, accompanied by varying amounts of epidote and hornblende.

Temperature-Pressure Conditions of Late Magmatic Alteration

The conditions that existed during the late magmatic alteration of biotite pyroxenite to amphibole pyroxenite are best explained by work carried out by Bailey (1969) on the hydration of aegirine. The similarity that exists between the alkaline rich mineral system, acmite ($\text{NaFe}^{+3}[\text{Si}_2\text{O}_6]$) - arfvedsonite-riebeckite ($\text{Na}_{2.5}\text{Ca}_{.5}\text{Fe}_5^{+2}\text{Si}_{7.5}\text{Al}_{.5}\text{O}_{22}(\text{OH})_2$), and the calcium rich mineral system aegirine-augite ($(\text{Na,Ca})(\text{Fe}^{+3},\text{Fe}^{+2},\text{Mg})[\text{Si}_2\text{O}_6]$) - ferrohastingsite ($\text{NaCa}_2\text{Fe}_4^{+2}(\text{Al},\text{Fe}^{+3})\text{Al}_2\text{Si}_6\text{O}_{22}(\text{OH},\text{F})_2$) is such that results obtained by Bailey may be extrapolated for an approximate interpretation of the conditions existing at Whiterocks Mountain. That is, the replacement of aegirine-augite rich, biotite pyroxenite by amphibole pyroxenite rich in ferrohastingsite likely occurred by moderately oxidizing (magnetite field of stability) fluids that were sufficiently hot enough to react with the pyroxenes to form amphibole plus magnetite. Bailey (1969) showed experimentally that aegirine by itself was stable in the presence of fluid H_2O ($P = 2$ to 4 k bars) and temperatures 700 - 750°C (subsolidus) for oxygen fugacities of the nickel + nickel oxide equilibrium, but for the more reducing conditions of the iron + wustite equilibrium, $T = 600$ to 700° (subsolidus), aegirine is replaced by arfvedsonite. This reaction would release sodium disilicate or consume $\text{SiO}_2 + \text{Al}_2\text{O}_3$; the absence of albite or nepheline suggests the latter. The presence of magnetite as a product suggests that some Ca and Al were available to permit release of iron instead of its incorporation into the amphibole.

CHAPTER VII

PETROCHEMISTRY

Introduction

Mapping of the Whiterocks Mountain stock indicated two different suites of rocks existed, one a biotite bearing, quartz-rich suite, and the other an augite bearing, quartz-poor suite of the alkaline family of rocks. Analysis of 39 rock specimens from the stock for major and minor elements plus the trace elements Ba, Rb and Sr and an additional 7 specimens analyzed only for the trace elements (Tables 4 and 5) has confirmed the presence of two distinct, though probably related suites of rocks, one alkalic, the other calc-alkalic.

Major and Minor Elements

A. Alkalic Suite of Rocks

The alkalic suite of rocks is characterized by little to no modal or normative quartz in all but the most felsic phase (leucocratic quartz monzonite, Appendices A and B) and by the occurrence of normative olivine and nepheline in most of the analyzed rocks and of normative leucite in most of the analyzed pyroxenites (Appendix D).

On a total alkalis vs. SiO_2 diagram (Figure 20), the quartz-poor rocks plot in the alkaline field, in an area determined by Currie (1976) to belong to the alkali basalt family of rocks.

In a similar diagram that includes the relationship between CaO and SiO_2 (Figure 21), the intersection of the two trends (CaO vs. SiO_2 and $\text{Na}_2\text{O} + \text{K}_2\text{O}$ vs. SiO_2) can be used to determine the Peacock index (Peacock, 1931). For the alkalic rocks the index is about 52, which puts them in the alkalic-calcic group of Peacock, but as it is close to the boundary

TABLE 4

MAJOR, MINOR AND TRACE ELEMENT CONTENTS OF SOME ROCKS FROM THE ALKALIC PORTION OF THE		WHITEROCKS MOUNTAIN STOCK										Trace Elements (in p.p.m.) ²										
		Major and Minor Elements (in Weight %) ¹																				
		SiO ₂	Al ₂ O ₃	Fe ₂ O ₃	FeO	MgO	CaO	Na ₂ O	K ₂ O	TiO ₂	P ₂ O ₅	MnO	L.O.I.* TOTAL	Ni	Cu	Ba	Sr	Rb	K			
pyroxenite	39	41.96	5.78	8.87	8.18	11.55	17.61	0.76	1.13	1.10	1.47	0.26	1.23	68	28	396	378	47	9380			
	196	39.06	5.50	11.50	8.62	10.79	17.99	0.69	0.65	1.29	1.51	0.25	0.97	69	357	278	361	35	5396			
	198	38.99	5.58	11.20	9.50	10.11	18.26	0.58	0.51	1.49	1.52	0.31	1.07	44	246	495	375	34	4234			
	128a	41.43	9.21	6.63	9.64	8.20	16.39	1.39	1.25	1.16	1.38	0.39	1.64	47	784	271	600	17	10376			
biotite	166	39.48	9.05	7.24	9.93	9.06	15.98	1.08	1.58	1.58	1.76	0.35	1.72	50	857	280						
	170	40.63	9.28	6.18	10.37	8.92	15.78	1.08	1.44	1.30	1.16	0.31	2.61	43	190	195	516	32	13116			
	175	37.29	9.19	9.49	10.37	8.11	16.25	0.95	1.14	1.61	0.58	0.32	2.33	32	310	266	499	23	11953			
	71b	42.21	12.86	18.27		5.79	14.31	1.65	1.53	1.31	0.74		0.51		70	412	1672	41	12701			
hornblende amphibole	191	43.45	14.37	7.13	7.45	5.13	12.97	1.95	1.72	1.19	1.15	0.27	1.61	32	152	577	1480	42	14278			
	189	51.87	16.70	4.09	4.67	2.67	7.72	3.04	4.65	0.74	0.72	0.19	1.15	22	98	914	1306	82	38600			
	187	52.64	16.41	3.73	4.53	2.87	7.60	3.32	5.07	0.63	0.73	0.22	1.01	30	134	1149	1821	68	42086			
	134	50.52	15.42	3.20	6.72	4.61	9.02	2.94	4.37	0.70	0.79	0.19	1.32	22	115	927	1071	86	36275			
	119a	53.50	17.02	2.76	4.97	2.72	7.06	3.30	4.89	0.67	0.67	0.18	1.12	19	76	1175	1270	83	40592			
	105	52.03	16.32	3.69	5.11	3.13	8.00	3.38	4.40	0.73	0.71	0.19	1.09	19	56	837	1090	81	36524			
pyroxenite	190	52.16	16.47	4.70	4.09	2.70	7.87	2.53	5.89	0.65	0.66	0.18	1.12	178	172	1224	1717	96	48893			
	186	50.21	17.13	3.75	3.80	1.98	7.47	3.33	4.15	0.73	0.59	0.21	5.81	12	25	800	1311	69	34449			
	137	56.27	18.12	2.63	2.63	1.31	5.76	4.06	5.35	0.55	0.46	0.14	0.61	10	12	1017	1573	127	44410			
	130	56.23	18.01	3.06	2.63	1.56	5.83	3.94	6.12	0.39	0.48	0.15	0.65	15	43	1240	2135	71	50802			
	72b	60.74	19.67	3.25		0.38	4.31	5.10	4.86	0.33	0.09		0.52		1	1040	1479	83	40343			
leucocratic quartz monzonite	192	61.74	18.84	1.65	1.02	0.54	3.56	4.79	5.05	0.27	0.27	0.11	0.87	14	2	1145	1326	93	41920			
	114b	68.96	17.03	0.94	0.43	0.01	2.10	4.59	4.88	0.14	0.03		0.30			1149	896	100	40509			
	115b	63.71	18.30	1.28	1.43	0.09	3.47	5.11	4.91	0.30	0.07		0.35			1068	1262	110	40758			
	188	66.25	16.51	0.61	1.75	0.84	2.75	4.69	2.47	0.32	0.32	0.06	1.01	32	2	1147	700	42	20503			
	182	67.64	16.34	0.67	1.75	0.56	3.18	4.22	2.09	0.27	0.29	0.09	0.94	22	4	2058	440	25	17349			
leucocratic diorite	63	68.39	17.01	1.07		0.01	1.17	4.93	6.43	0.18	0.03		0.54			773	313	232	53375			
	75	67.71	16.40	2.60		0.82	3.19	5.07	2.09	0.33	0.11		0.41			10	1282	543	42	17349		
	78	61.24	17.82	4.63		1.80	4.70	5.19	2.51	0.56	0.20		0.49			996	616	53	20836			
	79	68.57	16.30	2.52		0.85	3.09	4.74	2.14	0.33	0.10		0.54			1336	533	32	17764			
	A-1	48.43	12.03	1.89	1.09	1.09	1.94	3.83	1.64	0.28	0.11		1.31	7		144400	881	77	13614			
pyroxenite	A-2	58.79	14.62	2.64	0.51	2.89	2.89	3.53	2.05	0.29	0.11		1.24			54300	588	43	17017			
	A-3b	67.99	16.16	2.53		0.43	2.87	4.52	2.58	0.33	0.11		0.47				527	54	19756			

* Loss on ignition includes H₂O⁺, H₂O⁻, CO₂. L.O.I. determined gravimetrically.1. All major and minor elements determined by Cominco Ltd. Research Lab. in Toronto; Method of analysis is Li borate fusion/XRF. Approximate limits of error are $\pm 0.1 - 0.3\%$.2. Trace elements determined by Cominco Ltd. Research Lab. in Vancouver, B.C. 5r and Rb determined by X-ray fluorescence. Limits of error are $\pm 10\%$. Cu determined by atomic absorption, limits of error are $\pm 10\%$. Total Ni determined by hydrofluoric/perchloric acid digestion followed by atomic absorption. Limits of error are ± 5 ppm. K calculated from wt. % K₂O.

NOTE: Sample locations are given in Figure 7.

TABLE 5

MAJOR, MINOR AND TRACE ELEMENT CONTENTS OF SOME ROCKS FROM THE CALC-ALKALINE
PORTION OF THE WHITEROCKS MOUNTAIN STOCK

Major and Minor Elements (in Weight %) ¹														Trace Elements (in p.p.m.) ²				
	SiO ₂	Al ₂ O ₃	Fe ₂ O ₃	FeO	MgO	CaO	Na ₂ O	K ₂ O	TiO ₂	P ₂ O ₅	MnO	L.O.I.*	TOTAL	Cu	Ba	Sr	Rb	K
dyke 237 ³	76.03	12.56	0.98		0.01	0.54	4.54	3.85	0.07	0.02		0.46	99.06	19	232	56	121	31959
quartz porph. I ³	67.61	15.39	2.85		0.92	2.17	4.80	2.97	0.32	0.15	0.07	0.72	97.97	13	1166	497	67	24654
	68.16	15.10	2.63		1.00	2.48	4.79	2.84	0.27		0.07	0.63	97.97	20	3634	588	67	23575
	68.60	15.08	2.47		0.80	2.26	4.51	3.02	0.27	0.13	0.06	0.68	97.88	8	1342	498	68	25069
	67.18	15.31	2.88		1.03	2.76	4.27	2.69	0.33		0.07	0.85	97.37	5	1286	575	60	22330
	73.28	13.15	1.55		0.25	1.08	4.17	4.02	0.14	0.06	0.05	0.52	98.27	7	1441	184	90	33370
quartz porph. II ³	68.73	15.63	2.62		0.88	2.49	4.46	2.89	0.29		0.06	0.75	98.80	8	1366	515	64	23990
	72.82	12.89	1.16		0.18	0.81	3.75	4.18	0.14	0.05	0.03	0.84	96.85	7	1594	139	85	34698
undifferentiated gneiss ³														18	444	101	102	
														53	2049	418	36	
														13	1571	499	90	
														8	1496	391	103	
														10	1271	299	110	
														10	1142	287	126	
														9	1541	603	50	

- * L.O.I. loss on ignition includes H₂O⁺, H₂O⁻, CO₂, L.OI determined gravimetrically;
1. All major and minor elements determined by Cominco Ltd. Research Lab. in Toronto; Method of analysis is Li borate fusion /XRF. Approximate limits of error are ± 0.1 - 0.3%
2. Trace elements determined by Cominco Ltd. Research Lab. in Vancouver. Ba, Sr, and Rb determined by X-ray fluorescence. Limits of error ± 10%. Cu determined by atomic absorption, limits of error ± 10%. K calculated from wt. % K₂O.
3. Samples used in Rb/Sr age dating.

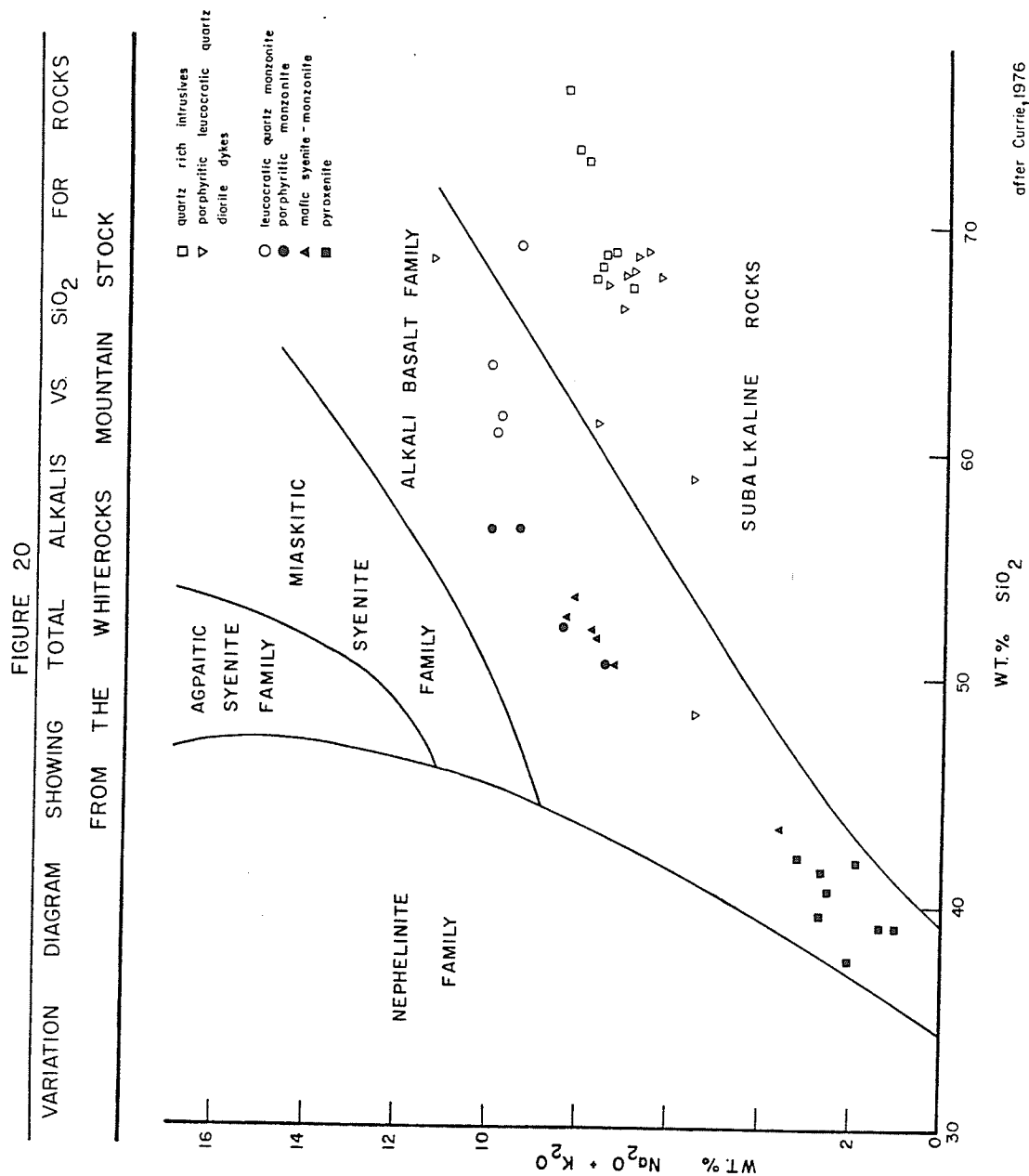
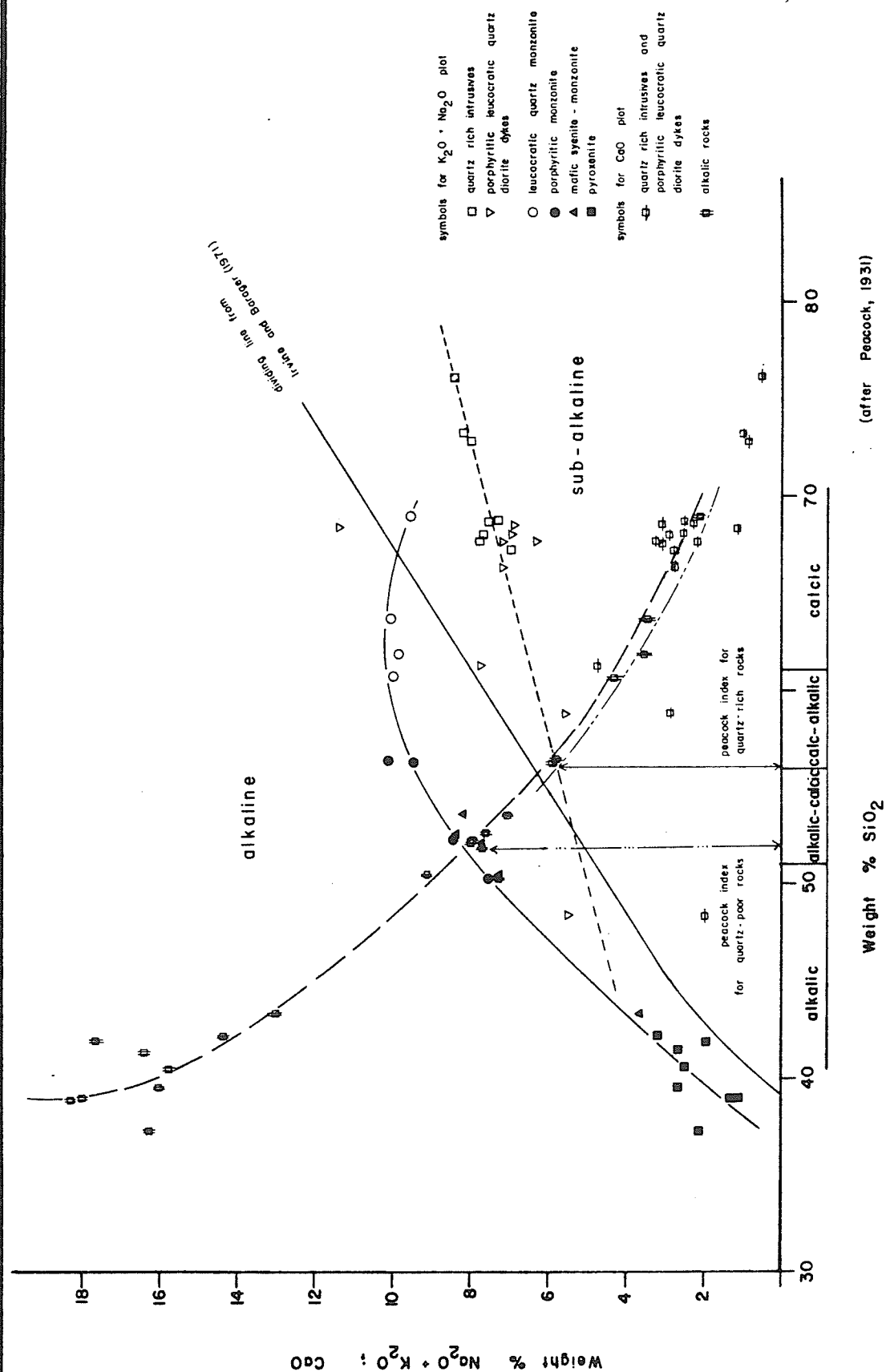


FIGURE 21

CHEMICAL VARIATION DIAGRAM SHOWING $K_2O + Na_2O$ AND CaO vs. SiO_2 AND THE PEACOCK INDEX FOR ROCKS FROM THE WHITEROCKS MOUNTAIN STOCK



they will continue to be called "alkalic" in this report. This name is also in accordance with Currie's classification in Figure 20 (Currie, 1976).

Harker variation diagrams for the alkalic rocks show that CaO, total Fe and MgO decrease with increasing SiO_2 while Na_2O , K_2O and Al_2O_3 increase with increasing SiO_2 (Figure 22). Lines drawn by inspection through the plotted points define smooth curves with few specimens aside from some pyroxenites plotting far from them. The regularity in the variation of the oxides from the different alkalic phases corresponds to a change from ultramafic to leucocratic rocks. This suggests that all the alkalic rocks have a common magmatic origin, probably through a process of crystal fractionation.

A similar conclusion may be arrived at by drawing a curve through the data points plotted on the total alkalis vs. SiO_2 diagram (Figure 20). In this case, the line drawn by inspection depicts a trend that shows the pyroxenites, mafic syenite-monzonite and porphyritic monzonite becoming more "alkaline" with increasing SiO_2 , however the leucocratic quartz monzonite unit diverges sharply from this trend and plots as a transitional phase between the alkalic and sub-alkaline rocks. The relative smoothness of the curve suggests that the data may define a magma that has fractionated from a quartz-deficient, undersaturated pyroxenite through monzonites to a weakly saturated, quartz-bearing leucocratic quartz monzonite.

Additional support for relating the alkalic pyroxenites to the leucocratic quartz monzonite through a process of crystal fractionation may be obtained from data plotted on an A.F.M. ternary diagram (Figure 23). Here, as in previous examples, data points from the various

FIGURE 22

HARKER VARIATION DIAGRAMS SHOWING MAJOR OXIDES
VS. SiO_2 FOR THE ALKALIC ROCKS FROM THE
WHITEROCKS MOUNTAIN STOCK

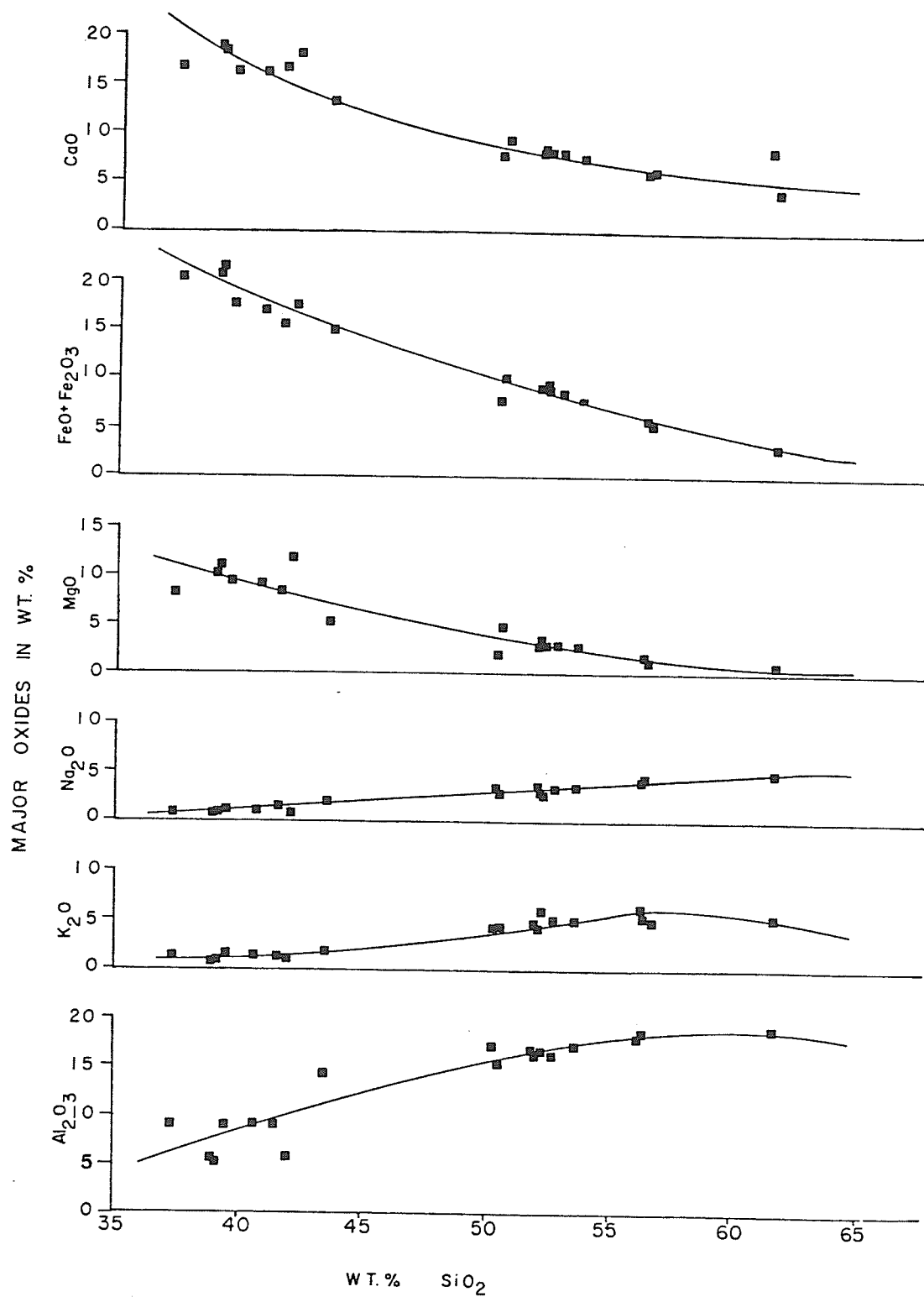
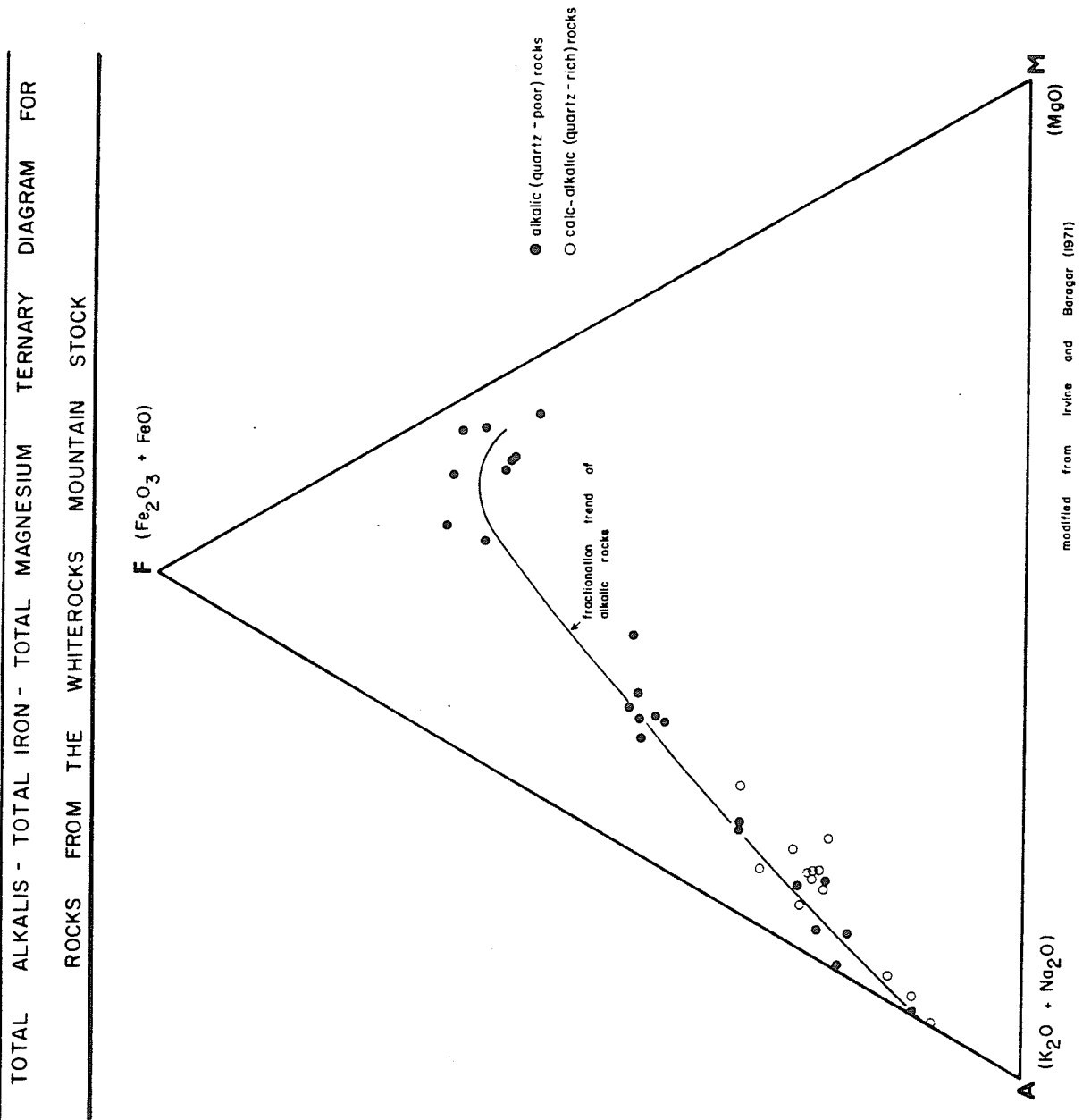


FIGURE 23



alkalic phases may be connected by a relatively smooth curve that runs through the pyroxenites, mafic syenite-monzonites, porphyritic monzonites and leucocratic quartz monzonites in a systematic and orderly fashion.

B. Calc-Alkalic Suite of Rocks

The second major component of the Whiterocks Mountain stock is the calc-alkalic group of rocks. These are characterized by abundant (15% - 25%) modal and normative quartz, normative corundum and hypersthene and no normative feldspathoids or olivine (refer to Appendix D, samples 182, 188).

On an alkalis vs. SiO_2 variation diagram, the samples all plot in a fairly small area within the sub-alkaline field (Figure 20). By attempting to extrapolate possible fractionation trends, a Peacock index of just over 56 can be inferred, making the rocks calc-alkalic by this method of classification (Figure 21).

On the A.F.M. diagram (Figure 23), the calc-alkalic rocks plot in line with the alkalic rocks, and no distinction between the two suites of rocks can be made.

C. Porphyritic Leucocratic Quartz Diorite Dykes

The geochemical data obtained on the porphyritic leucocratic quartz diorite dykes has been included on all diagrams and though there is a scatter, the dykes tend to plot in the same field as the calc-alkalic rocks. This adds to the textural and mineralogical evidence already given in suggesting that the dykes originated from the calc-alkalic portion of the Whiterocks Mountain stock. The scatter in the data is thought to be the effect of associated hydrothermal fluids. For example, dyke sample A-1 contains over 14% Ba and sample A-2 contains over 5% Ba (Table 4).

In addition, these and many other dykes in the central and western portions of the alkaline complex (Figure 7) are associated with hydrothermal alteration, which has resulted in development of biotite and sericite. However, some of the variation likely reflects a primary chemical diversity which is expressed as mineralogical and textural differences between different exposures of the same dykes or between different dykes. Overall, the similarity in chemistry, mineralogy and texture between the calc-alkaline rocks and the least altered porphyritic leucocratic quartz diorite dykes when combined with the field relationships infers they are of a similar age and origin.

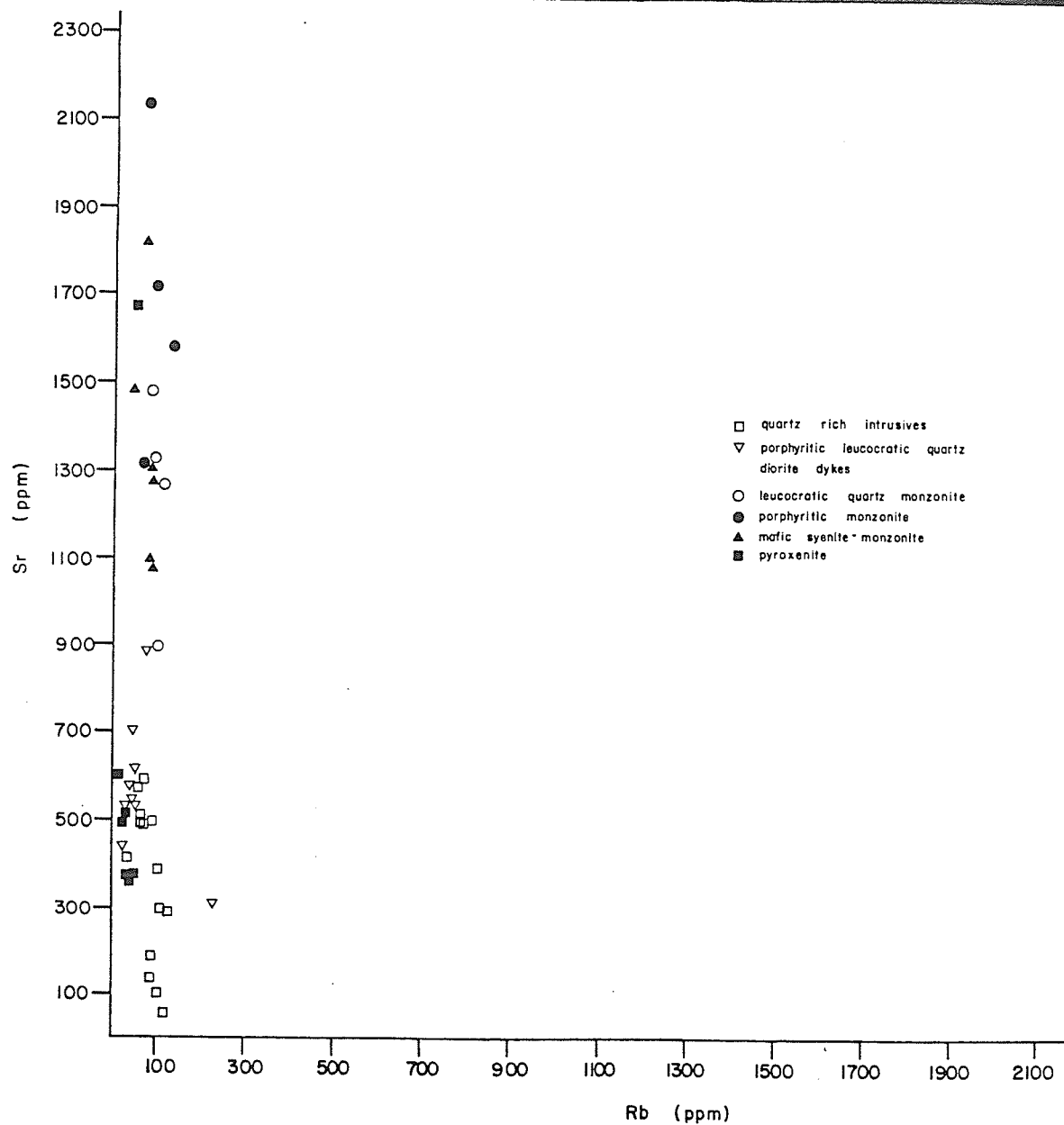
Petrogenetic Trace Elements: Ba, Rb, and Sr

During a process of crystal fractionation within a magmatic melt, Ba, Rb and Sr are typically enriched in the residual liquid as incompatible elements (Mason, 1966; Carmichael et al., 1974; Krauskopf, 1979) and as such become progressively enriched in the more felsic rock types. Strontium substitutes for Ca, and Rb and Ba for K, though Ba seems to be enriched in early formed K minerals whereas Rb is enriched in late formed K rich minerals. Because of this, all rock samples from the Whiterocks Mountain stock were analyzed for Sr, Ba and Rb and their values plotted on a number of variation diagrams.

Sr is enriched from 361 ppm to 2135 ppm for the pyroxenites through to the porphyritic monzonite, it decreases slightly to an average 1241 ppm for the leucocratic quartz monzonite and decreases further to an average 571 ppm for porphyritic leucocratic quartz diorite dykes and 400 ppm for quartz monzonites and granodiorites.

Rb values show no systematic change and range from 17 to 127 ppm for the alkaline rocks and from 25 to 232 for the calc-alkaline rocks. The lack of variation in the Rb contents is unexplained.

FIGURE 24
 CHEMICAL VARIATION DIAGRAM SHOWING Sr vs. Rb FOR THE WHITEROCKS
 MOUNTAIN STOCK



On the Sr vs. Ba variation diagram (Figure 25), the data is much more scattered, with a greater increase of Sr than Ba for the pyroxenites through to the porphyritic monzonite. This trend is broken by a sudden drop in Sr values for the leucocratic quartz monzonite. The calc-alkalic rocks (primarily quartz monzonites) have similar Sr contents to the alkalic pyroxenites, but contain more Ba. Anomalously high contents of Ba are found in some of the dyke specimens which are known to come from areas where hydrothermal alteration is evident.

On the Ba vs. Rb variation diagram (Figure 26) the pyroxenites, mafic syenite-monzonite and porphyritic monzonite all show strong progressive enrichment in Ba relative to Rb, inferring increasing fractionation. The leucocratic quartz monzonite however, shows a reverse in the trend with a slight decrease in Ba content. The calc-alkalic rocks show tremendous variation in Ba, ranging from values equal to those of the alkalic pyroxenites to values far exceeding those of the porphyritic monzonite.

On the Ca/Sr vs. K/Rb variation diagram (Figure 27), the data plotted shows a change from high Ca/Sr for the biotite pyroxenite to low Ca/Sr values for the felsic, leucocratic quartz monzonite. However, within each of the alkalic rock units there is considerable variation in the K/Rb ratio. The calc-alkalic rocks show similar variation in the K/Rb values. The porphyritic leucocratic quartz diorite dykes have tremendous differences which likely reflect a combination of primary magmatic differences and hydrothermal alteration effects.

Rock Geochemical Results and their Interpretation

Under normal magmatic fractionation processes, Sr, Ba and Rb should be enriched in the residual liquid and hence occur in increased amounts

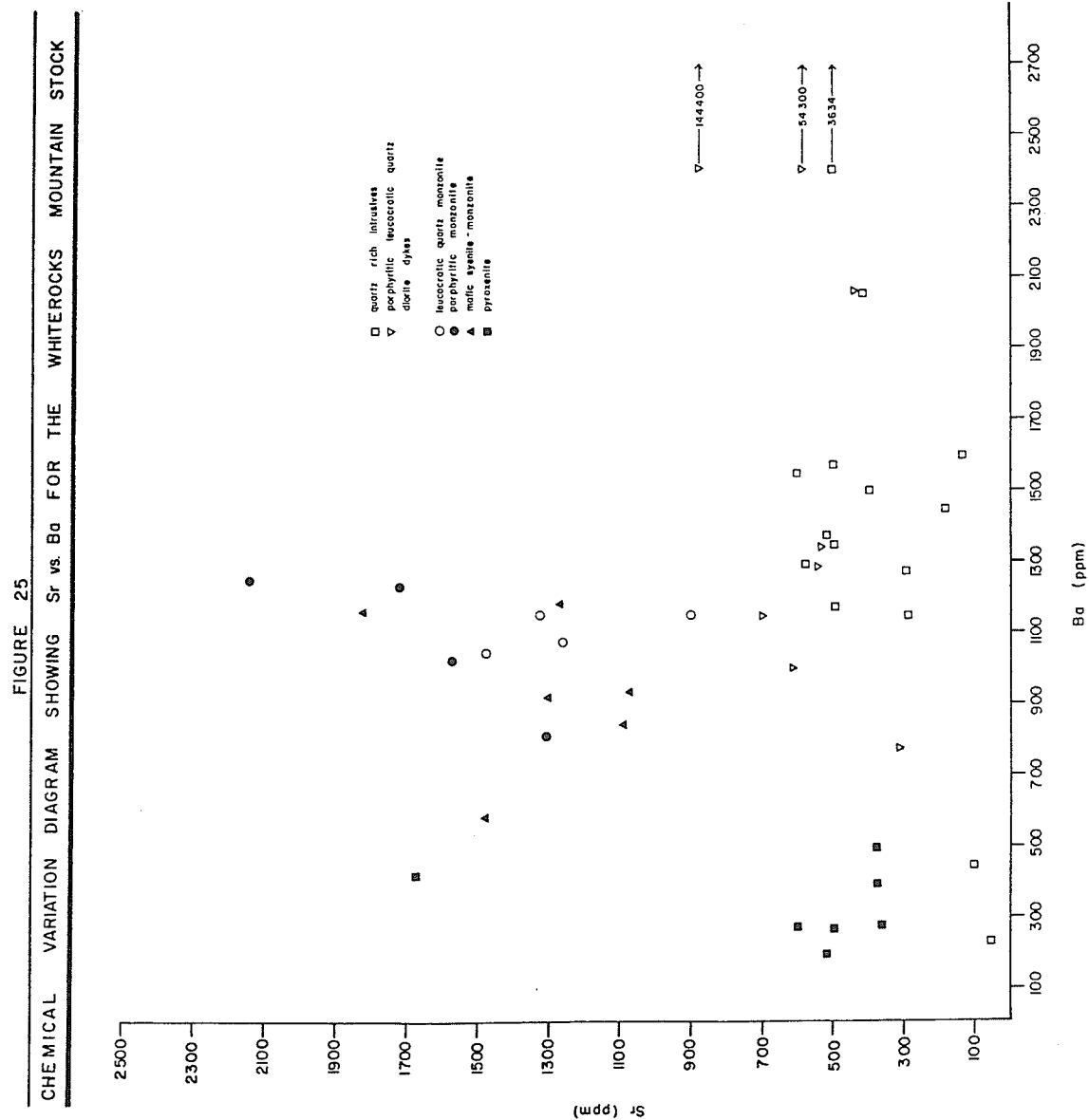
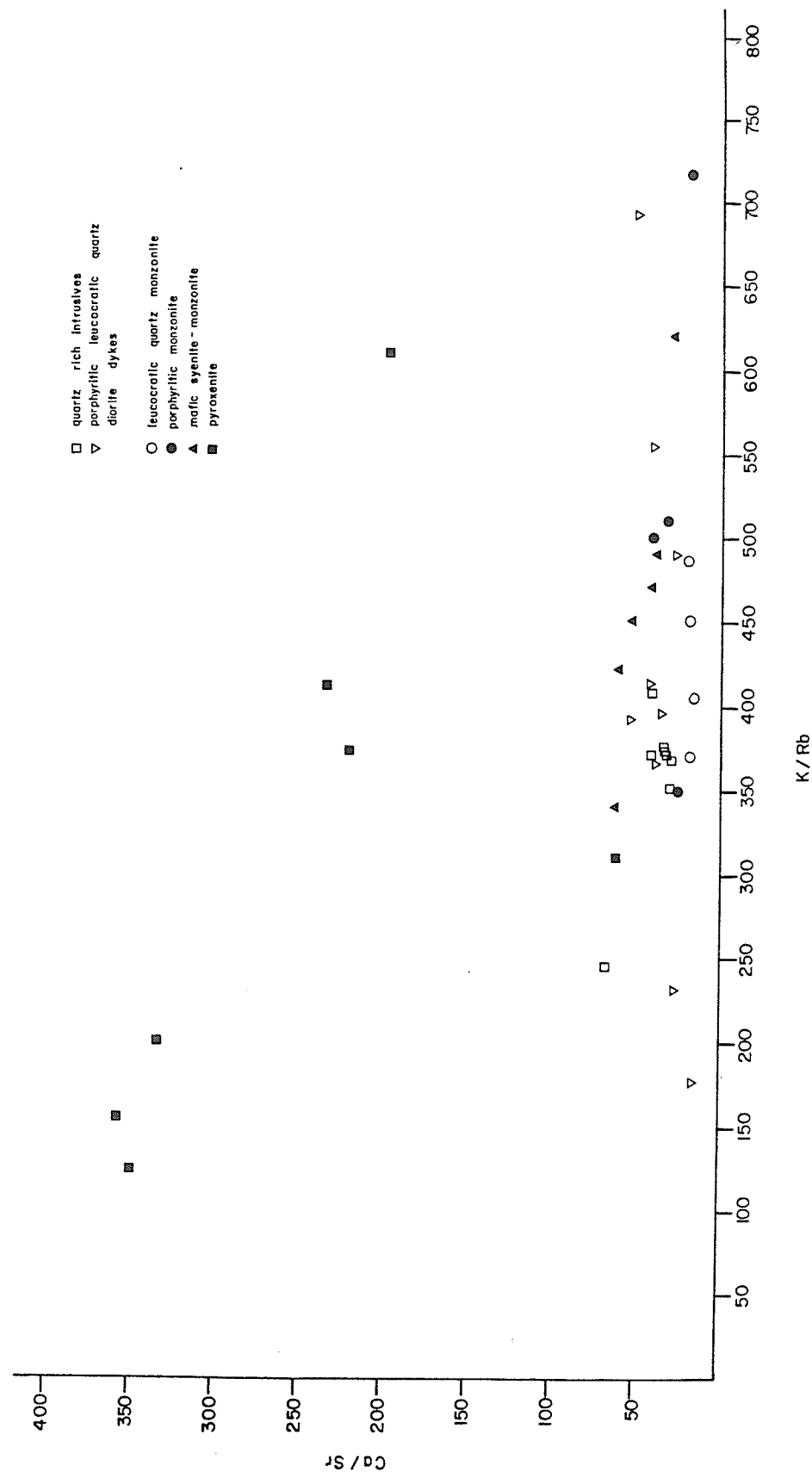


FIGURE 27

CHEMICAL VARIATION DIAGRAM SHOWING Ca/Sr vs. K/Rb FOR THE WHITEROCKS MOUNTAIN STOCK



in the more felsic rock members of a fractionated series. The K/Rb and Ca/Sr ratios should decrease with increasing fractionation and the K/Ba and Rb/Sr ratios should increase with increasing fractionation (Mason, 1966; Carmichael et al., 1974; Krauskopf, 1979).

For the Whiterocks Mountain alkalic complex, the K/Rb ratio (Appendix E) increases from a low of 124.5 for a biotite pyroxenite to a high of 715.5 for a porphyritic monzonite. The K/Ba ratio does show an increase from the pyroxenites to the mafic syenite-monzonite as expected, but is fairly constant for porphyritic monzonite, and in the leucocratic quartz monzonite phase it drops and continues to decrease for the calc-alkalic suite of rocks.

The Rb/Sr ratio also behaves differently than expected, as is apparent in Figure 24. The ratio actually decreases in value from the alkalic pyroxenites through to the porphyritic monzonite. The leucocratic quartz monzonite generally has higher Rb/Sr values than the porphyritic monzonite and as in the other ratios (K/Rb, K/Ba, Ba/Rb) signifies an apparent change in the fractionation trend.

These chemical trends appear to be contrary to those expected under normal magmatic differentiation processes. However, they can be explained by separation of biotite from the melt as shown by Hanson (1978) in his study on mineral/melt distribution coefficients for Ba, Rb, Sr and K in granitic rocks.

Since Ba and Rb readily substitute for K in biotite, the result of crystallizing out biotite is to leave a melt depleted in Ba and Rb or to produce decreasing Rb/Sr and increasing K/Rb and K/Ba ratios. Such a phenomenon could be responsible for the Rb/Sr ratios that show a decrease and the K/Rb and K/Ba ratios that show an increase up to the porphyritic

monzonite phase. It is likely that the effects of the early crystallization of biotite have been lost from the melt by this stage and more "normal" crystal fractionation can then take place.

The Ca/Sr ratio does not show any deviation from that expected under normal magmatic differentiation because neither elements substitute appreciably into any of the early forming minerals in the stock.

Although the early crystallization of biotite largely determined the chemical pattern of the mafic syenite-monzonite and porphyritic monzonite, the subsequent fractionation of ferrohastingsite and plagioclase were likely responsible for forming the rocks that followed and the change in the geochemical patterns.

The significance of this explanation for the observed geochemical patterns is that it adds support to the hypothesis that all the rocks in the Whiterocks Mountain stock could be related through a process of crystal fractionation.

Even the biotite pyroxenite has characteristics which suggest it is the magmatic residual of another magma which fractionated at depth. These features include the cumulate nature of the biotite pyroxenite shown by the presence of two essential minerals: aegirine-augite and biotite. No trace of olivine was found which is rare for an alkalic pyroxenite.

In addition to the mineralogy, the geochemistry of the pyroxenites, when compared to other ultramafic bodies as in Table 3, suggests the Whiterocks Mountain ultramafics are not derived straight from the mantle. This is evident in their depletion in MgO and enrichment in P_2O_5 and total Fe, especially the Fe_2O_3 component. Also, the Whiterocks Mountain ultramafic is strongly depleted in Ni and enriched in Sr, Ba and Rb when compared to other ultramafics.

The closest similarity in chemistry to that of the Whiterocks, Mountain alkaline pyroxenite is with average alkaline basalts (Table 3), suggesting the pyroxenites are more equivalent to a partially evolved mafic rock. This is most evident in the trace elements, where the alkaline basalts show similar, though slightly higher values for Ni, Sr, Ba and Rb. However, differences in the major oxides do exist (excluding those that may be simply related to differences between mafic and ultramafic rocks), including much higher TiO_2 content and lower P_2O_5 content and $\text{K}_2\text{O}/\text{Na}_2\text{O}$ ratios for the alkaline basalts.

CHAPTER VIII

AGE DETERMINATIONS

Introduction

The age of the Whiterocks Mountain stock was guessed at by comparing the rocks with similar looking rocks of known ages from other areas. This method led Cairnes (1937) and Jones (1959) to group the rocks with the nearby "Jurassic or Later" intrusives. Little (1961), however, considered the rocks to be much younger, i.e. Oligocene. Recently, Okulitch (1979) mapped the area and considered the rocks to be Eocene or Paleocene in age.

The results of the present study indicate the stock is composed of two different suites of rocks that may be related to a common source but appear to be of different ages. Intrusive relationships suggest that the alkalic rocks are older than the calc-alkalic rocks. In order to establish the approximate ages of the plutonic rocks K-Ar and Rb-Sr ages were determined.

Ages and Interpretation

In consideration of possible resetting of K-Ar age dates by an intense regional thermal event associated with the intrusion of Coryell plutonic rocks 50 m.y. ago, as suggested by Medford (1975), age determinations were attempted using Rb-Sr methods. However, high Sr contents of the alkalic rocks produced low Rb/Sr ratios and precluded any attempt at obtaining a whole rock Rb-Sr age date for the alkalic complex. Instead a 6-point, whole rock Rb/Sr isochron, giving an age of 147 ± 6 m.y. and an initial $\text{Sr}^{87}/\text{Sr}^{86}$ ratio of $.7039 \pm .0002$ was obtained (by R. L. Armstrong, 1979, at U.B.C. for Cominco Ltd.) from an aplite dyke and

five quartz monzonite samples from the calc-alkalic portion of the stock. In addition, a Rb-Sr age of 149 ± 22 m.y. was determined (by R. L. Armstrong, 1980, at U.B.C. for Cominco Ltd.) from two biotite mineral concentrates obtained from the biotite pyroxenite. One specimen consisted of coarse biotite taken from a hydrothermal biotite breccia and the second sample was of relatively fresh biotite pyroxenite with only minimal secondary biotite development.

The overlap in the two Rb-Sr ages indicates that either both the alkalic and calc-alkalic portions of the stock are so similar in age that within the limits of error the two complexes cannot be separated by Rb-Sr age dating methods, or it means that only the secondary biotite is similar in age to the calc-alkalic complex. Because the secondary biotite is hydrothermal in origin and appears to have formed as a direct result of the emplacement of the calc-alkalic dykes, it appears that the Rb-Sr age dates obtained likely reflect emplacement of the calc-alkalic portion of the Whiterocks Mountain stock. This hypothesis is supported by K/Ar dates of 147 ± 5 m.y. and 145 ± 5 m.y. and a Rb-Sr date of 154 ± 6 m.y. with an initial $\text{Sr}^{87}/\text{Sr}^{86}$ ratio of 0.7050 obtained by Wilkins (1981) for the porphyritic leucocratic quartz diorite dykes.

In an attempt to narrow down the age of the alkalic complex, K/Ar dates of 169 ± 6 m.y. for the porphyritic monzonite and 174 ± 6 m.y. for the amphibole pyroxenite were obtained. Also, whole rock plus orthoclase, plagioclase and hornblende mineral separates produced a Rb-Sr isochron of 291 ± 38 m.y. with an initial $\text{Sr}^{87}/\text{Sr}^{86}$ ratio of 0.70355 ± 0.00017 for the porphyritic monzonite and 338 ± 37 m.y. with an initial $\text{Sr}^{87}/\text{Sr}^{86}$ ratio of 0.7037 ± 0.00013 for the leucocratic quartz monzonite (Wilkins, 1981).

The K/Ar results obtained in the dating of the alkaline complex are similar to K/Ar dates obtained for other alkaline complexes of comparable composition in southern B.C. These include a 200-181 m.y. age for the Copper Mountain intrusives (Preto, 1972), a 191-177 m.y. age for the Kruger alkaline complex (Pet8 and Armstrong, 1976), a 168-149 m.y. age for the Ollala alkaline complex (Wilkins, 1981), and a 174 m.y. age for the Tulameen ultramafic complex (Fox, 1973).

Of the above, the Kruger alkaline complex most closely resembles the alkaline rocks of the Whiterocks Mountain stock. Not only is it similar in lithology and chemistry, it also has a similar K/Ar age and occurs at the periphery of the Similkameen intrusive complex (southeastern edge) where it is intimately associated with quartz-rich rocks (Campbell, 1939; Fox, 1973). As such it was thought these rocks may represent the oldest phases of the Similkameen and Okanagan intrusive complexes. Also, based on a similar K/Ar age and the presence of ultramafic to mafic alkaline rocks, the Ollala alkaline complex may be part of these oldest intrusive groups.

However, the Rb-Sr dates of 291 ± 38 m.y. and 338 ± 37 m.y. suggest the alkaline rocks of the Whiterocks Mountain stock may be Lower Mississippian to Middle Pennsylvanian in age. If so, these rocks are not only considerably older than the calc-alkaline rocks making up the remainder of the stock, they are older than all other intrusive rocks in the area (except the serpentized, Mississippian or older, Old Dave intrusions).

In order to confirm these older ages for the alkaline rocks, Armstrong (in progress) is attempting to date the porphyritic monzonite and leucocratic quartz monzonite with zircons. If this work should agree with Paleozoic Rb-Sr ages obtained by Wilkins (1981), then it seems quite possible other

alkalic complexes of comparable lithology and geochemistry that have K/Ar ages in the 200-150 m.y. range have been wrongly interpreted. Examples include the Ollala and Kruger alkalic complexes.

In contrast to the age discrepancies observed for the alkalic rocks, K/Ar and Rb-Sr ages for the calc-alkalic rocks of the Whiterocks Mountain stock are in agreement with one another. The ages of about 150 m.y. are also in agreement with the 154 ± 6 m.y. age determined for granites, quartz monzonites and granodiorites of the Okanagan complex to the south (Petß and Armstrong, 1976). In addition, these dates are within one standard deviation of the 146 m.y. K/Ar date obtained from a hydrothermal biotite sample at the Brenda porphyry copper-molybdenum mine, (Figure 1), 23 km southwest of the Whiterocks Mountain stock (Soregaroli and Whitford, 1976).

The results of age dating show the calc-alkalic portion of the Whiterocks Mountain stock is coeval to the younger phases of the Okanagan complex. It also indicates the magmatic episode responsible for producing the Brenda copper-molybdenum deposit is very close in age and possibly related to the magmatic activity that produced the calc-alkalic rocks of the Whiterocks Mountain stock. The older, associated alkalic rocks of the stock may be coeval with the oldest rocks in the Okanagan intrusive complex, as suggested by the K/Ar dates, or may be the oldest intrusive complexes in the area as indicated by the Rb-Sr dates.

CHAPTER IXCONCLUSIONS

The Whiterocks Mountain stock is composed of a Middle Jurassic to possibly Lower Mississippian suite of alkalic rocks that range from biotite pyroxenite to leucocratic quartz monzonite. They are generally characterized by the absence of quartz and the presence of aegirine-augite and ferrohastingsite. Intruding these rocks are a number of porphyritic leucocratic quartz diorite dykes that texturally, mineralogically and chemically resemble the quartz rich, biotite bearing calc-alkalic rocks making up the remainder of the stock. Examination of C.I.P.W. norms, major and minor element geochemistry, petrogenetic trace elements Ba, Rb and Sr and modal mineralogy all indicate the amphibole pyroxenite, mafic syenite-monzonite, porphyritic monzonite and leucocratic quartz monzonite are related to the biotite pyroxenite through crystal fractionation. Initial geochemical trends, particularly those involving Rb and Ba were determined by the early separation of biotite from the melt. Subsequent fractionation of ferrohastingsite and plagioclase established more "normal" magmatic differentiation trends and likely account for the transition of the alkalic rocks into quartz-bearing calc-alkalic rocks. The leucocratic quartz monzonite unit appears to be the transitional phase between the quartz-poor and quartz-rich rocks.

Isotopic dating of the calc-alkalic portion of the stock has established it as being about 150 m.y. (Upper Jurassic) in age. This is similar in age to rocks of comparable composition belonging to the Okanagan intrusive complex to the south. In addition it is very close in agreement with the age of hydrothermal activity occurring at the Brenda porphyry copper-molybdenum mine, 23 km southwest of the Whiterocks Mountain

stock. It also is the age of the secondary biotite observed in the alkalic complex although it is definitely not the age of mineralization associated with the amphibole pyroxenite.

The age of the alkalic rocks varies from 169 m.y. to 174 m.y. (Middle Jurassic) according to K/Ar age dating methods to 291 m.y. to 338 m.y. (Middle Pennsylvanian to Lower Mississippian) by Rb-Sr dating methods. Country rocks adjacent to the stock are Mississippian to Triassic in age and therefore do not aid in further delineating the age of the rocks.

Although the biotite pyroxenite appears to be the second phase to have crystallized in the Whiterocks Mountain stock, its origin is uncertain. The cumulate nature of the unit suggests it may be a fractionated phase of a larger ultramafic body occurring at depth. Its geochemistry, particularly the low MgO, Ni, TiO_2 and Rb/Sr values combined with relatively high total Fe, P_2O_5 , K, Sr and $\text{K}_2\text{O}/\text{Na}_2\text{O}$ values indicate the rock is highly evolved.

Initial $\text{Sr}^{87}/\text{Sr}^{86}$ ratios of 0.7035 ± 0.0002 and 0.7037 ± 0.0001 obtained for the alkalic rocks, and 0.7039 and 0.7050 for the calc-alkalic rocks are consistent for magmas derived from mantle sources. However they more likely represent magma derived from melting subducted oceanic lithosphere or pre-intrusive volcanogenic rocks as previously suggested by Petß and Armstrong (1976).

CHAPTER XACKNOWLEDGEMENTS

The author wishes to acknowledge the assistance of Cominco Ltd. in supporting this project. Special thanks are due to Myron Osatenko of Cominco Ltd. for arranging the project, supplying maps, thin sections, chemical analysis and providing unlimited assistance and guidance. The author would also like to thank Dr. L. D. Ayres for many helpful discussions, Dr. F. Hawthorne and Dr. P. Cerny for assistance and Dr. P. Laznicka and Dr. A. C. Turnock for reading the manuscript and providing many helpful suggestions.

He would also like to thank Ms. F. Elwick for considerable assistance in putting the thesis together and his wife Candis, who aided with maps and diagrams and provided unlimited moral support during the long stretches.

REFERENCES

- Bailey, D. K. 1969. The stability of acmite in the presence of H_2O . American Journal of Science, Vol. 267-A, pp. 1-16.
- Barr, D. A., Fox, P. E., Northcote, K. E. and Preto, V. A. 1976. The alkaline suite of porphyry copper deposits - A summary, in Porphyry Deposits of the Canadian Cordillera, C.I.M. Special Volume 15, pp. 359-367.
- B.C. Department of Mines and Petroleum Resources. 1969. Geology, exploration and mining in B.C., pp. 299-300.
- _____. 1970. Geology, exploration and mining in B.C., pp. 406.
- B.C. Ministry of Mines and Petroleum Resources. 1975. Exploration in B.C., pp. E52.
- _____. 1977. Exploration in B.C., pp. E79-E80.
- _____. 1978. Exploration in B.C., pp. E93.
- Borley, G. and Frost, M. T. 1962. Some observations on igneous ferro-hastingsites. Mineralogical Magazine, Vol. 33, pp. 646-662.
- Bowen, R. and Gunatilaka, A. 1977. Copper. Its geology and economics, John Wiley and Sons, Toronto, 366 p.
- Cairnes, C. E. 1937. Mineral deposits of the west half of Kettle River area, B.C., scale 1 inch = 4 miles, Geological Survey of Canada Paper 37-21.
- _____. 1940. Kettle River (west half) map sheet, 1 inch = 4 miles, Map 538A, Geological Survey of Canada.
- Campbell, C. D. 1939. The Kruger Alkaline Syenites of Southern British Columbia. American Journal of Science, Vol. 237, No. 8, pp. 527-549.
- Campbell, R. B. and Okulitch, A. V. 1972. Stratigraphy and structure of the Mount Ida Group, Vernon (82L), Adams Lake (82M, W $\frac{1}{2}$, and Bonaparte (92P) map areas in Report of Activities, Part A, April to October 1972, Geological Survey of Canada, Paper 73-1A, pp. 21-23.
- Carmichael, I. S. E., Turner, F. J. and Verhoogen, J. 1974. Igneous Petrology, McGraw-Hill Inc., New York, 739 p.
- Christopher, P. A. and Carter, N. C. 1976. Metallogeny and metallogenic epochs for porphyry mineral deposits of the Canadian Cordillera, in Porphyry Deposits of the Canadian Cordillera, C.I.M. Special Volume 15, pp. 64-71.
- Church, B. N. 1979. Geology of the Terrace Mountain Tertiary Outlier: scale, 1:50,000, Province of British Columbia Ministry of Energy, Mines and Petroleum Resources, preliminary map 37.

- Currie, K. L. 1976. The alkaline rocks of Canada, Geological Survey of Canada Bulletin 239, 228 p.
- Fox, K. 1973. The geology of alkalic complexes in north-central Washington, unpublished Ph.D. thesis, Stanford University.
- Gabrielse, H. and Reesor. 1974. The nature and setting of granitic plutons in the central and eastern parts of the Canadian Cordillera, Pacific Geology (P.G.E.O.B.Y.), Vol. 8, pp. 109-138.
- Graybeal, F. T. 1973. Copper, manganese and zinc in coexisting mafic minerals from Laramide intrusive rocks in Arizona, Economic Geology, Vol. 68, pp. 785-798.
- Hanson, G. N. 1978. The Application of Trace Elements to the Petrogenesis of Igneous Rocks of Granitic Composition, Earth and Planetary Science Letters, Vol. 38, pp. 26-43.
- Hibbard, M. J. 1965. Origin of some alkaline feldspar phenocrysts and their bearing on petrogenesis, American Journal of Science, Vol. 263, pp. 245-261.
- Hyndman, D. W. 1972. Petrology of Igneous and Metamorphic Rocks, McGraw-Hill Inc., New York, 533 p.
- Irvine, T. N. and Barager, W. R. A. 1971. A guide to the chemical classification of the common volcanic rocks, Canadian Journal of Earth Sciences, Vol. 8, pp. 523-548.
- Jakes, P. and White, A. J. R. 1972. Major and trace element abundances in volcanic rocks of orogenic areas, Geological Society of America Bulletin, Vol. 83, pp. 29-40.
- Jones, A. G. 1959. Vernon map area, B.C., Geological Survey of Canada Memoir 296, 186 p.
- Krauskopf, K. B. 1979. Introduction to Geochemistry: second edition, McGraw-Hill Inc., New York, 617 p.
- Little, H. W. 1960. Nelson map area, west half, British Columbia, Geological Survey of Canada Memoir 308, 205 p.
- _____. 1961. Kettle River, west half map area, Geological Survey of Canada, map 15-1961.
- Lo, H. H. and Goles, G. G. 1976. Compositions of Formosan basalts and aspects of their petrogenesis, Lithos, Vol. 9, pp. 149-159.
- Macdonald, C. C. 1975. Geology and Geochemistry of the Whit Claim Group, Vernon Mining Division, B.C., Assessment Report 5692.
- Mason, B. 1966. Principles of Geochemistry, John Wiley and Sons, New York, 329 p.

- Medford, G. A. 1975. K-Ar and fission track geochronometry of an Eocene thermal event in the Kettle River (west half) map area, southern British Columbia, Canadian Journal of Earth Sciences, Vol. 12, pp. 836-843.
- Minister of Mines, B.C. 1968. Annual Report, pp. 223.
- Monger, J. W. H. 1975. Upper Paleozoic rocks of the Atlin Terrane, northwestern British Columbia and south-central Yukon, Geological Survey of Canada Paper 74-47, 63 p.
- Monger, J. W. H. and Price, R. A. 1979. Geodynamic evolution of the Canadian Cordillera - progress and problems, Canadian Journal of Earth Sciences, Vol. 16, pp. 770-791.
- Ney, C. S. and Hollister, V. F. 1976. Geological setting of porphyry deposits of the Canadian Cordillera, in Porphyry Deposits of the Canadian Cordillera, C.I.M. Special Volume 15, pp. 21-29.
- Nockolds, S. R. 1954. Average chemical composition of some igneous rocks, Geological Society of America Bulletin, Vol. 66, pp. 1007-1032.
- Okulitch, A. V. 1979. Geology and mineral occurrences of the Thompson-Shuswap-Okanagan region; south central British Columbia (parts of 82 and 92); scale 1:250,000, Geological Survey of Canada Open File 637.
- Osatenko, M. J. 1978. Geological, stream silt and soil geochemical and ground magnetic work on the Dobbin property (Tad claims 1-6), Tadpole Lake area, Vernon Mining Division, NTS. 82L/4W, Assessment Report 6732.
- _____. 1979. Assessment Report of Geology, Soil Geochemistry, Percussion and Diamond Drilling on the Dobbin Property (Tad 1-3, 5-12, 14, 19 and Esperon 11 claims), Tadpole Lake, Vernon and Nicola M.D., N.T.S. 82L/4W, Assessment Report 7596.
- Peacock, M. A. 1931. Classification of igneous rock series, Journal of Geology, Vol. 39, pp. 54-67.
- Petö, P. 1973 a. Petrochemical study of the Similkameen Batholith, British Columbia, Geological Society of America Bulletin, Vol. 84, pp. 3977-3984.
- _____. 1973b. Potassium-argon ages of igneous rocks from the area near Hedley, southern B.C.: Discussion, Canadian Journal of Earth Sciences, Vol. 10, pp. 1357-1358.
- Petö, P. and Armstrong, R. L. 1976. Strontium isotope study of the composite batholith between Princeton and Okanagan Lake, Canadian Journal of Earth Sciences, Vol. 13, pp. 1577-1583.

- Pilcher, S. H. and McDougall, J. J. 1976. Characteristics of some Canadian Cordilleran porphyry prospects in Porphyry Deposits of the Canadian Cordilleran, C.I.M. Special Volume 15, pp. 79-82.
- Preto, V. A. 1972. Geology of Copper Mountain. British Columbia Dept. of Mines and Petroleum Resources, Bulletin 59, 87 p.
- _____. 1974. Petrochemical study of the Similkameen Batholith, British Columbia: Discussion, Geological Society of America Bulletin, Vol. 85, pp. 841-842.
- Roddick, J. C., Farrar, E. and Procyshyn, E. L. 1972. Potassium-argon ages of igneous rocks from the area near Hedley, southern B.C., Canadian Journal of Earth Sciences, Vol. 9, pp. 1632-1639.
- Ross, J. V. 1974. A Tertiary thermal event in south-central British Columbia, Canadian Journal of Earth Sciences, Vol. 11, pp. 1116-1122.
- Smith, J. V. 1974. Feldspar Minerals, Vol. 1, Springer-Verlag.
- Soregaroli, A. E. and Whitford, D. F. 1976. Brenda in Porphyry Deposits of the Canadian Cordillera, C.I.M. Special Volume 15, pp. 186-194.
- Stanton, R. L. 1972. Ore petrology, McGraw-Hill Inc., New York, 713 p.
- Streckeisen, A. 1976. To each plutonic rock its proper name, Earth-Science Reviews, Vol. 12, pp. 1-33.
- Sutherland-Brown, A., Cathro, R. J., Panteleyev, A. and Ney, C. S. 1971. Metallogeny of the Canadian Cordillera, C.I.M. Bulletin, May, pp. 37-61.
- Wilkins, A. L., 1981. K-Ar and Rb-Sr Dating of the Whiterocks Mountain Alkalic Complex in the Intermontane Belt West of Okanagan Lake, South-Central B.C. Unpublished B.Sc. Thesis, U.B.C.

APPENDIX A																
MODAL MINERALOGY IN VOLUME PERCENT FOR SOME ROCKS FROM THE ALKALIC PORTION																
OF THE WHITEROCKS MOUNTAIN STOCK																
	AGAIRINE - AUGITE	BIOTITE	FERRORHASTINGSITE	HORNBLLENDE	OPAUDES	EPIDOTE	CHLORITE	PLAGIOCLASE	K-FELDSPAR	PERTHITE	QUARTZ	SERICITE & CLAY	CARBONATE	SPHENE	APATITE	TOTAL
23	17.5	.5	58.7	5.9	.9	9.4	—	.9	1.9	—	—	—	2.2	.2	2.0	100.1
44	88.6	—	.8	.1	.7	.5	.1	.2	—	—	—	—	tr.	.3	1.7	99.9
120	41.9	1.1	16.7	18.9	12.0	6.2	—	.1	.1	—	—	—	—	.6	8.4	100.0
128a	51.5	1.9	38.3	.4	1.6	2.7	—	.7	1.1	—	—	—	tr.	—	2.0	99.9
166b	1.0	1.4	40.9	32.5	7.1	11.3	—	.8	—	—	—	—	.1	.1	1.0	100.1
179	12.8	.7	46.3	23.5	4.9	6.9	.1	.5	—	—	—	—	1.0	.3	1.7	100.0
179b	51.9	1.2	12.9	7.1	10.6	13.6	—	.5	—	—	—	—	—	tr.	1.8	100.0
39	62.2	15.1	5.6	7.0	6.8	1.2	—	tr.	—	—	—	—	2.5	1.0	1.4	99.9
45	65.1	21.1	4.0	2.4	4.8	.5	—	tr.	—	—	—	—	—	.2	1.6	100.0
70	48.9	27.7	12.8	2.1	1.1	3.3	.1	—	2.9	—	—	—	—	—	2.1	99.9
196b	71.4	12.9	1.5	.7	12.4	.5	—	—	—	—	—	—	—	—	.5	99.9
19	23.4	6.6	12.0	.8	5.0	5.0	.6	23.2	18.8	—	—	2.8	—	.6	1.1	99.9
23a	16.6	2.6	14.7	3.7	2.2	5.8	.3	24.0	29.1	—	—	—	.3	—	.8	100.1
25	—	21.4	—	—	.9	1.2	1.2	49.5	5.1	—	13.1	3.9	2.9	—	.8	100.0
31	18.7	4.2	28.7	4.8	1.2	1.1	—	11.0	29.0	—	—	1.0	—	—	.2	99.9
38	10.3	—	17.1	.8	2.3	.3	—	—	—	—	—	—	—	—	.5	99.9
187	13.2	.5	13.5	1.7	2.1	1.0	1.0	21.2	41.0	—	—	3.3	.7	—	.8	100.0
100	3.4	.3	24.2	2.3	1.4	7.9	2.3	38.1	23.9	—	—	—	—	—	—	100.1
105	7.5	.3	21.1	3.7	2.6	2.6	—	38.1	23.9	—	—	—	—	—	—	99.9
105a	9.0	1.5	20.8	1.2	2.1	2.5	1.2	36.7	23.0	—	—	1.9	—	—	.2	100.1
119a	2.7	6.2	.5	24.6	1.3	.9	2.1	61.2	—	—	—	—	—	.4	—	99.9
119b	10.0	2.5	13.1	2.5	1.6	1.1	.6	40.2	26.9	—	—	1.1	—	—	.3	99.9
159	1.6	26.6	1.6	.4	1.4	7.4	—	57.4	.1	—	—	—	—	.5	3.0	100.0
166e	5.4	2.3	36.3	4.8	.1	6.2	1.7	42.5	—	—	—	—	—	—	1.1	99.9
181	14.9	.5	19.1	3.8	2.9	3.3	—	29.8	22.8	—	—	2.3	—	.1	.7	100.1
191	17.7	1.3	23.7	2.3	2.3	1.5	.2	50.2	—	—	—	—	—	—	.7	99.9
38c	7.9	.2	9.7	.8	1.1	5.9	.4	22.8	—	—	—	6.2	—	.2	.3	100.1
40	14.2	1.9	9.3	.5	5.3	5.8	.3	27.1	—	—	.4	10.6	.1	—	.3	100.0
60a	—	2.9	14.5	.2	.5	5.5	.4	24.8	—	—	1.8	2.3	—	.5	.4	100.0
99	2.5	—	4.4	5.7	2.0	11.3	6.4	23.0	38.8	—	—	4.1	—	.9	1.0	100.1
122c	6.4	.2	1.3	1.0	.2	6.6	.7	25.8	56.6	—	.7	—	—	.3	.2	100.0
122b	.6	1.2	11.1	14.0	3.0	15.4	.4	15.6	26.5	—	.6	10.2	—	.8	.6	100.0
130	6.7	.4	4.9	.7	1.3	4.9	.1	25.2	53.7	—	—	2.6	—	.4	.1	100.1
138	—	1.6	7.7	13.2	1.9	13.3	.4	11.7	34.5	—	—	7.8	1.6	.6	.8	100.1
106	.2	tr.	2.5	1.3	.6	4.3	—	51.3	5.5	24.7	9.1	—	—	.1	.3	99.9
126	—	tr.	1.7	.9	.8	7.7	.1	44.0	2.8	3.5	8.0	.1	.1	.2	.1	100.0
200	—	—	3.3	.6	.3	6.7	—	47.0	5.7	31.1	4.9	—	.3	.1	—	100.0
58a	—	.1	5.3	.8	—	1.7	.1	26.1	22.5	29.0	14.3	—	—	tr.	—	99.9
95	—	.5	.1	.1	.6	1.8	.3	28.2	16.6	32.2	19.0	.6	—	—	—	100.0
133	.8	10.5	—	—	1.4	—	.9	—	84.7	—	—	.5	—	1.1	—	99.9
188	—	2.5	—	—	.7	—	8.3	—	84.5	—	—	.5	2.7	.8	—	100.0

Notes: Sample locations given in Figure 7

APPENDIX B

PARTIAL MODES IN VOLUME PERCENT FOR SOME
ROCKS FROM THE WHITEROCKS MOUNTAIN ALKALIC
COMPLEX

	sample numbers	mafic plus opaques	plagioclase	k-spar	quartz	total
mafic syenite - monzonite	2a	48.1	16.0	35.8		99.9
	11	43.0	22.2	34.8		100.0
	30b	70.3	3.8	25.8		99.9
	32	50.3	16.7	33.0		100.0
	40	25.3	29.8	44.9		100.0
	42	31.9	37.3	30.7		99.9
	65	55.4	15.3	29.3		100.0
	134	42.4	15.1	42.4		99.9
	151	39.6	24.3	36.0		99.9
	158	37.9	20.8	40.8	0.4	99.9
	166c	36.3	16.0	47.3	0.5	100.1
	183	38.2	31.3	30.5		100.0
porphyritic monzonite	35	2.9	45.8	50.3	0.9	99.9
	54	20.4	35.4	38.2	6.0	100.0
	60b	14.8	43.9	41.0	0.2	99.9
	71	22.3	32.8	45.0		100.0
	78	23.4	49.0	27.6		100.0
	114	25.5	27.0	41.7	5.8	100.0
	121a	39.0	28.9	32.1		100.0
	185	12.0	49.4	37.3	1.4	100.0
leucocratic quartz monzonite	104	3.7	46.2	40.5	9.6	100.0
	104a	9.2	49.2	36.2	5.3	99.9
	107	7.3	50.4	33.6	8.7	100.0
	108	2.3	47.2	40.4	10.1	100.0
	58b	5.6	49.7	36.2	8.5	100.0
	58c	1.9	38.2	43.9	15.9	99.9
	58d	2.1	38.2	43.9	15.9	100.1
	91	4.3	48.5	37.9	9.2	99.9

Note: sample locations shown on Figure 7

APPENDIX C

X-RAY RESULTS FROM THREE ANALYZED K-SPAR PHENOCRYSTS FROM THE PORPHYRITIC MONZONITE OF THE WHITEROCKS MOUNTAIN ALKALIC COMPLEX				
Sample	99	130	185	
Triclinicity	$d_{131} = 3.046 \text{ A} ; d_{1\bar{3}1} = 2.974 \text{ A}$ $= 12.5 (d_{131} - d_{1\bar{3}1})$ $= 0.9$	$d_{131} = 3.030 \text{ A} ; d_{1\bar{3}1} = 2.988 \text{ A}$ $= 12.5 (d_{131} - d_{1\bar{3}1})$ $= 0.53$	$d_{131} = 3.024 \text{ A} ; d_{1\bar{3}1} = 2.954 \text{ A}$ $= 12.5 (d_{131} - d_{1\bar{3}1})$ $= 0.88$	
% Na in Solid Solution	$d_{201} = 4.216$ $= 8\%$	$d_{201} = 4.208$ $= 13\%$	$d_{201} = 4.218$ $= 7\%$	
Or Content	64%	71%	54%	

Note: Sample locations in Figure 7.

APPENDIX D

C.I.P.W. NORMS FOR SOME ROCKS FROM THE WHITEROCKS MOUNTAIN ALKALIC COMPLEX

	Q	C	Or	Ab	An	Ne	Lc	Di			Hy		Ol			Mt	Il	Ap	H ₂ O	Os
								Wo	En	Fs	En	Fs	Fo	Fa						
pyroxenites biotite	39		6.12		8.90	3.41	0.44	28.77	21.24	4.62			5.32	1.22	12.76	2.13	3.36	1.23		
	196		0.56		10.01	3.12	2.62	29.00	22.14	3.83			3.36	1.22	16.70	2.43	3.70	0.97		
	198		1.11		11.12	2.56	1.74	29.12	21.11	5.28			2.94	1.63	16.24	2.89	3.70	1.07		
	128a		7.23	0.52	15.29	6.25		23.90	14.65	7.92			4.06	2.45	9.51	2.28	3.36	1.64		
	166		2.78		15.29	4.83	5.23	22.04	14.15	6.47			6.02	3.06	10.44	3.04	4.03	1.72		
amphibolite	170		2.78		6.12	4.83	4.36	22.74	13.84	7.66			5.88	3.88	9.05	2.43	2.69	2.61		
	175				17.51	4.26	6.54	18.68	12.04	5.41			5.74	2.86	13.69	3.04	1.34	2.33	4.47	
malic syenite - monzonite	191		10.01	14.67	25.30	1.14		13.22	8.45	3.83		1.29	0.79	3.08	1.63	10.44	2.28	2.69	1.61	
	189		27.80	25.68	18.07			6.50	3.76	2.39				1.12	0.82	6.03	1.37	1.68	1.15	
	187		30.02	22.53	15.01	3.12		9.51	5.04	4.22				0.28	0.20	5.34	1.22	1.68	1.01	
	134		26.13	17.82	15.85	3.98		9.86	5.39	4.09				4.34	3.67	4.64	1.37	2.02	1.32	
	119a		28.91	27.77	17.24			5.68	2.92	2.64		0.82	0.79	2.10	2.04	3.94	1.22	1.68	1.12	
	105		26.13	26.20	16.40	1.42		7.89	4.42	3.17				2.38	1.84	5.34	1.37	1.68	1.09	
porphyllite monzonite	190		35.03	19.91	16.12	0.85		7.77	5.09	2.11				1.12	0.61	6.73	1.22	1.68	1.12	
	186		24.46	28.30	19.46			5.80	3.38	2.11				1.12	0.82	5.34	1.37	1.34	5.81	
	137	0.47	31.69	34.58	15.29			4.29	2.54	1.58	0.74	0.53				3.71	1.06	1.01	0.61	
	130		36.14	29.87	13.34	1.70		5.22	3.27	1.58			0.42	0.20	4.41	0.76	1.01	0.65		
porph. leuco- cratic qtz monz.	192	6.77	30.02	40.35	15.01			0.46	0.31	0.13	1.04	0.26				2.32	0.46	0.67	0.87	
porph. leuco- cratic qtz diorite	188	22.32	14.46	39.82	11.68						2.10	2.24				0.93	0.76	0.67	1.01	
	182	27.19	12.23	35.63	13.90						1.40	2.38				0.93	0.46	0.67	0.94	

Note: Values listed are weight percentages of each normative mineral.
Sample locations are given in Figure 7

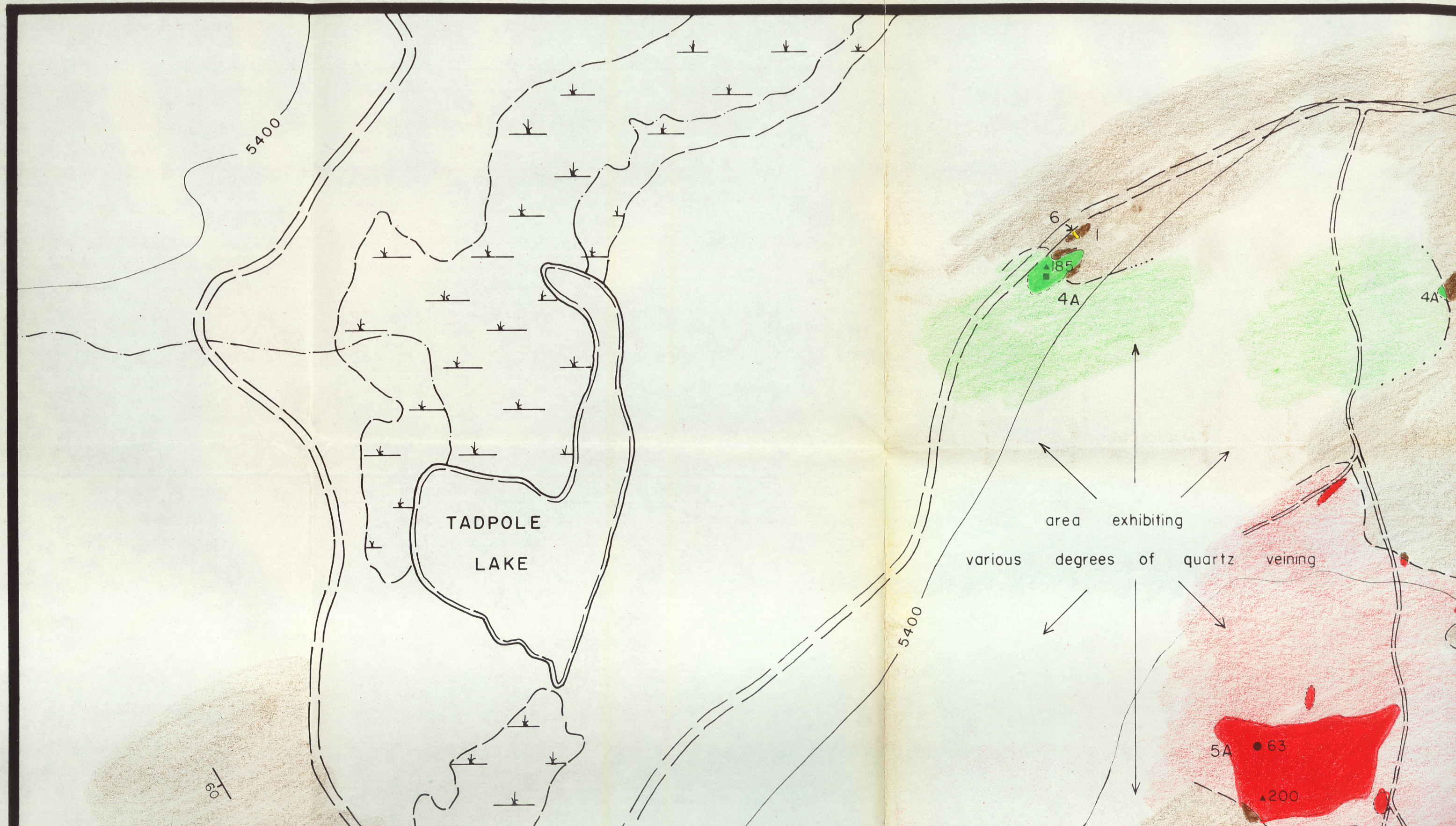
APPENDIX E

CALCULATED RATIOS OF VARIOUS ELEMENTS AND OXIDES FOR ROCKS FROM THE WHITEROCKS MOUNTAIN STOCK							
sample	K ₂ O/Na ₂ O	K/Rb	K/Ba	Ba/Rb	Ca/Sr	Sr/Ba	Rb/Sr
COMPLEX pyroxenites	39	1.49	199.6	23.7	8.4	333.0	0.955
	196	0.94	154.2	19.4	7.9	356.2	1.299
	198	0.88	124.5	8.6	14.6	348.0	0.758
	128a	0.90	610.4	38.3	15.9	195.2	2.214
	166	1.46					
	170	1.33	409.9	67.3	6.1	218.6	2.646
	175	1.20	519.7	44.9	11.6	232.7	1.876
	71b	0.93	309.8	30.8	10.0	61.2	4.058
	191	0.88	340.0	24.7	13.7	62.6	2.565
	189	1.53	470.7	42.2	11.1	42.2	1.429
COMPLEX mafic syenite - monzonite	187	1.53	618.9	36.6	16.9	29.8	1.585
	134	1.49	421.8	39.1	10.8	60.2	1.155
	119a	1.48	489.1	34.5	14.2	39.7	1.081
	105	1.30	450.9	43.6	10.3	52.5	1.302
	190	2.33	509.3	39.9	12.8	32.8	1.403
	186	1.25	499.3	43.1	11.6	40.7	1.639
	137	1.32	349.7	3.5	8.0	26.2	1.547
	130	1.55	715.5	41.0	17.5	19.5	1.722
	72b	0.95	486.1	38.8	12.5	20.8	1.422
	192	1.05	450.8	36.6	12.3	19.2	1.158
COMPLEX leucocratic quartz monzonite	114b	1.06	405.1	35.2	11.5	16.8	0.780
	115b	0.96	370.5	38.2	9.7	19.7	1.182
	188	0.53	488.2	17.9	27.3	28.1	0.610
	182	0.50	694.0	8.4	8.3	51.7	4.860
	63	1.30	230.1	69.0	3.3	26.7	0.405
	75	0.41	413.1	13.5	30.5	42.0	0.424
	78	0.48	393.1	20.9	18.8	54.5	0.618
	79	0.45	555.1	13.3	41.8	41.4	0.399
	A-1	0.43	176.8	0.1	1875.3	15.7	0.006
	A-2	0.58	395.7	0.3	13575.0	35.1	0.011
ALKALIC porphyritic quartz monzonite	A-3b	0.53	365.9			38.9	0.102
	237	0.85	244.1	137.8	1.9	68.9	0.241
	238b	0.62	368.0	21.1	17.4	31.2	0.426
	239	0.59	351.9	6.5	54.2	30.1	0.162
	248	0.67	368.7	18.7	19.7	32.4	0.371
	285	0.63	372.2	17.4	21.4	34.3	0.447
	295	0.96	370.8	23.2	16.0	41.9	0.128
	265	0.65	374.8	17.6	21.3	34.6	0.377
	298	1.11	408.2	21.8	18.8	41.6	0.087
	238a			4.4		0.227	1.010
CALC - ALKALIC undifferentiated diorites & quartz monzonites	242			56.9		0.204	0.086
	247			17.5		0.318	0.180
	271			14.5		0.261	0.263
	273			11.6		0.235	0.368
	284			9.1		0.251	0.439
	292			30.8		0.391	0.083

WHITEROCKS

MOUNTAIN

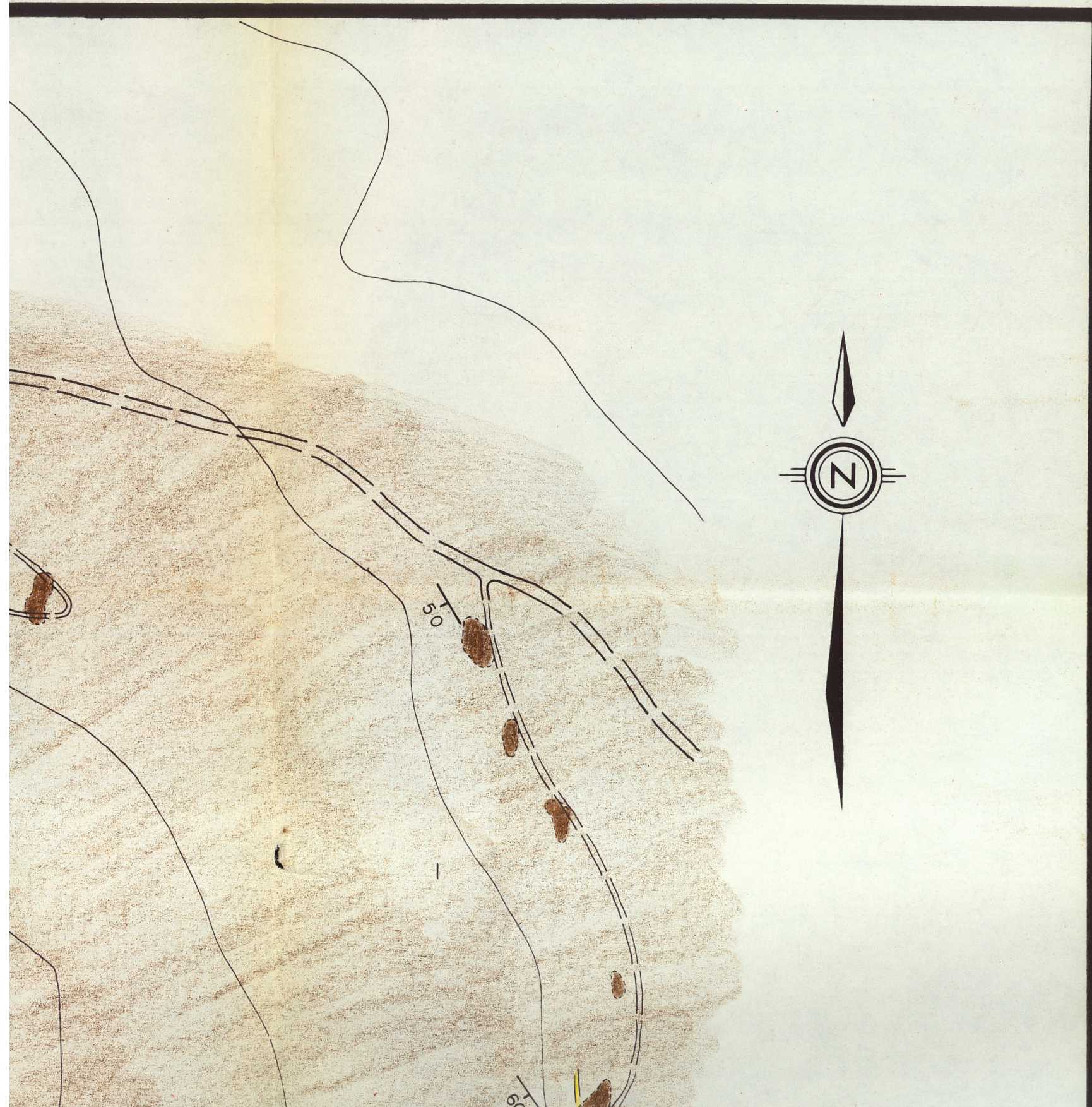
ALKALIC



ALIC

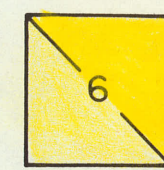
COMPLEX





LEGEND

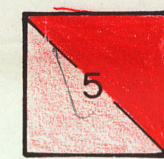
UPPER JURASSIC



Porphyritic Leucocratic Quartz
Diorite

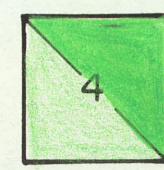
intrusive contact

UPPER MISSISSIPPIAN TO UPPER JURASSIC



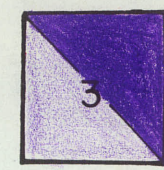
Leucocratic Quartz Monzonite
A. less than 10% quartz
B. greater than 10% quartz

intrusive contact



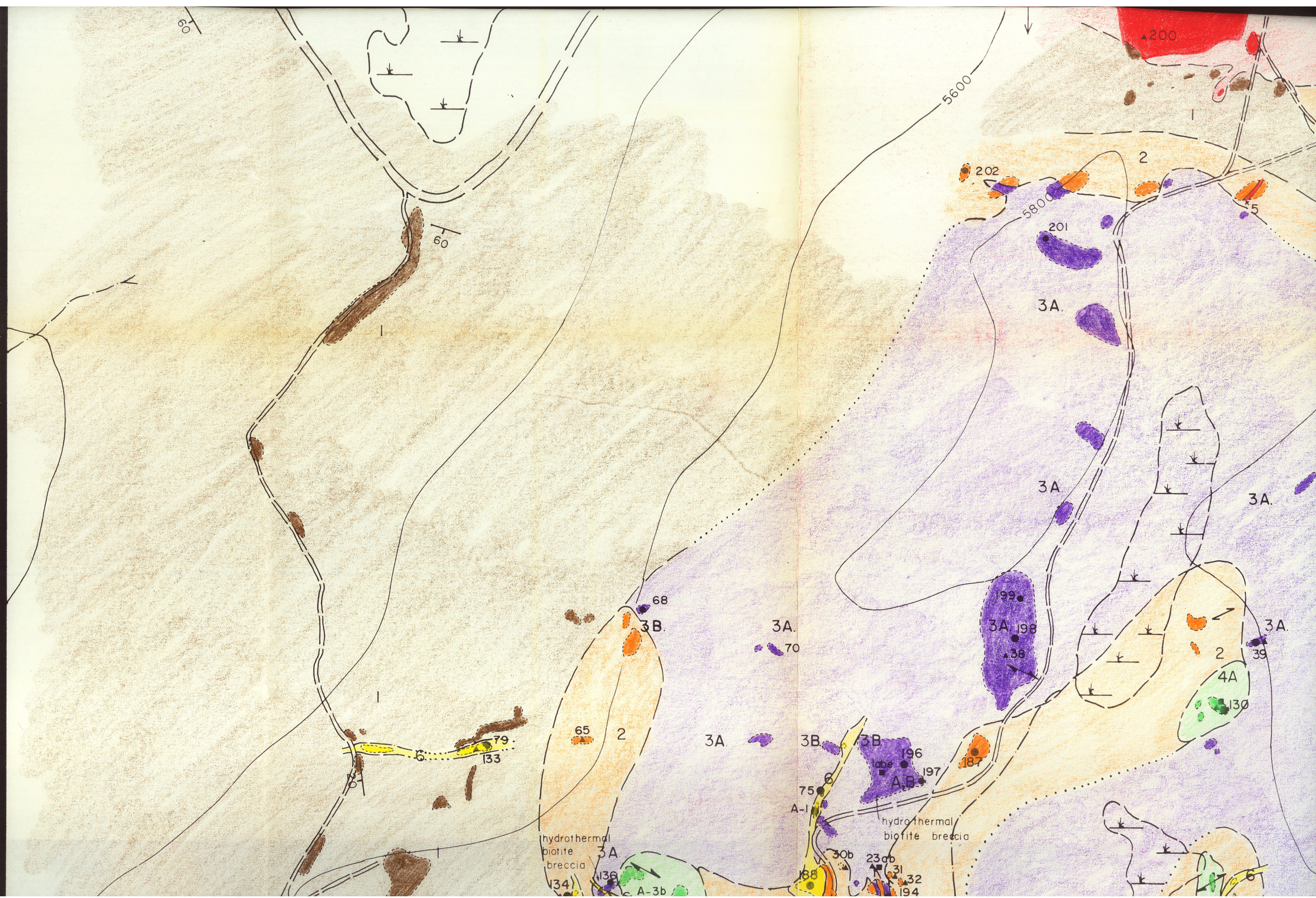
Porphyritic Monzonite
A. microcline phenocrysts less than 2cm.
B. microcline phenocrysts 2-15cm.

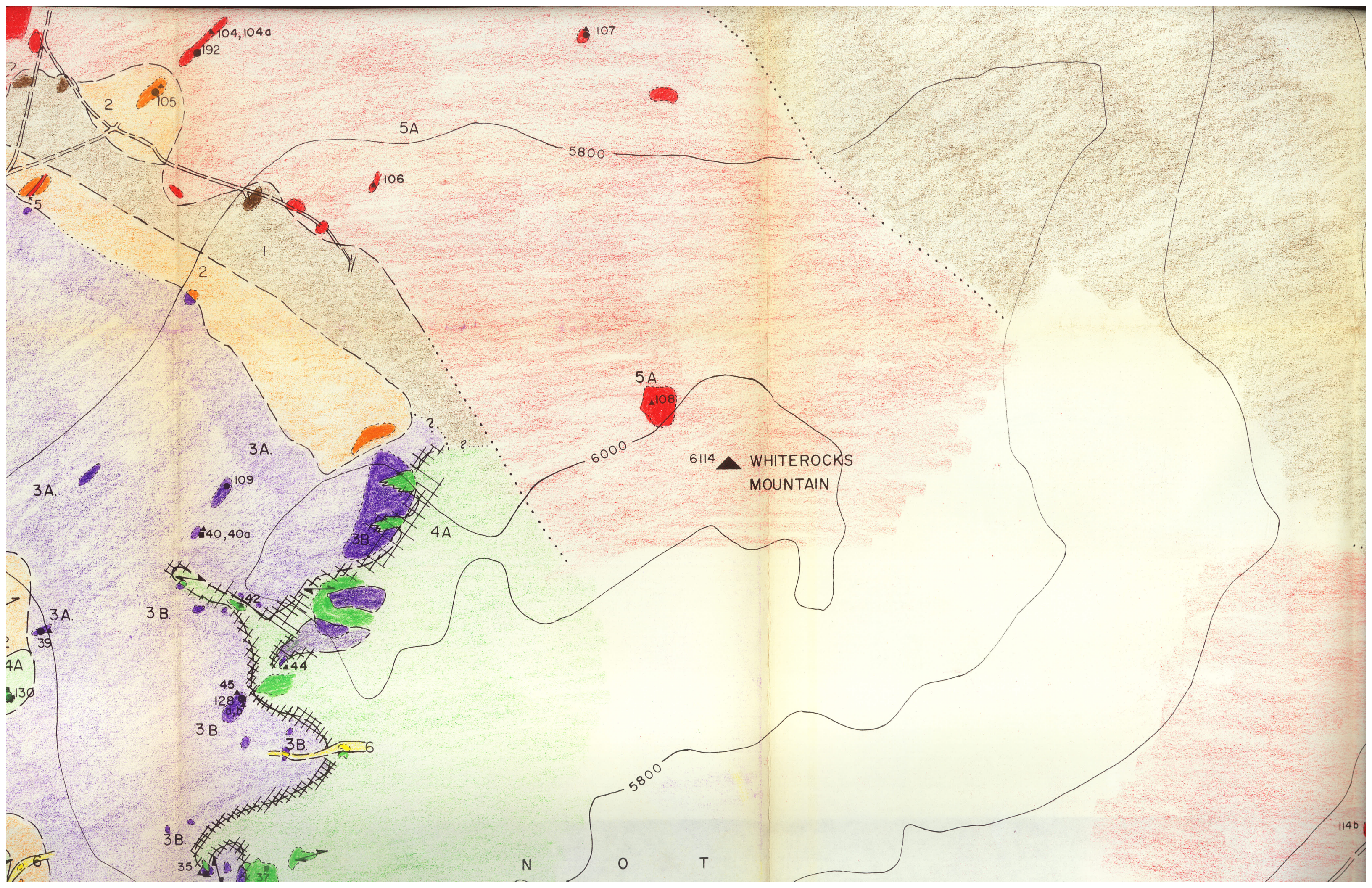
intrusive contact

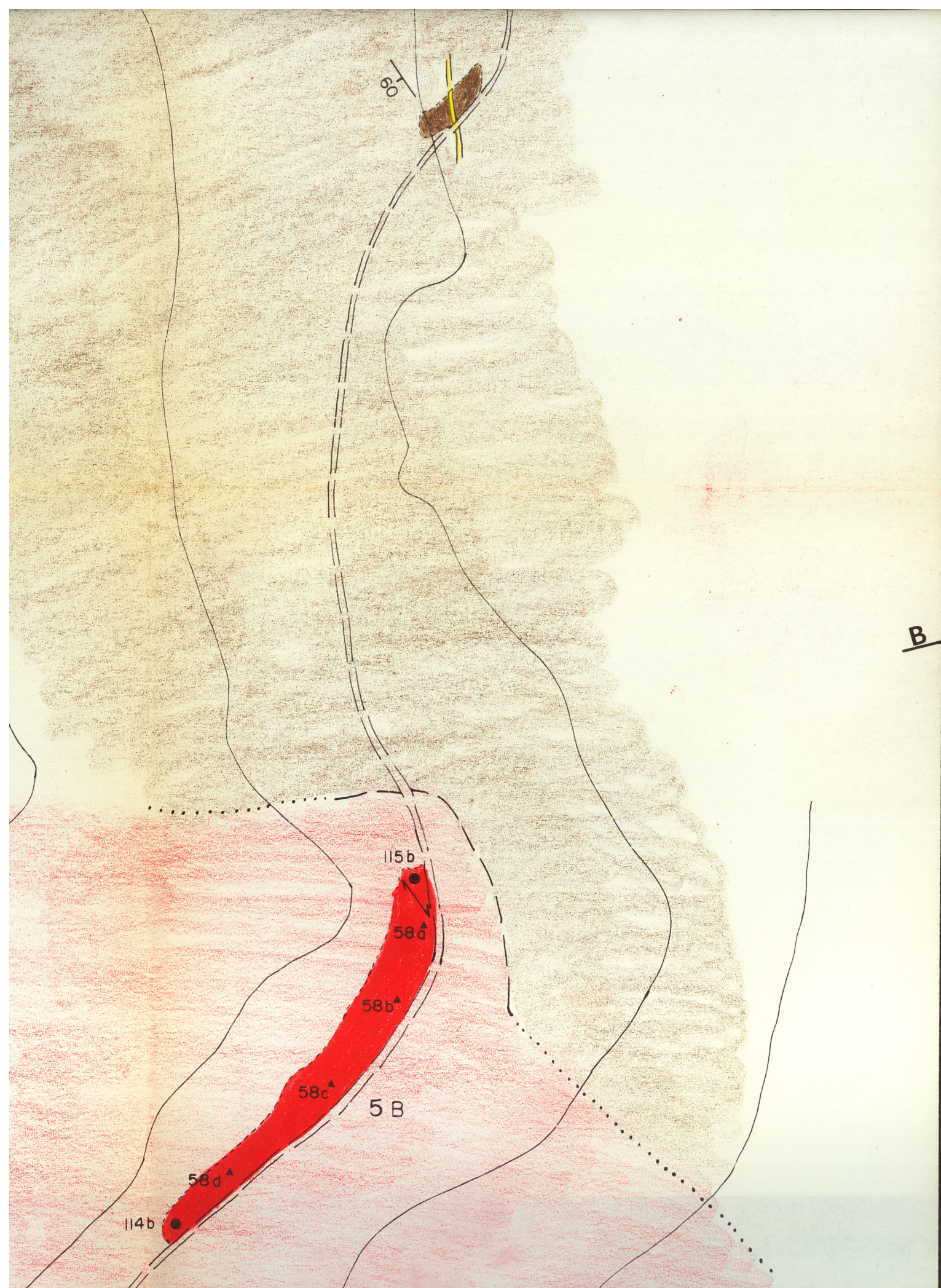


Alkalic Pyroxenite
A. biotite pyroxenite
B. amphibole pyroxenite

MOUNTAIN ALKALIC COMPLEX





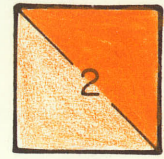


WHITEROCKS



A. biotite pyroxenite
B. amphibole pyroxenite

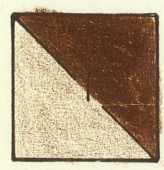
intrusive contact



Mafic Syenite- Monzonite

intrusive contact

UPPER MISSISSIPPIAN TO TRIASSIC



Metasediments and Metavolcanics

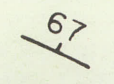
SYMBOLS



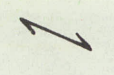
outcrop



geologic contact:
defined, approximate, assumed



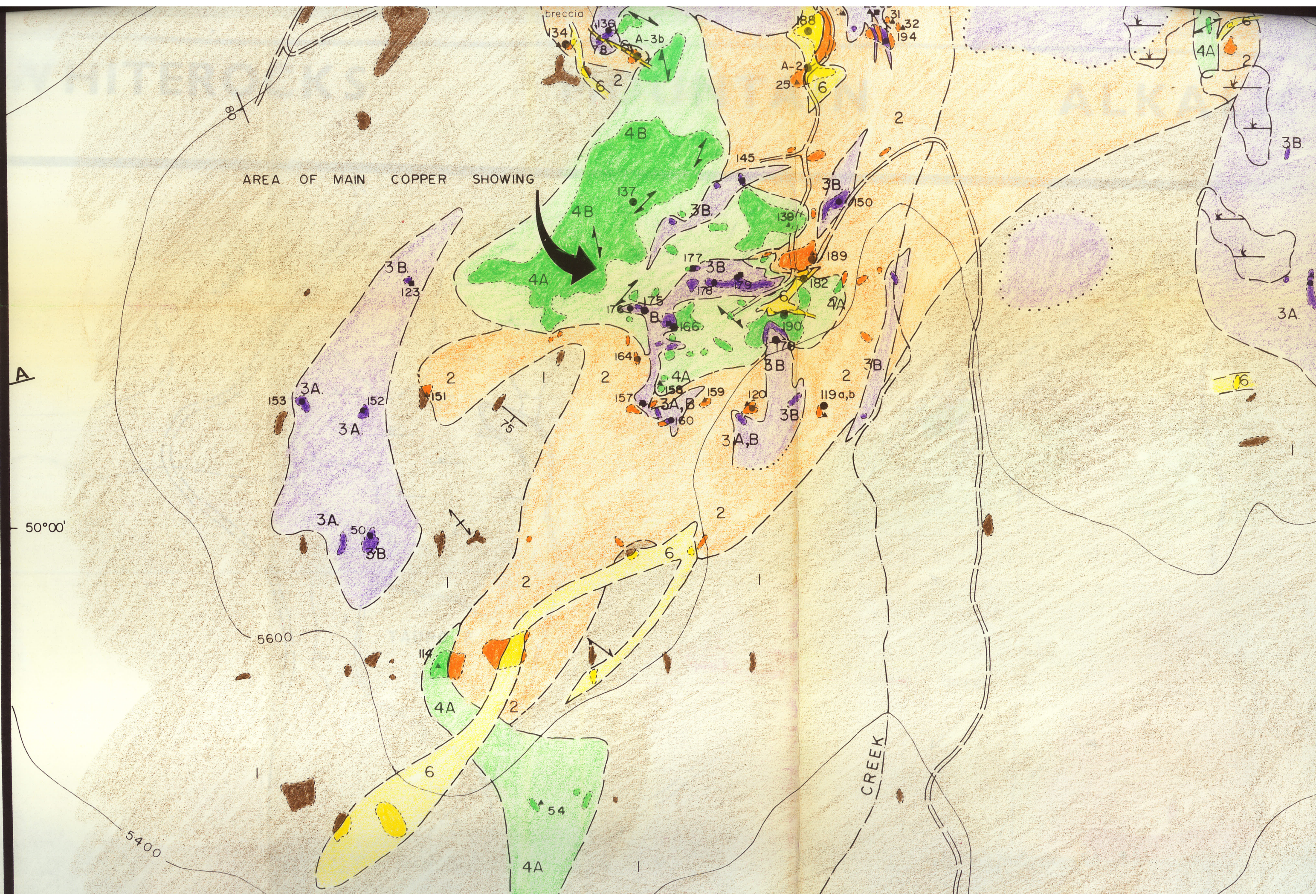
bedding

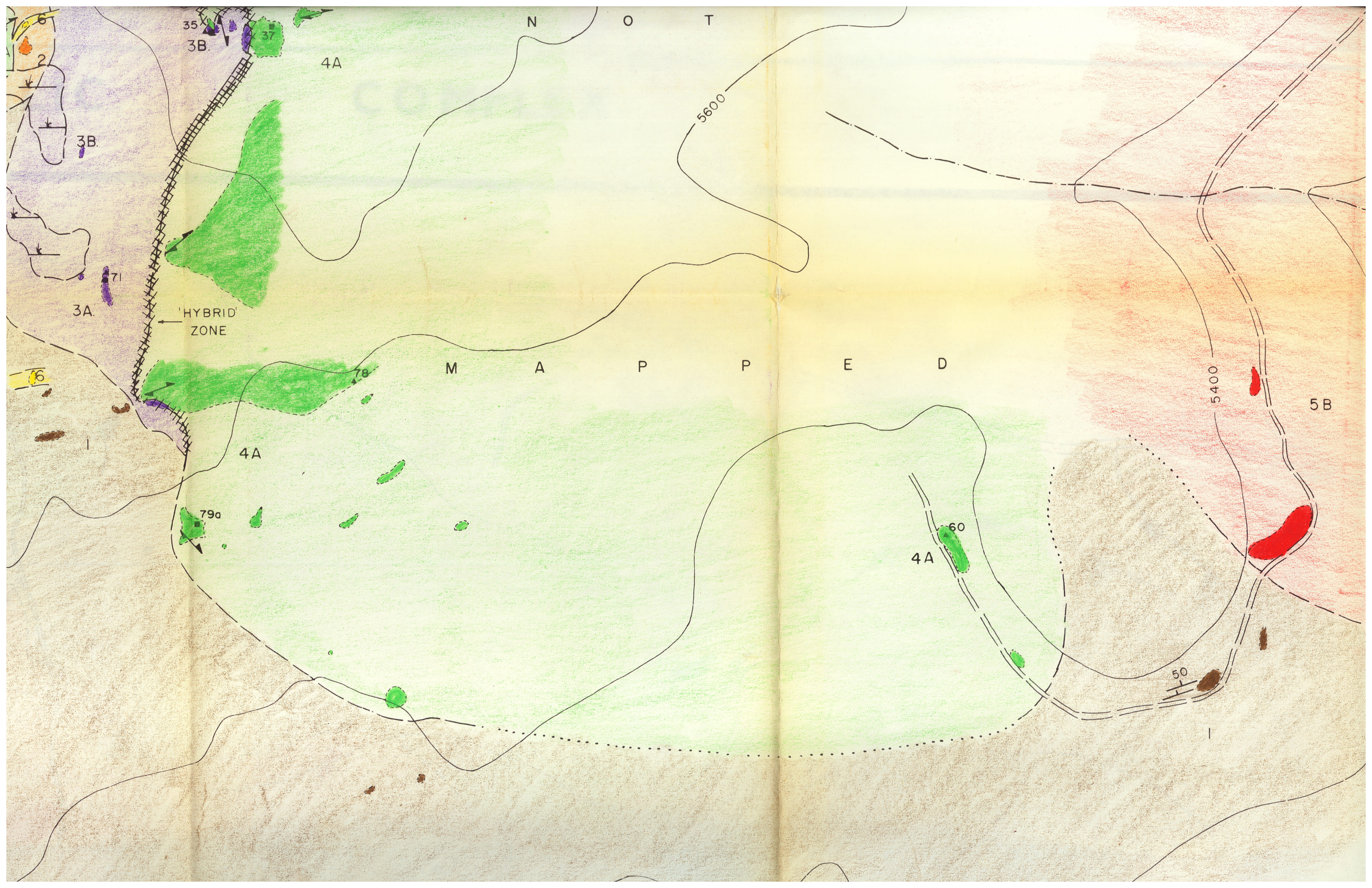


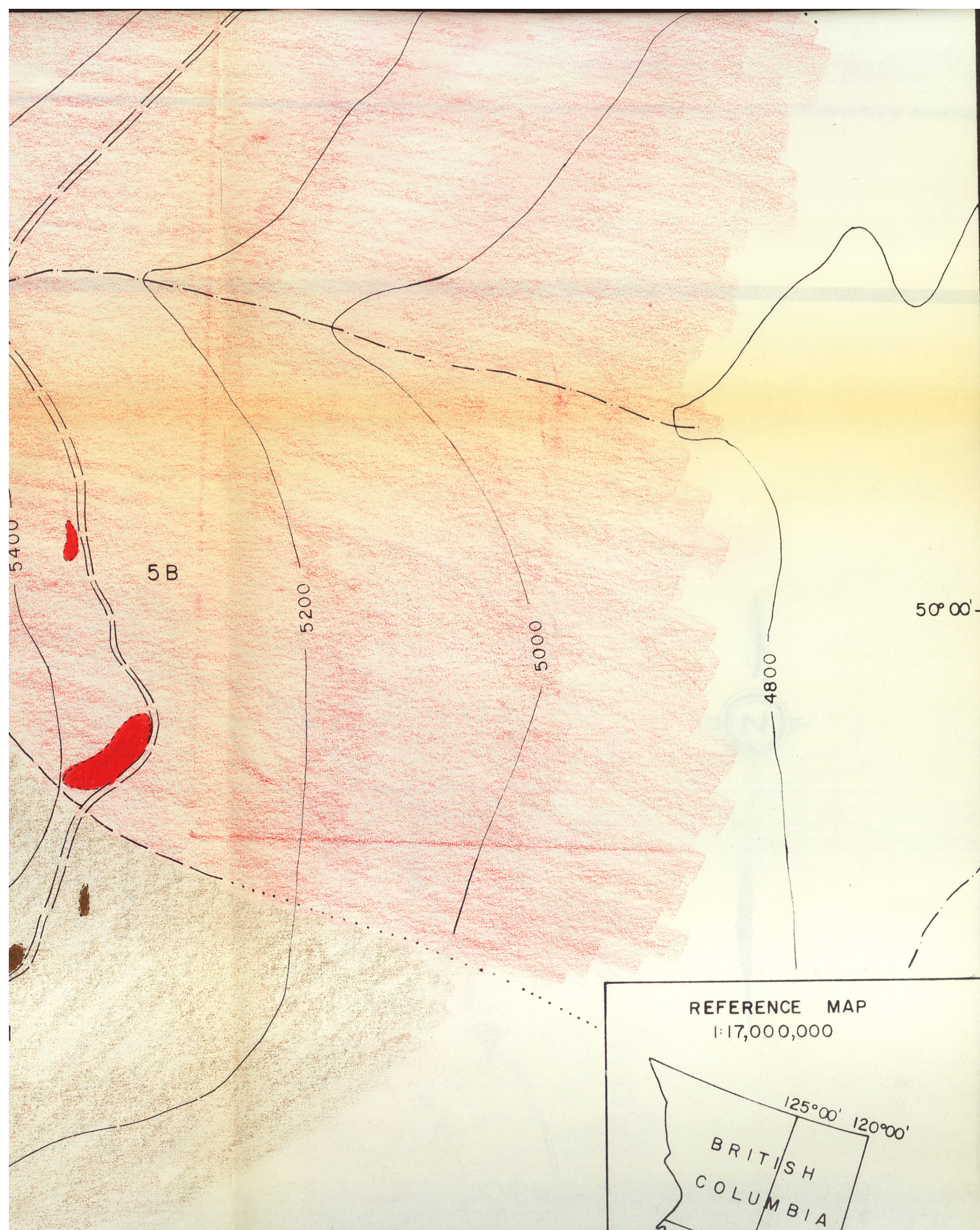
metamorphic foliation



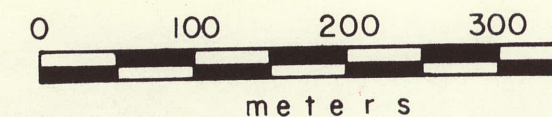
primary alignment of minerals







- primary alignment of minerals
- 170 sample number and location for whole rock and trace element analysis
- 40 sample number and location for x-rayed amphiboles and k-spars
- 12 sample number and location for point counted specimens
- pyroxenite - monzonite hybrid zone
- access road
- contours in feet above sealevel
- swamp
- creek



SCALE 1:5000

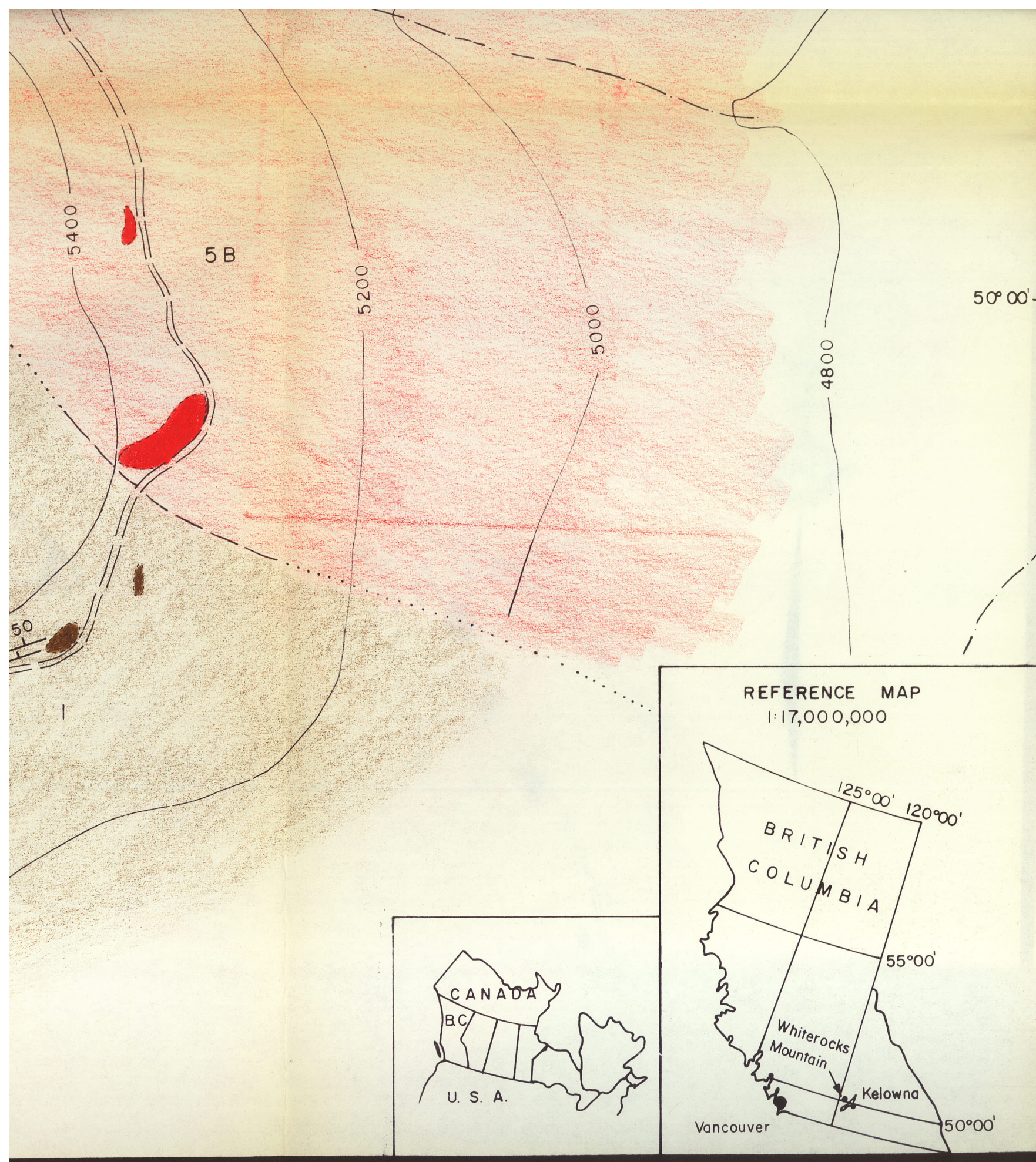
GEOLOGY MAPPED BY D.T. MEHNER, 1978, 1980

NOTE: positions of some contacts were determined from ground magnetic survey data obtained from assessment reports on the TAD mineral claims, N.T.S. 82L/4W obtainable from Mining Recorder's office in Vernon or Victoria, B.C.

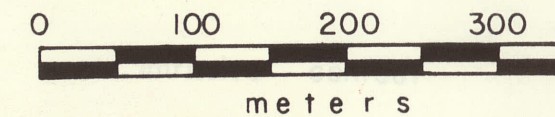
FIGURE 7







- sample number and location for point
counted specimens
- pyroxenite - monzonite hybrid zone
- access road
- contours in feet above sealevel
- swamp
- creek



SCALE 1:5000

GEOLOGY MAPPED BY D.T. MEHNER, 1978, 1980

NOTE: positions of some contacts were determined
from ground magnetic survey data
obtained from assessment reports on the TAD
mineral claims, N.T.S. 82L/4W obtainable from Mining
Recorder's office in Vernon or Victoria, B.C.

FIGURE 7

GEOLOGICAL MAP OF WHITEROCKS MOUNTAIN ALKALIC COMPLEX